THE INFLUENCE OF PFA PARTICLE SIZE ON THE WORKABILITY OF CEMENTITIOUS PASTES

Jan Hendrik Christoffel Pretorius

A dissertation submitted in partial fulfillment of the requirements for the degree of

MASTER OF SCIENCE (TRANSPORTATION)

In the

FACULTY OF ENGINEERING, THE BUILT ENVIROMENT AND INFORMATION TECHNOLOGY

UNIVERSITY OF PRETORIA

August 2002

SUMMARY

THE INFLUENCE OF PFA PARTICLE SIZE ON THE WORKABILITY OF CEMENTITIOUS PASTES

Jan Pretorius

Supervisor: Professor E.P. Kearsley

Department: Civil & Biosystems Engineering

University: University of Pretoria

Degree: Master of Science (Transportation)

In this dissertation the effects of different types of Pulverized Fuel Ash (PFA)-types on the workability of cementitious pastes containing relative large amounts of PFA were investigated. The different types of PFA were produced at the same source thus they were chemically similar but differed in terms of average particle size and size distribution (grading). By using a two-point measurement technique based on flow through a J-shaped tube it was possible to detect relative small differences in workability between pastes. It was found and concluded that the different types of PFA had a significant effect on the workability of pastes containing cement and PFA as well as PFA alone.

The physical differences between the PFA-types were quantified and their effects on workability investigated. It was concluded that PFA with a broader particle size distribution range produced pastes with higher workability at constant water content. It was found that compressive strength as measured after 28 days were solely a function of the water/cementitious ratio for the curing regime employed. It was concluded that for curing conditions used the type of PFA used could have a significant effect on compressive strength when constant workability is required.

ACKNOWLEDGEMENTS

I wish to express my appreciation to the following organizations and persons who made this dissertation possible:

1. Ash Resources and PPC for supplying the raw materials. Permission to use the material is gratefully acknowledged. The opinions expressed are those of the author and do not necessarily represent the policy of these organizations.

2. The following persons are greatly acknowledged for their assistance during the coarse of the study:

   Mrs. Hanli Turner
   Mrs. Ansie Martinek
   Mr. Jaap Peens
   Mr. Herman Booysen
   Mr. Derek Mostert
   Mrs. Jenny Callanan
   Personnel of the concrete laboratory at the Civil Engineering department of the University of Pretoria

3. Professor E.P. Kearsley, my supervisor, for her guidance and support.

4. My family, especially my wife for their encouragement and support during the study.

5. To my creator

TABLE OF CONTENTS

LIST OF FIGURES

LIST OF TABLES

1 INTRODUCTION

1.1 Background

Workability is one of the most important properties of fresh concrete, cementitious pastes and grouts thus measurement and control thereof is of outmost importance. The relevance of this property is associated with placing and processing of concrete, the more workable the easier it is to place and the less energy is required for compaction.

The primary contributing factor in workability is the water content of the mix, which is usually measured and referred to as the water/cement ratio. The higher the water/cement ratio, the more dispersed are the cement and other solid particles thus the more workable the slurry. The water/cement ratio should however be kept at a minimum to allow for appropriate strength development.

Concrete however does not only consist of cement and water but also fine and coarse aggregate and sometimes cement extenders such as Pulverized Fuel Ash (PFA) and ground granulated blast furnace slag. These constituents also contribute to the workability of the resulting concrete. The extent as well as mechanism of their contribution should thus be thoroughly understood in order to predict and control workability.

Pulverized Fuel Ash (PFA), more commonly known as fly ash, is a by-product from coal combustion in the electricity-generating process at thermal power plants and has cementitious properties. Replacing part of cement with PFA in a concrete mix has many advantages such as its cost effectiveness, it is environmentally friendly and it also enhances the durability and late-age strength of concrete. It also has an effect on workability and the extent thereof is investigated in this dissertation. In general, it has been accepted that the inclusion of PFA into concrete improves workability at constant water content.

The use of PFA as a partial replacement for cement in the construction and manufacturing industry is controlled by user specifications and minimum requirements, including amongst others size and strength reactivity requirements. These requirements is limited to the use of PFA as a replacement for ordinary Portland cement (OPC), however PFA can also be used in

association with other types of cements like rapid hardening cements. When measuring strength activity, most specifications take into account the effect of PFA on the water requirements to achieve constant workability thus the relative strength activity amongst different PFA-types may partially or fully dependent on their water reducing effect.

To assess the effect of PFA on workability a useful, accurate and sensitive test method is needed. Standard test methods have previously been criticized as not being sensitive enough and also that they do not describe workability in full. Other methods have been developed that fulfil these shortcomings but these methods are often not practical for use on site.

1.2 Objectives of the study

The main objective of this study is to assess the effects of different types of PFA on the workability of cementitious pastes. If PFA affects workability, the water demand of mixes will be affected when a certain level of workability is required and this will in turn affect the strength obtained.

To assess the effect of different types of PFA on workability an appropriate method of measuring workability is established which is user-friendly, accurate and sensitive to small differences in workability.

The second objective is to quantify the properties of the different types of PFA and assess them in terms of their influence on workability. The results are then compared to current requirements for PFA properties, especially size requirements. The effect of various material properties on workability is determined.

1.3 Scope of the study

The experimental side of the study is limited to high workability mixes containing cement and relatively high volumes of PFA. The use of high volumes of PFA (up to 67% by mass) in cementitious pastes to produce foamed concrete has been reported by Kearsley and Wainwright (1998).

High workability measuring techniques specified in standard specifications are assessed, as well as an alternative technique identified in the literature review that is suitable for workability ranges. A two-point method for measuring workability of high workability cement/PFA-pastes is established. This method can be used in quality control and mix design applications. At given water content it can also be used to assess variations in PFA or cement sources and properties on the workability of the resulting pastes.

In this study, different properties of PFA including particle size distribution and R_{45} (residue larger than 45μm) and their effects on workability of pastes containing cement from a single source is established. PFA-samples with different particle sizes and size distributions were obtained from a single power station thus the effect of variations in chemical content is minimized and assumed insignificant.

1.4 Methodology

Standard workability tests performed include the slump and flow table-methods. The alterative test method is based on a J-shaped tube. This method was assessed by preliminary testing as to establish its practicality and credibility. The J-tube is a two-point method and yield value and plastic viscosity-values can be determined. This method has been employed as a standard in Japan for testing the workability of highly flowable grouts.

The methods are compared by analyses of cement/PFA pastes with varying water/binder ratios. The measured plastic viscosity and yield values obtained with the j-tube test are compared to slump and flow-table values to establish relationships between these values and determine water content ranges where these relationships are valid.

The influence of five different PFA-types (from the same source) on the flow properties of cement-PFA pastes is analysed by preparing cement-PFA pastes with a constant PFA/cement ratio of 2. Workability measurements are performed and compared to those for cement and PFA-pastes alone. For all mixes, the total mass of the solids is to remain constant.

Particle size distribution analyses as well as X-ray fluorescence spectrometry are performed on all materials to assess particle size, grading-influence and chemical composition on paste and mortar properties. It is accepted that the chemical composition of all the PFA-types is similar and that

this effect is insignificant. Other tests include the measurement of Blaine specific surface area and relative density measurements.

1.5 Organisation Of Report

The report consists of the following chapters and appendices:

- Chapter 1 contains the introduction and will familiarize the reader with the scope of the research study
- Chapter 2 consists of a thorough literature survey, performed to assist the researcher with the technical background and knowledge on the subject that is needed to perform the relevant experimental tests.
- Chapter 3 outlines and explains the experimental tests undertaken during the study together with motivation for each.
- Chapter 4 shows the results obtained as graphical representations.
- Chapter 5 discusses the results.
- In chapter 6 conclusions are drawn and recommendations for further research are given.
- The list of references follows the end of the report.
- Appendix A contains data obtained from preliminary tests.
- Appendix B contains data from j-tube tests.

2 LITERATURE REVIEW

An intensive literature survey was conducted to firstly gain background knowledge on the workability of concrete, cementitious pastes and grouts and why it is an important parameter. Current standard workability test methods are reviewed followed by a more thorough study on the science of workability and the development of the more rigorous so-called two-point test methods.

The experimental part of the study is to assess the effects of different PFA-types that differed only in terms of particle size and distribution on the workability of cementitious pastes. The remainder of the literature survey thus focuses on the effects of different constituents in mixtures on workability, with emphasis on the use of PFA in concrete and cementitious pastes as a replacement material for cement. The science of particle size distribution and the quantification thereof is investigated in order to establish test parameters. Lastly an overview of South African PFA-types is given as well as standard specifications and test methods that these PFA-types must comply with.

2.1 Introduction to the Workability of Cementitious and Concrete Mixes

Concrete is semi-fluid in the fresh state due to the presence of water in the mix which allow for spacing between solid particles as well as lubrication. Because of this it is inevitable that more water in a mix will result in increased workability. Several factors are believed to contribute to the water demand of the different constituents (cement, coarse and fine aggregate, and extenders like fly ash) of a concrete mix. These constituents do not necessarily contribute equally to the water demand of the whole system.

Surface area of solids varies with size and shape and is measured as area per unit weight. If a certain mass of material were to be ground fine, the same mass of the now finer material would have an increased surface area. Particle shape also has an effect on surface area. Irregular shaped particles has got a larger surface area per unit mass than spherical ones. Solids with a relatively large surface area will therefore need more water to be wetted and such solids in a concrete mix will decrease workability or flow at a given water content relative to solids with lower surface area (at the same mass). Also, round smooth particles will cause less internal friction in a suspension than angular particles because there are less contact points between round particles than between angular particles.

It must also be remembered that for a surface to be wetted, it must have some affinity for water. Hydrophobic material such as non-polar hydrocarbons will therefore not absorb as much water as a more hygroscopic material such as cement. In the same way two different constituents in a concrete mix such as cement and fly ash may have different affinities for water. According to Hobbs (1980) the fly ash in a mix absorbs a negligible amount of water and its only influence on workability is due to viscous drag of the particles.

Abrahams (1918) concluded in his well-documented work that concrete strength depended on one factor namely the water cement ratio and he gave the following equation:

$$S = \frac{A}{B^x} \qquad \text{(Eq. 2.1)}$$

Where:

S = Compressive strength of the concrete,
x = Water/cement ratio and
A and B = Constants for a given material and conditions.

Thus to optimize compressive strength, the water-cement ratio should be kept at a minimum. Enough water should still be added to allow for complete cement hydration, and this minimum water-cement ratio was established to be 0.36 (Neville and Brooks, 1998).

The restricting factor for keeping water content at a minimum is workability of the mix. Enough water must be added into a mix to reach the minimum workability for an application. This factor has opened the way for the development of water reducers and plastisizers. These are chemical admixtures that can increase the workability of a concrete mix at a given water-cement ratio. Several researchers such as Bai et al (1999) have claimed that the introduction of fly ash and other mineral admixtures to a concrete mix may improve workability.

2.2 Measurement of the workability of cementitious pastes and fresh concrete

When fresh concrete or paste is subjected to a minimum level stress it starts to flow or shear like any liquid will do. The applied stress can be due to gravity as in the case of the slump test or can be applied as in the case of the flow table test. The measurement of workability can be defined as the measurement of shear strain of a unit volume of fresh concrete subjected to a standard level of stress.

Previous researchers have introduced several workability tests, according to Banfill (1990) over a hundred. Only a handful of these tests have been accepted as standards by different countries. Different test methods for different ranges of workability is normally recommended, for instance four different tests are recommended by the British Standards 1881 as illustrated in Table 2.1.

Table 2.1: Recommended ranges for test methods as in BS 1881, Part 102-105 (Tattersall, 1991)

Workability	***Method***
Very low	Vebe time
Low	Vebe time, compaction factor
Medium	Compaction factor, slump
High	Compaction factor, flow table
Very high	Flow table

The difference in the tests is the stress level to result in measurable strain or flow. The five workability ranges shown in Table 2.1 are all subjected to their own standard stress level so that variations in each range can be clearly identified.

Some of these more common methods used in field applications as well as by researchers referred to later on in this literature survey will be reviewed briefly.

2.2.1 The slump test (BS 1881: Part 102, 1983)

The slump test is probably the most well known and most frequently used workability test. A cone made of metal sheet (height 300mm, bottom diameter 200mm, top diameter 100mm) is filled with concrete to the top in three layers and rodded in a specified way. The cone is then

lifted and the concrete allowed to slump. The amount of slump is measured and recorded to the nearest 5mm. The apparatus is shown in Figure 2.1.

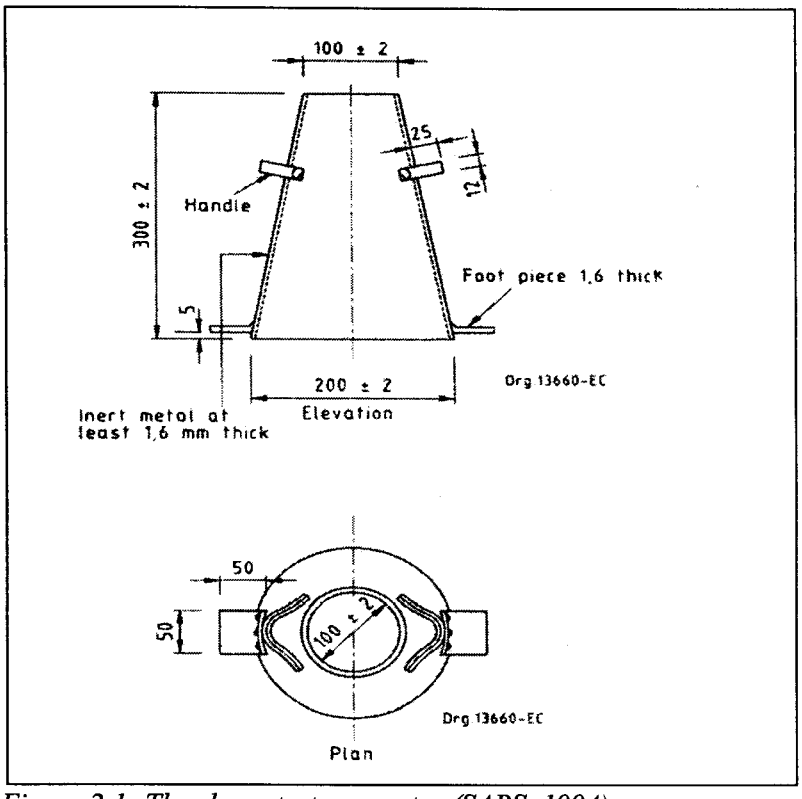

Figure 2.1: The slump test apparatus (SABS, 1994).

The various types of slump are shown in Figure 2.2 and only true slump can be reliably measured.

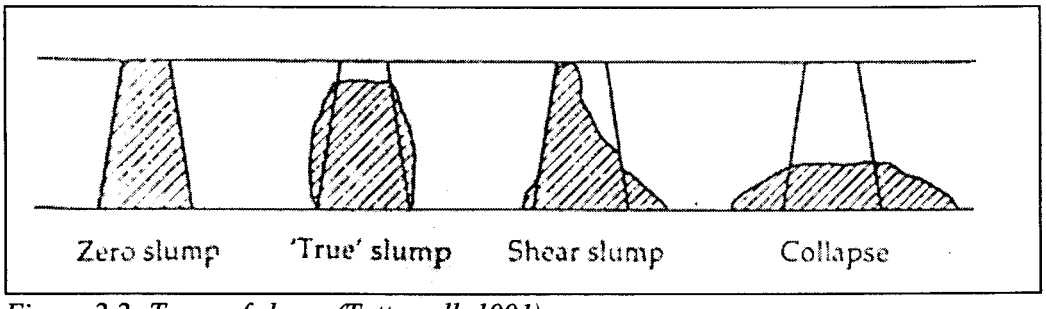

Figure 2.2: Types of slump (Tattersall, 1991)

The test is not sensitive enough to different levels of low workability mixes, which all result in zero slump. The test has also been criticized as being too sensitive to operator technique (Tattersall, 1991).

2.2.2 *The Compaction-factor test (BS 1881: Part 103, 1993)*

The compacting-factor test was devised by Glanville (1947). These researchers worked on the basis of compaction and were out to test the ability of concrete to compact as the criteria for its workability. The test apparatus is shown in Figure 2.3.

The volume capacity of the two cones and bottom cylinder decreases from top to bottom. The top cone is filled with concrete and then the door at the bottom of this cone is opened. The concrete then falls into the second cone which it fills to overflowing. Subsequently the door of this cone is then opened and the concrete falls into the cylinder. The excess concrete is scraped of the top of the cylinder and the partially compacted concrete is then weighed. The weight of concrete for full compaction of the cylinder is also measured and the compacting factor is then calculated as the weight of concrete for partial compaction divided by that for full compaction.

Cusens (1956) showed that the compacting factor might not always give a good indication of the ability of the concrete to compact. He showed in one instance that a concrete mix with a compacting factor of 0.70 achieved a density ratio of 0.88 after it was vibrated under mild conditions of 1.5g at 100Hz and thus concluded that the test is unsuitable for relatively dry mixes.

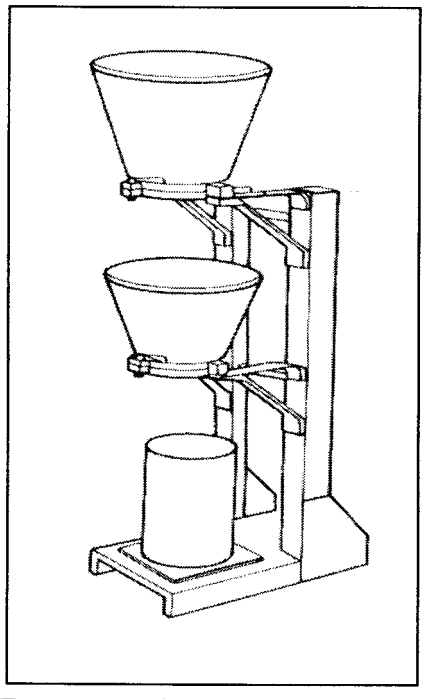

Figure 2.3: The compacting factor apparatus (Neville & Brooks, 1998)

2.2.3 The Vebe consistometer (BS 1881: Part 104, 1983)

The test apparatus is shown in Figure 2.4.

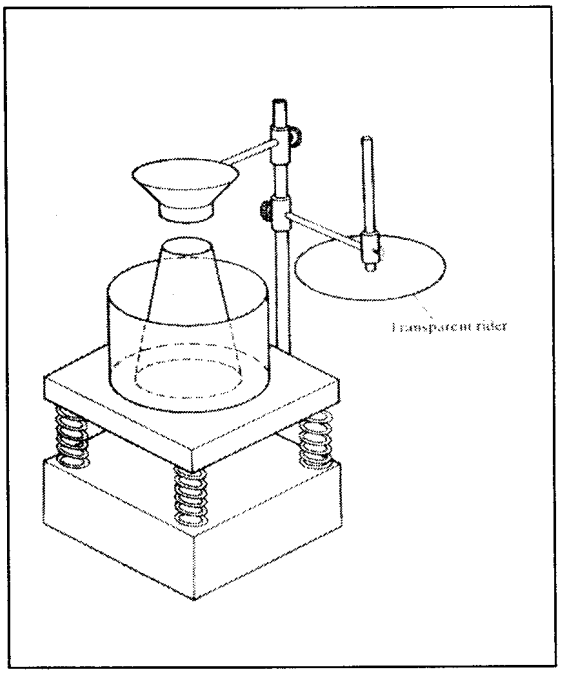

Figure 2.4: The Vebe-test (Neville & Brooks, 1998).

A standard slump cone is placed inside a cylinder and on top of a vibrating table. The cone is filled with concrete in the standard slump-method manner. Thereafter the cone is removed and a transparent disc-shaped rider is put on top of the concrete. The concrete is then vibrated until the whole face of the disc is covered by concrete, judged visually and the time taken recorded. The only source of errors for the test is establishing the start and end points. According to Tattersall (1991) the vibration needs time to "start up" and the visual estimation of the end point may also prove to be inconsistent between different operators.

2.2.4 The flow table test (BS 1881: Part 105, 1985)

The flow table test was introduced in the advent of the use of superplastisizers for the development and production of very high workable concrete. The slump test was not adequate anymore because these high workable concretes all produced collapse slumps. The other methods like Vebe-time and compacting factor was designed for concretes of lower workability so they were also inadequate (Tattersall, 1991). The test is illustrated in Figure 2.5.

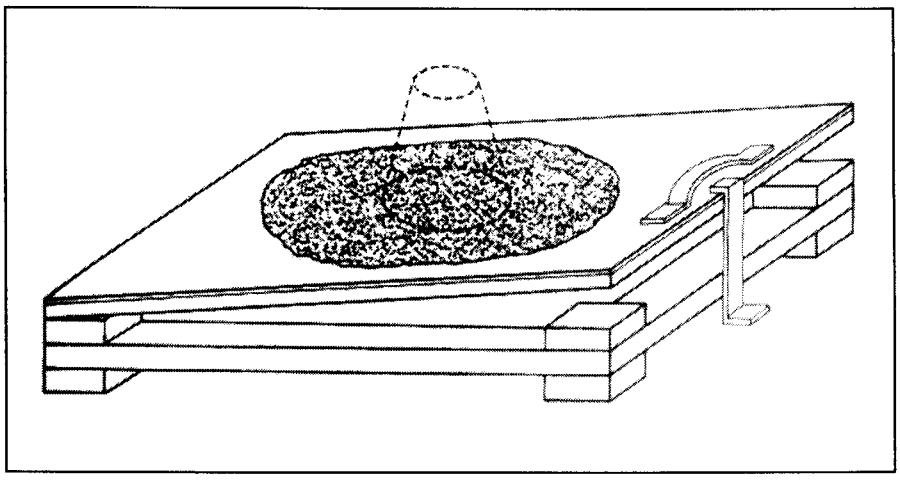

Figure 2.5: Flow table test (Neville & Brooks, 1998).

An upper wooden board is connected to a baseboard by means of hinges on one side so that it can lift up on the other side. A metal plate is attached on top of this upper board which is marked with a cross and concentric circles. The lift of the upper board is limited to 40mm by means of a stopper. A truncated cone of the concrete to be tested is formed on the metal plate, centered inside the concentric circles by means of a cone shaped form similar as that used for the slump test. The upper board holding the concrete is then lifted 40mm (until it touches the stopper) and dropped. This is repeated 15 times. The bumping action causes the concrete to spread and the two diameters parallel to the sides of the table is measured and the mean calculated, expressed to the nearest 5mm. The flow table test is described in ASTM (ASTM C109, 1998) as well as British Standards specifications (BS 3892, 1997) as part of the assessment of the quality of fly ash.

Diamond and Bloomer (1977) severely criticized the test giving several reasons for this. They claimed that the test is operator-sensitive mainly because of uncertainties about the force at which the limiting stop is struck when the table is raised. Morat, et. al. (1993) showed that when testing the effect of fly ash on workability of concrete, the test is a significant source of errors at relative low water contents. Their work will be discussed in more detail later.

2.2.5 Standard flow tests for cementitious grouts

Standard workability tests for highly fluid grouts for which above mentioned tests are not appropriate have been developed (ASTM 939, 1998; BS 3892, 1997). In ASTM C939 the Flow Cone method is described and workability is measured as the time of efflux of a specified volume

off cement grout through a standardized flow cone. The apparatus is shown in Figure 2.6. Measurement is performed by means of a stopwatch and the end point is taken as the time of the first break in continuous discharge of the grout from the cone. The method is intended for use with grouts having an efflux time of not more than 35 seconds. The specification states that if an efflux time of more than 35 seconds is measured, the flow table method (ASTM C109) should rather be used to measure workability, however the table should only be dropped 5 times in a time space of 3 seconds.

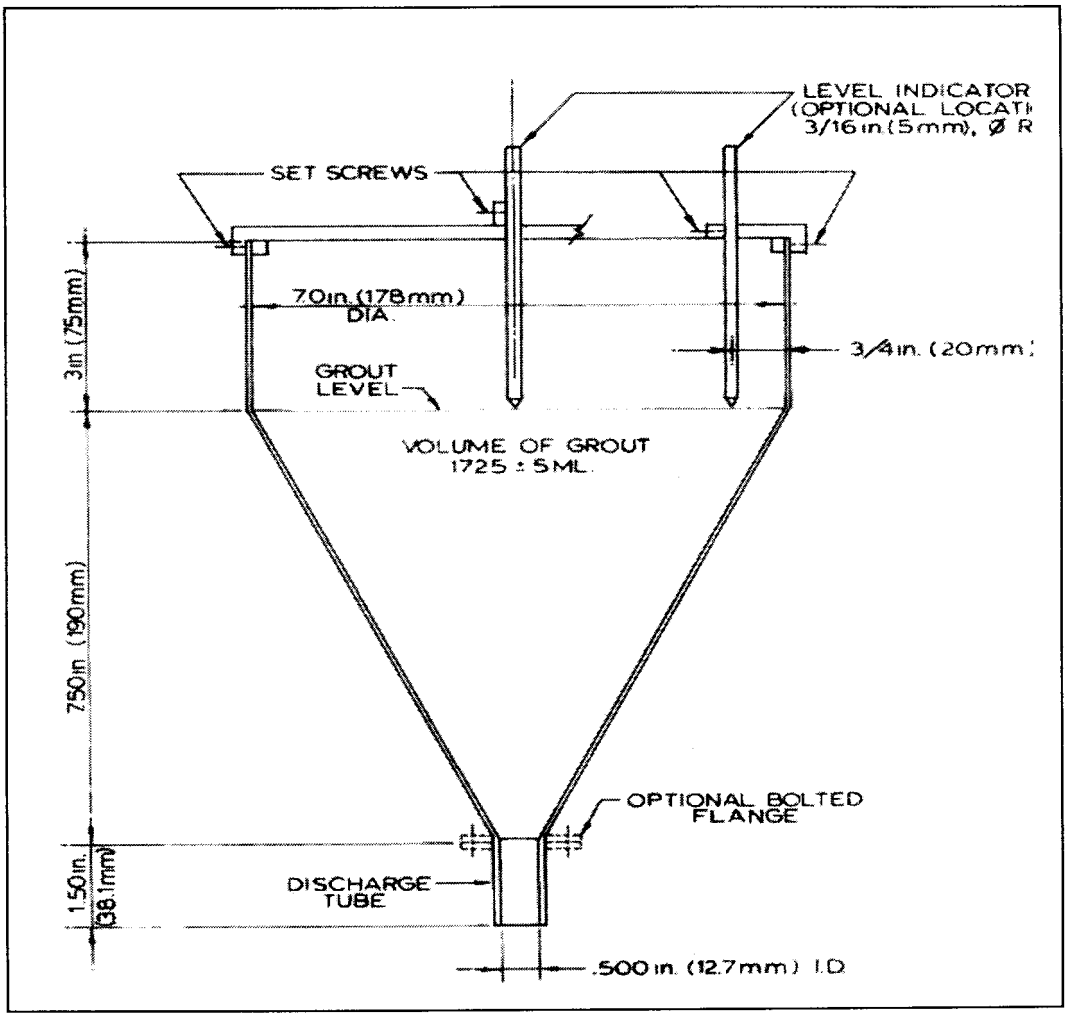

Figure 2.6: The Flow Cone (ASTM 939, 1998).

British Standards (BS 3892, 1997) describes the flow channel method and quantifies workability as the flow distance of a standard volume of grout in a channel with a minimum value being specified. A top as well as side illustration of the apparatus is shown in Figure 2.7

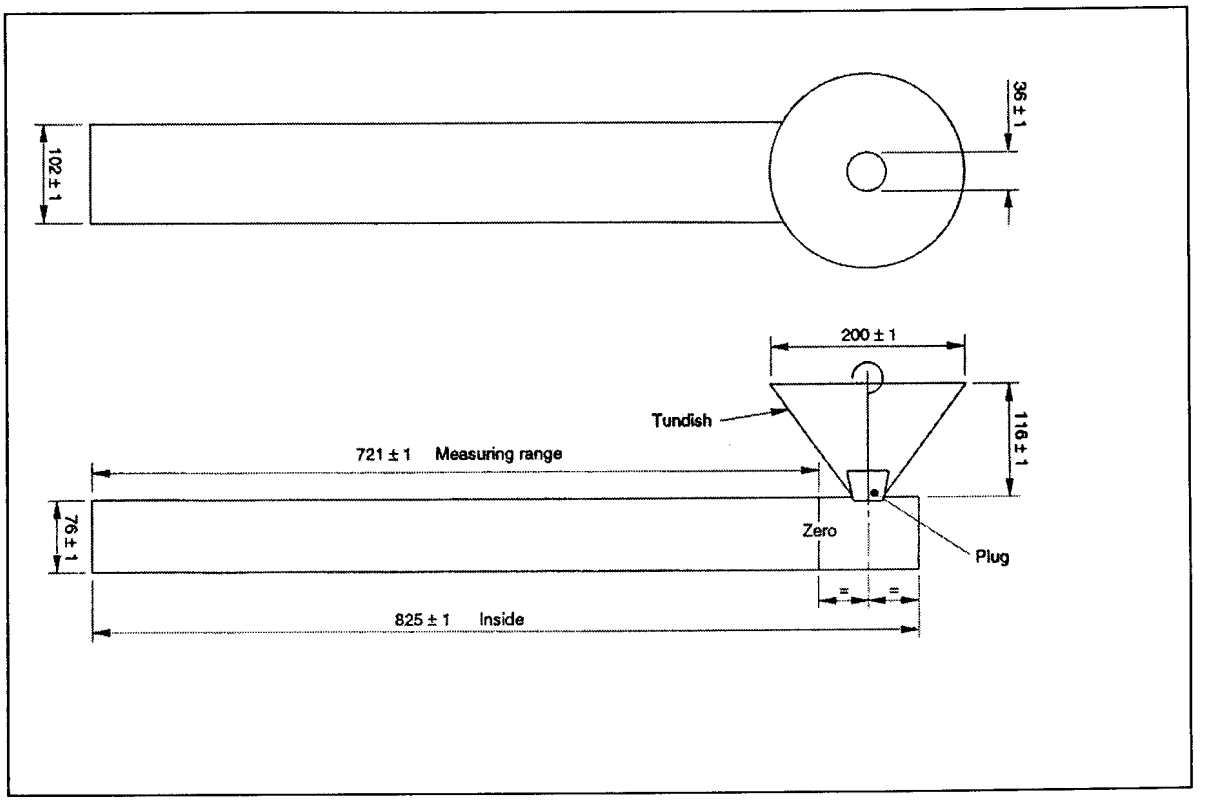

Figure 2.7: The flow channel (B.S., 1997).

All of the mentioned workability measurement tests are termed one-point tests because measurements are taken only at one stress level.

2.3 The Rheology Of Fresh Concrete and the Development of the Two-Point Test

Tattersall and Banfill (1983) described in their book why the workability of concrete should be assessed by a two-point (measuring shear at more than one stress level) instead of a one-point test. Newton described the laminar flow of a liquid by the following equation:

$$\tau = \eta \times \gamma \qquad \text{(Eq. 2.2)}$$

Where:

τ = Shear stress,

γ = Rate of shear and

η = Coefficient of viscosity (a constant characteristically of a given liquid).

If a graph of shear rate as a function of shear stress is plotted, we find a straight line, passing through the origin and with a slope of $1/\eta$ as shown in Figure 2.8:

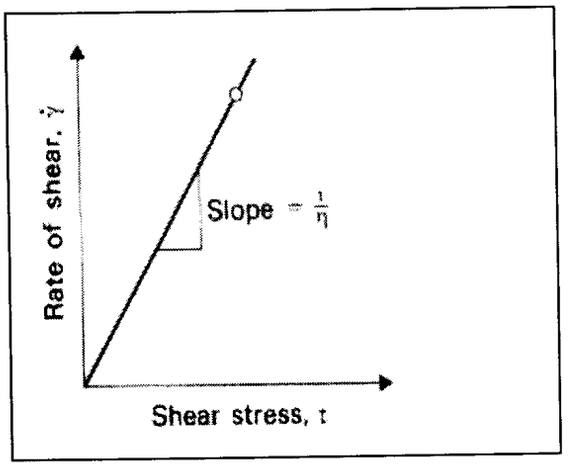

Figure 2.8: Newtonian liquid: $\tau = \eta \times \gamma$ (Tattersall & Banfill, 1983)

Thus the higher the shear rate at a given shear stress value, the lower the viscosity. The plot only requires one experimental value because a straight line only requires two points to pass through, with the origin taken as the first point. Thus for a Newtonian fluid, but for a Newtonian fluid only, a single experimental measurement, i.e., a single-point method of determination, is sufficient.

Not all liquids follow the Newtonian-law, thus the quotient (shear stress)/(shear rate) is not constant but depends on the shear rate at which it is measured, as well as maybe the shear "history" of the sample being investigated. Also the quotient may be constant but the line does not pass through the origin. It is thus clear that such flow curves cannot be drawn by using one measurement point and the flow qualities can also not be described by only one constant. Take a

flow curve of a liquid that is a straight line but has an intercept on the stress axes. Here a minimum shear stress value, called the yield value, is identified and is read off at the point where the line crosses the shear stress axes. This is the minimum stress value to be applied to the liquid to initiate flow. The Newtonian equation thus changes to:

$$\tau = \tau_0 + \mu \times \gamma \qquad \text{(Eq. 2.3)}$$

And is known as the Bingham model and τ_0 is termed the yield value or yield stress.

Thus for a fluid following Bingham flow characteristics, at least two measurement values are needed to draw a flow curve and the flow characteristics are described by the yield value, τ_0, and the viscosity, μ. A Bingham-plot is shown in Figure 2.9.

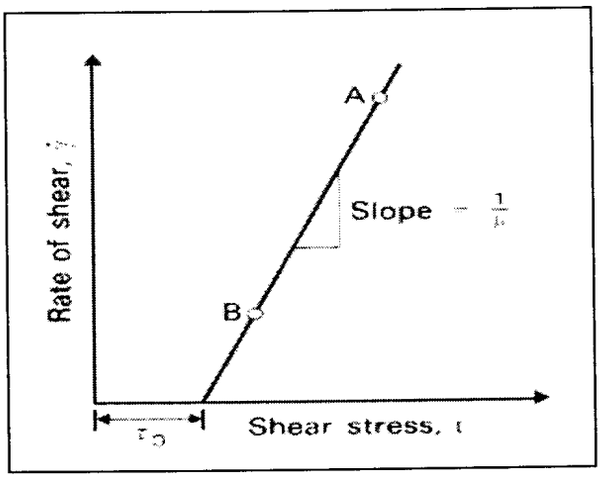

Figure 2.9: The Bingham model: $\tau = \tau_0 + \mu \times \gamma$ (Tattersall and Banfill, 1983).

Banfill (1994) explained further that simple visual observation is often enough to identify the existence of a yield stress, for example mortar on a trowel is capable of supporting its own weight without flowing.

Bingham plastics may also show time-dependent behavior in the form of reduction in shear stress at a constant shear rate, which is more severe at high shear rates. This thinning effect may be irreversible or the structure might be reformed after shear has stopped. The latter case is referred to as thixotropy. Because of this, a plot of shear stress versus shear rate when the controlled rate

is first increased then decreased, as for shear mixers, may result in a hysteresis loop thus the yield stress and plastic viscosity at any instant depend upon the previous shear history of the sample. Banfill further explain that a hysteresis loop cannot unambiguously characterize the structural breakdown in Bingham plastics. However when the structure has fully broken down, the downcurve (decreasing shear rate side of the loop) conforms to the Bingham model and the yield stress and plastic viscosity may be determined from it.

Workability can thus also be measured as the amount of shear stress required as to achieve a certain controllable level of shear strain. Tattersall initiated his development of 2-point workability measuring equipment based on power requirement during mixing. His first apparatus was a 3-speed Hobart food mixer equipped with a stirring hook. The electrical power input necessary to drive the hook at a constant rate was measured when the bowl contained the concrete (25-kg) and when it was empty by means of a dynamometer. The torque (T) on the shaft was calculated by dividing the difference between the two powers, P, by the speed, N. The apparatus is shown in Figure 2.10.

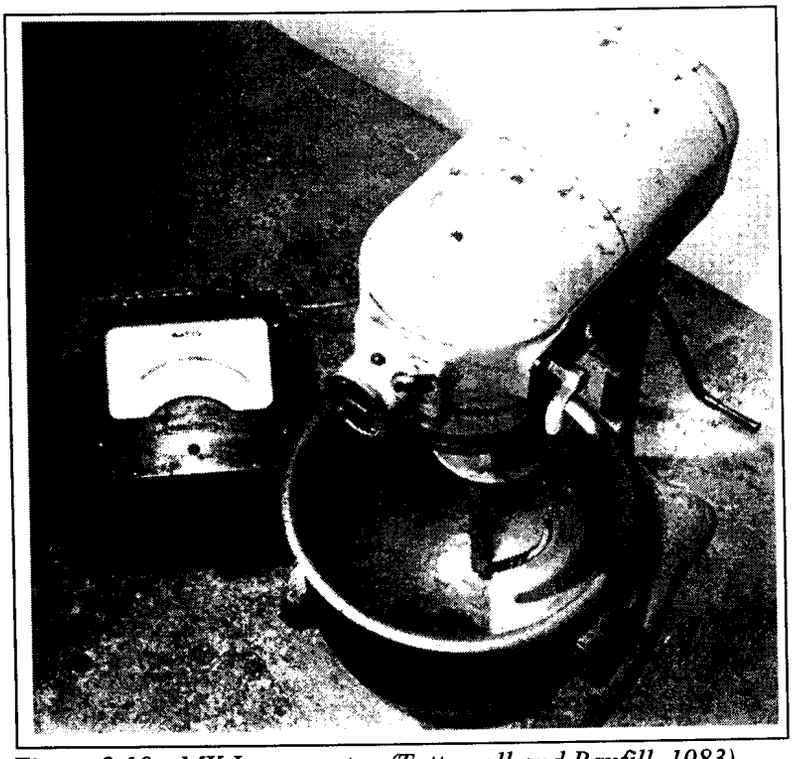

Figure 2.10: MK I- apparatus (Tattersall and Banfill, 1983).

Tattersall found, surprisingly, that when this torque value was plotted against speed, a linear relationship was obtained and the plot resembled the same plot as that of the Bingham model. This linear equation was given as:

$$T = g + hN \qquad \text{(Eq. 2.4)}$$

Where g is the intercept on the T axes and resembles the yield value. The h-term is relevant to the viscosity as explained by the Bingham model.

This method was termed the MK I-model and has since been revised to the MK II-model for high workability mixes and the MK III-model for low workability mixes. The differences between these models lie in the shape of the impellers. It was necessary to modify the impellers to eliminate problems associated with concrete being pushed away from the center of the bowl, therefore creating inconsistent shear environments. The MK II-impeller is shown in Figure 2.11 and has the shape of an interrupted helix. For the MK III model, it was changed to an H-shaped impeller with an offset gearing resulting in a planetary motion when mixing *(Tattersall and Banfill, 1983).*

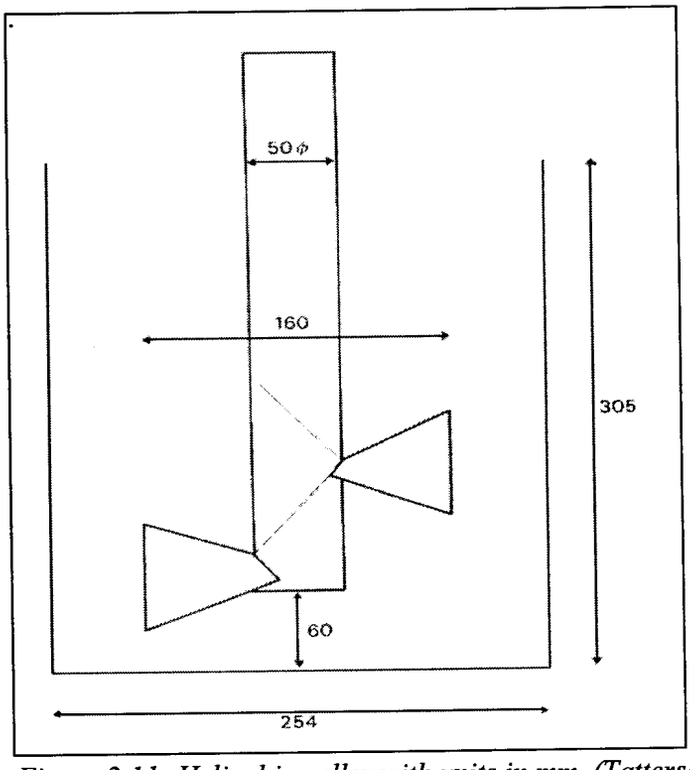

Figure 2.11: Helical impeller with units in mm. (Tattersall and Banfill, 1983).

The MK III-impeller is illustrated in Figure 2.12.

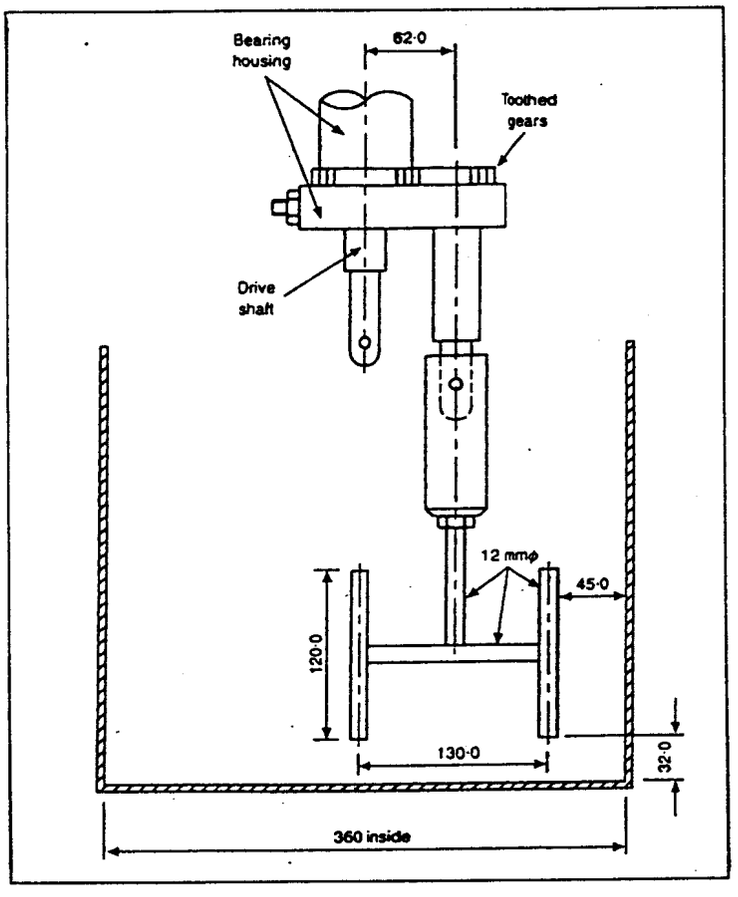

Figure 2.12: Offset H- impeller, with units in mm (Tattersall and Banfill, 1983).

Later, torque measurement was modified by simply recording the change in oil pressure generated by the electrical motor so that measurements could be assessed visually from a pressure gage. Wimpenny and Ellis (1987) added a pressure transducer to enable the oil pressure to be recorded by a chart or computer to reduce the subjective nature of the manual estimates from the pressure gage.

Banfill (1990) presented a two-point workability measurement apparatus, the Viscocoder, similar to the MK-apparatus of Tattersall. A diagram of the apparatus is shown in Figure 2.13.

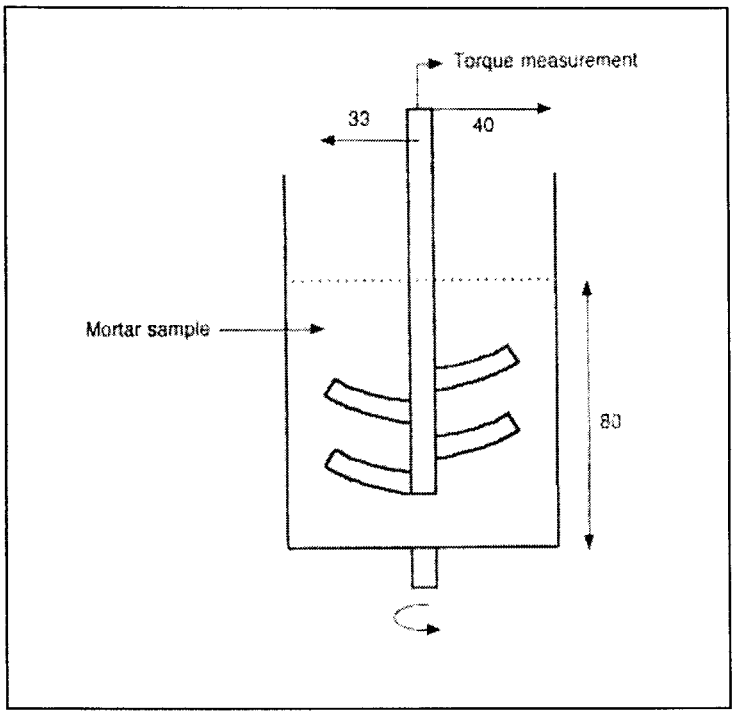

Figure 2.13: Schematic diagram of Viscomat and Viscocoder, with units in mm (Banfill, 1990.)

The concentric pedal is mounted on a torque measuring head containing a calibrated spring. As the cylinder rotates, the viscous resistance of the mortar flowing through the blades of the paddles turns it against the spring and moves a chart recorder pen across a chart which moves forward at a constant rate. The test is run for a certain time at different speeds. Breakdown of the concrete takes place as the test is initiated and commences until equilibrium is reached. Thereafter the flow curve conforms to a Bingham model. For a Newtonian fluid, no breakdown takes place. The flow curve, in the form of a plot of torque against time is constructed from values of torque obtained at each speed; in the case of the Bingham model these are the final values reached at the end of each speed. This is illustrated in Figure 2.14.

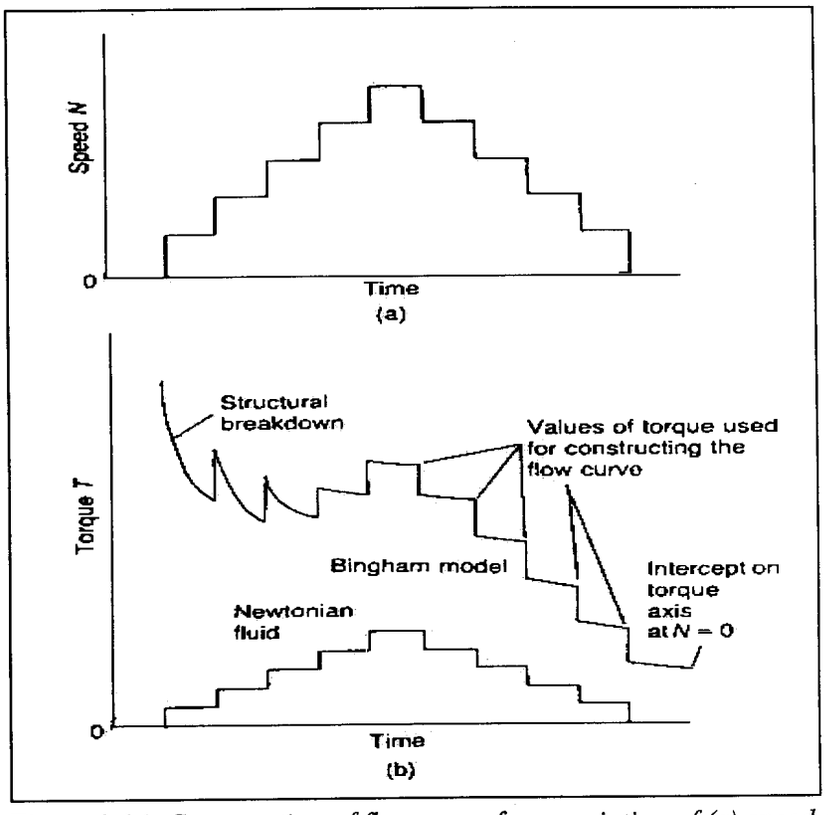

Figure 2.14: Construction of flow curve from variation of (a) speed and (b) torque with time (Banfill, 1990)

Different mortars were made and the flow curve of one of these mortars is shown in Figure 2.15, with measurements taken on the down curves, thus as the speed were reduced.

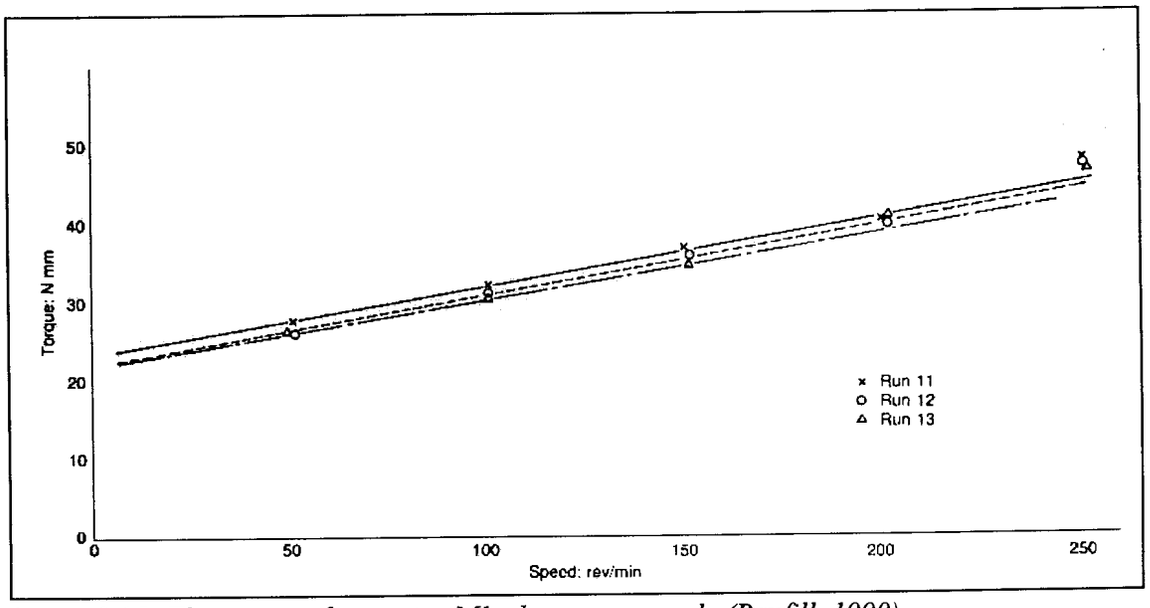

Figure 2.15: Flow curves for mortar M1: down curves only (Banfill, 1990).

Banfill claimed that for this program of 44 tests only two downcurves (from top speed to zero) gave correlation coefficients below 0.990, and those were mixes of low water content, which were probably too stiff for the ViscoCoder. Banfill later modified the ViscoCoder so that torque measurement is continuously monitored electronically as the sample is subjected to a predetermined speed and temperature program over a given time as controlled by the software in a personal computer.

Beaupre and Mindess (1994) designed their Rheometer based on Tattersal`s MKIII-model. The torque measurements were performed by the use of strain gages measuring the deflection of a small beam in bending. The apparatus is shown in Figure 2.16.

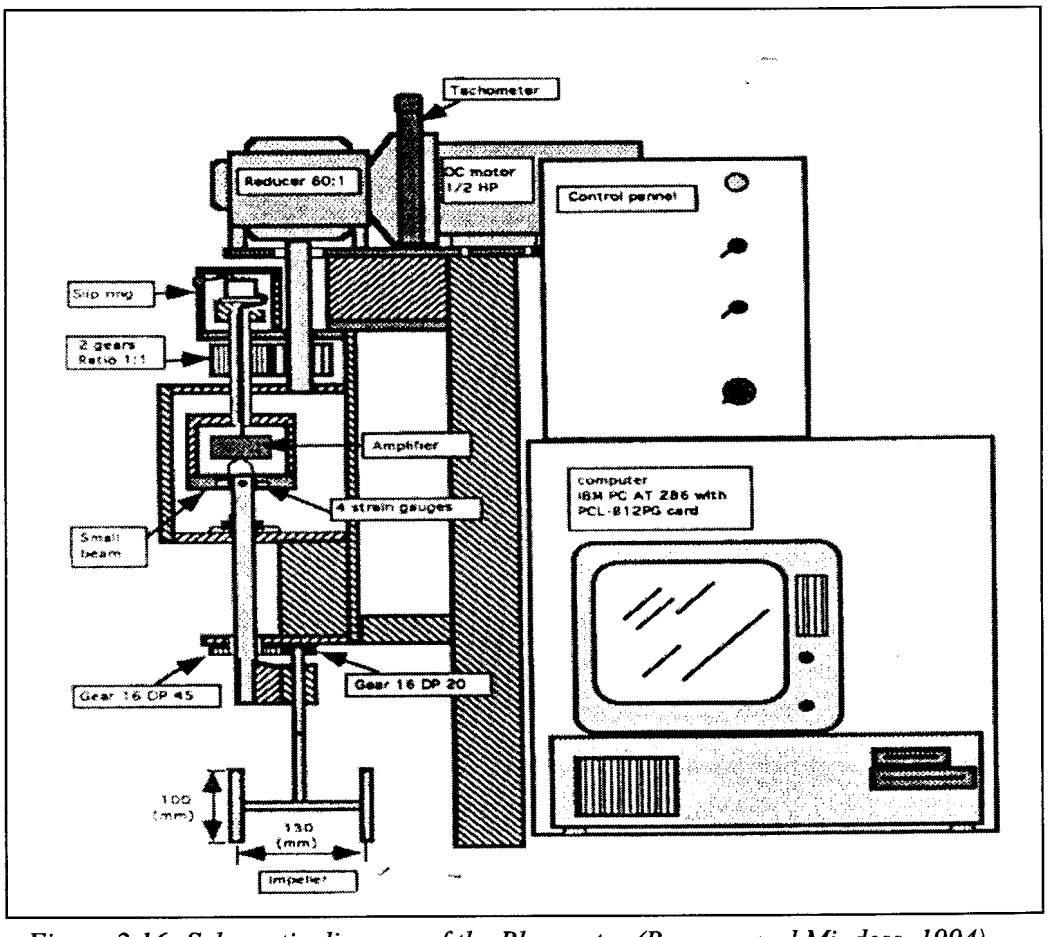

Figure 2.16: Schematic diagram of the Rheometer (Beaupre and Mindess, 1994)

Tests are controlled by a computer program, which can increase or decrease speeds at different intervals. A typical test program is shown in Figure 2.17 and torque measurements from the descending part of the speed-time curve are used to construct Bingham-graphs.

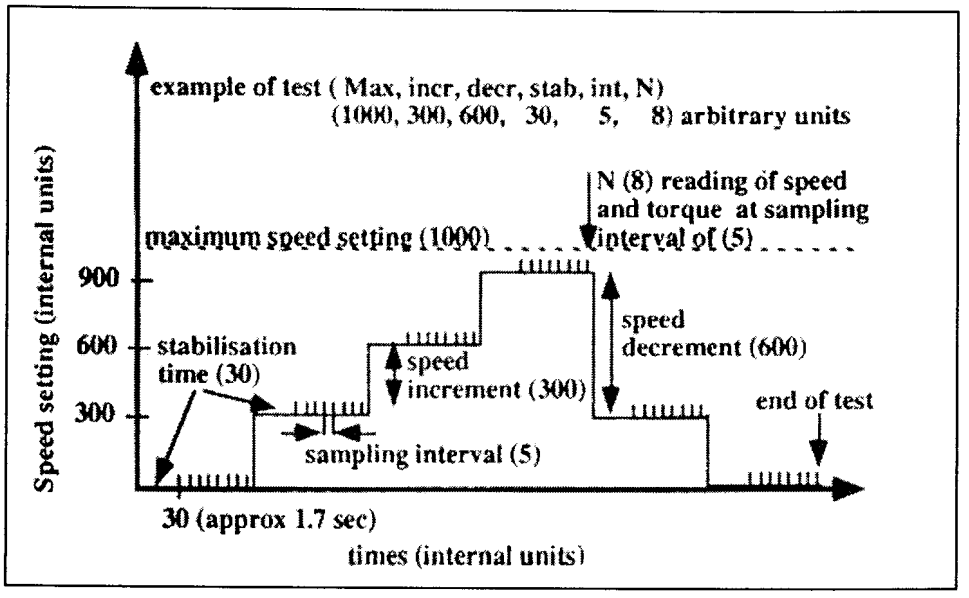

Figure 2.17: Schematic representation of Rheometer test (Beaupre and Mindess, 1994)

Another two-point test method developed earlier was the coaxial-cylinder viscometer, also known as the concentric-cylinders viscometer. The apparatus is shown in Figure 2.18.

The space between the two cylinders is filled with concrete and the outer cylinder then rotated at varying speeds. The torque applied on the inside cylinder to prevent it from also turning due to viscous drag is then measured and the relationship between torque and angular speed is plotted as shown in Figure 2.19.

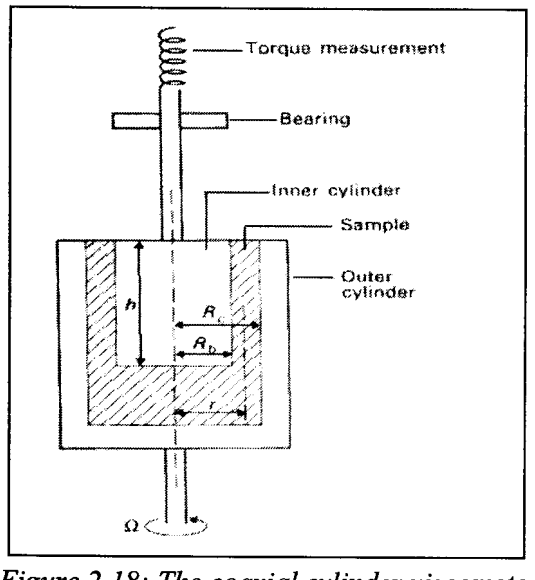

Figure 2.18: The coaxial cylinder viscometer (Tattersall, 1991).

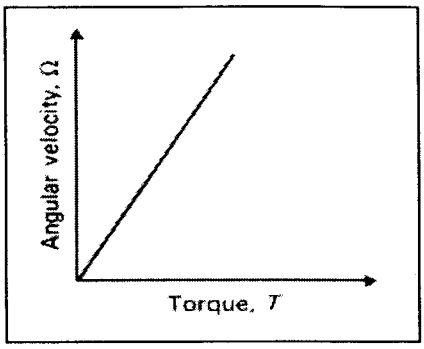

Figure 2.19: Torque-angular velocity relationship for a Newtonian liquid in concentric cylinders (Tattersall, 1991).

The slope of the line is proportional to the fluidity of the concrete and the reciprocal to the viscosity. Tattersall later discarded this test as a measure for his two-point test theory because according to him, a failure plain may develop in the concrete, creating a situation of "free-spin".

Homma et al (1998) devised a new method called the j-shaped flow test for testing highly workable concrete. They claim the method to be a two-point method. The test apparatus is shown in Figure 2.20.

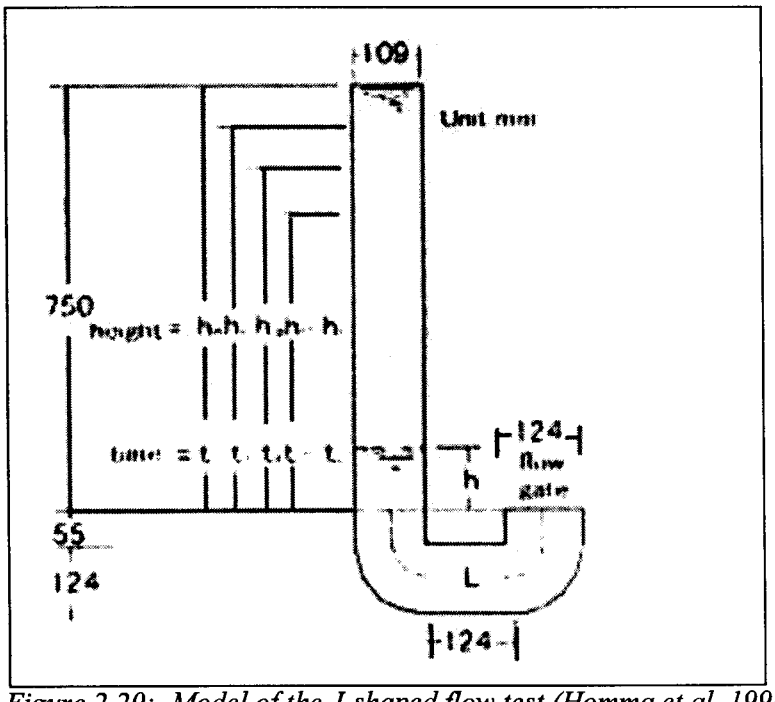

Figure 2.20: Model of the J-shaped flow test (Homma et al, 1998)

Concrete is packed inside the entire tube after closing the lower-end opening. The lower-end gate is then opened and the concrete starts to flow under the influence of differential pressure. The time for every 5 cm of flow is measured and the velocity calculated.

The authors explain that when a driving pressure, ΔP, acts on concrete in a tube and the concrete starts to flow laminary, it can be modeled as shown in Figure 2.21.

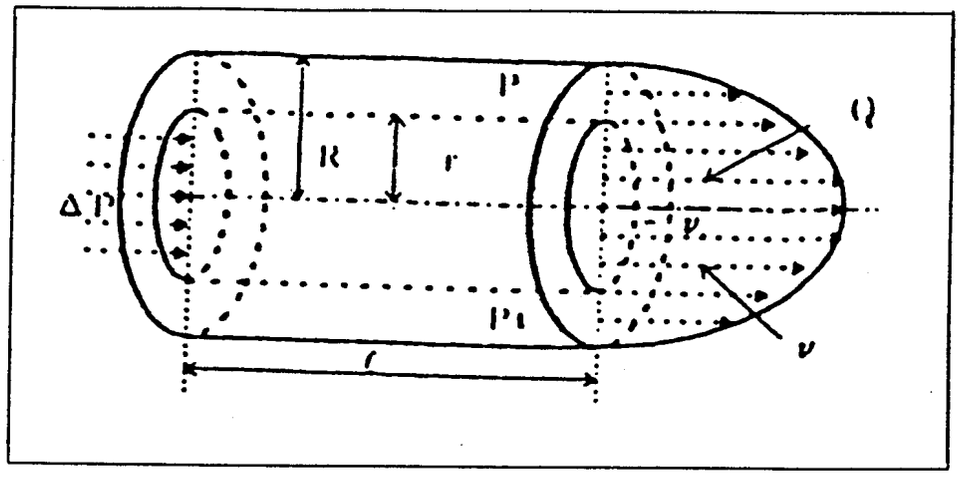

Figure 2.21: Laminar flow under pressure in a tube (Homma et al, 1998).

The flow velocity inside the tube will increase from 0 on the sidewalls to maximum at r = 0 in the center of the tube. In laminar flow the paths of individual particles of fluid do not cross, and so the pattern of flow may be imagined as a number of thin, concentric cylinders which slide over one another like the tubes of a telescope. The difference in velocity between these cylindrical rings is related to viscosity, and thus there are stresses along the interfaces between these layered cylinders so as to appose the relative motion. In laminar flow these stresses are entirely due to viscosity.

The j-tube test used by Homma was based on the principles for capillary viscometers as explained by Govier (1972). Govier explained that in a vertical pipe, the pressure force of the fluid (due to pressure drop) is counterbalanced by the viscous force (force due to wall shear stress).

A simple force balance yields the expression for wall shear stress (τ_w):

$$\tau_w = \frac{D \times \Delta P}{4L} \qquad \text{(Eq. 2.5)}$$

And with the flow velocity (V):

$$V = \frac{4Q}{\pi \times D^2} \qquad \text{(Eq. 2.6)}$$

The rate of shear at the capillary wall may be determined from the general equation of Rabinowitsch (1929) and Mooney (1931), which is

$$S_w = (\frac{1+3n}{4n}) \times \frac{8V}{D} \qquad \text{(Eq. 2.7)}$$

With:

Q = volumetric flow rate

D = inside diameter of capillary

L = effective length of capillary

ΔP = Pressure drop; and

$$n = \frac{\delta \ln \frac{D \times \Delta P}{4L}}{\delta \ln \frac{8V}{D}} \qquad \text{(Eq. 2.8)}$$

Here n is the slope of the logarithmic plot of $\frac{D \times \Delta P}{4L}$ versus $\frac{8V}{D}$. The slope, n, may vary and the applicable value should be used for each value of 8V/D. For Newtonian fluids, $n = 1$.

For a capillary viscometer where laminar flow takes place as a result of pressure drop, the general procedure for calculating shear stress and shear rate is as follows:

1. Calculate τ_w from the flow data obtained by using Equation 2.5
2. Plot τ_w versus $\frac{8V}{D}$ on logarithmic coordinates and determine n as a function of $\frac{8V}{D}$
3. Calculate S_w from Equation 2.7
4. Plot S_w versus τ_w on arithmetic or logarithmic coordinates as preferred, and
5. If desired, to fit an appropriate one of the constitutive equations to the data.

The last point would be applied for estimation of the plastic viscosity and yield stress from the slope and y-intercept of the graph respectively. Yield stress can also be calculated using equation 2.5 for the end height of the paste in the tube. As the height of the concrete in the tube reduces, the applied shear stress at the tube wall also reduces. With proper equipment it is thus possible to measure the height and consequently the shear stress as well as the resulting flow rate, thus rate of shear, at relative small time intervals like tenths of seconds.

Tattersall (1981) warned against using capillary flow tests as tools for measuring concrete workability because according to him a thin layer containing only paste will form on the tube wall thus creating an inconsistent shear environment throughout the diameter of the tube.

Hopkins and Cabrera (1994) have previously shown the importance of stress level when taking workability measurements. These authors illustrated the importance of taking workability measurements at at least two stress levels (two-point test) as can be seen from the plots in Figure 2.22. They explained that different results might be obtained from different single point tests at different stress levels.

Using the slump test (low stress level) concrete C proved to be the most workable, then B and lastly A. If a Vebe-test was performed at a higher shear stress level, different results might have been obtained. If the concrete were to be pumped (application at high stress level), concrete B would have proved to be the most workable and concrete C the least. It would thus have been foolish to decide on the most workable concrete for pumping using the slump test.

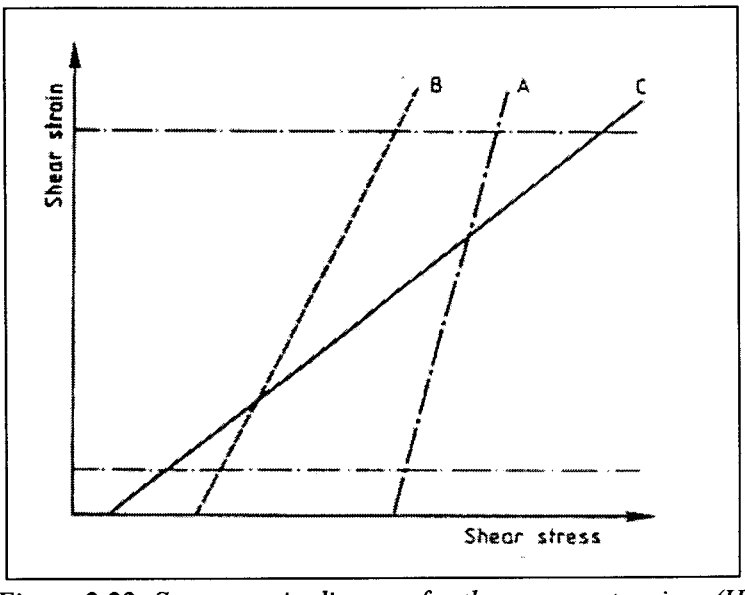

Figure 2.22: Stress-strain diagram for three concrete mixes (Hopkins & Cabrera, 1994).

The authors concluded that for a chosen mix where water is the only factor influencing workability, the slump test is adequate. Tattersall (1991) also explained that in mixes where workability is only a function of the water content, there exists a linear correlation between the yield value and plastic viscosity. Thus a relative measure of the one will also give a good indication of the other and therefore a one-point test that relates to one of these parameters would be appropriate. On the other hand he also explained that if a linear relationship is obtained between yield value and plastic viscosity at different water contents, then only the water content has an influence on workability. When the effects of other admixtures like water reducers were to be assessed, a much more rigorous test should be performed, like one of Tattersal`s two-point tests.

Other researchers such as Osbeak (1986) have obtained different results for the workability of the same mixes when different tests like slump or Vebe-time were used as assessment criteria. Morat et al (1993) showed that workability measurements done according to the flow table method only give accurate results when mortars with relatively high water contents are assessed. Their work will be reviewed in more detail later on.

Ferraris and de Larrard (1998) modified the standard slump test into a two-point test by introducing rate of slump. The authors described that there is a relationship between rate of slump and viscosity as well as between final slump and yield stress of fresh concrete. They however explained that the test is limited to concrete with a slump value of between 120 and 260mm. The rate must be measured between the initial slump (height of slump cone) and partial slump (intermediate to the final slump). The difference in height should not be too small, because this would lead to very small slump times and thus poor relative precision of measurement. A partial slump that is too large will rule out all concretes with a low final slump. A Partial slump height of 100m was chosen.

The standard slump base was modified by attaching a 350mm rod to the center of the base perpendicular to the base surface. A plate with a center hole fitting over the rod was designed so that it can slide along the rod on top of the slumping concrete to the level of the partial slump height, where a stopper terminates its movement. This partial slump time was measured by means of a stopwatch and the average slump rate could thus be calculated. The apparatus is shown in Figure 2.23 and the test procedure illustrated in Figure 2.24.

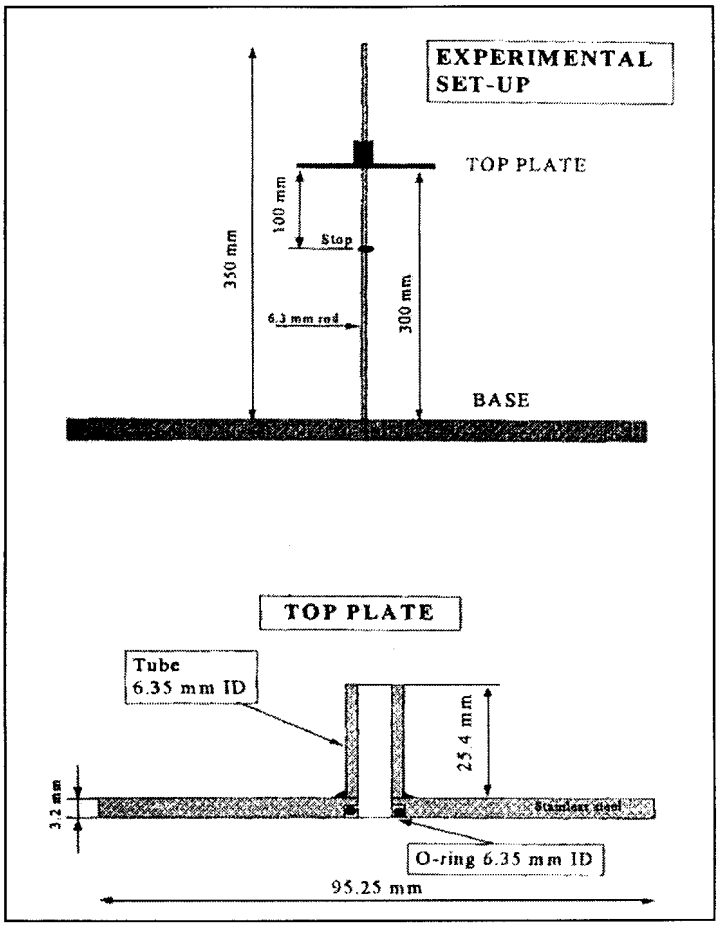

Figure 2.23: Rod and top plate in the modified slump apparatus (Ferraris and de Larrard, 1998)

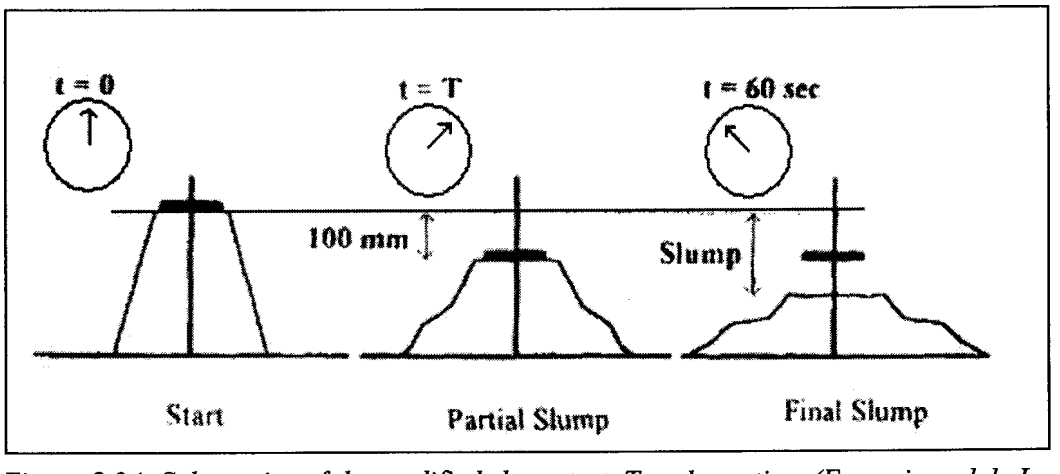

Figure 2.24: Schematics of the modified slump test. T = slump time (Ferraris and de Larrard, 1998)

After some tests the authors concluded that the modified slump tests and model presented allows an evaluation of the plastic viscosities of concretes but the test is most likely to be used as a quality control procedure in the field as it is less accurate than other workability mixer-measurement apparatuses like the BTRHEOM Rheometer (de Larrard et al, 1997) which in turn is more suitable for laboratory experiments.

2.4 The influence of particle properties on the flow of fresh mortar and concrete

Sakai et al (1997) investigated the fluidity of cement paste with various types of inorganic powders. Their work highlighted the influence of particle size, shape and packing density on fluidity. Others before them (Okamura and Ozawa, 1994) already reported results of such tests by blending inorganic powders into concrete mixes. They found that the fluidity and segregation-properties of flowing concrete could be improved and the dosage of water reducing agents reduced compared to concrete of the same fluidity without inorganic powders.

Sakai and his co-workers investigated the effect of shape of inorganic powders on the fluidity of cement paste containing superplastisizers according to the following test:
Two types of fused silica were prepared, spherical (PSS) and crushed (PCS), and these powders were substituted into a cement mortar at various percentages (between 10% and 40%) by weight.

Water to powder ratio of 0.9 was used and kept constant for all PSS and PCS replacements. A policarxylate-type water reducing agent was added at 1.6% by powder weight. Above this dosage all mixtures showed the same flow values. Grading analyses were performed on the three different materials, cement and the two types of fused silicas, by means of laser-type light scattering method and results are shown in Figure 2.25.

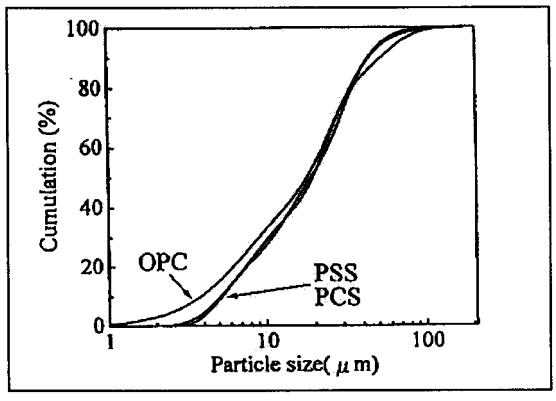

Figure 2.25: Particle size distribution (Sakai et al, 1997).

Apparent viscosity (u) measurements were performed on the different mortars, using a rotating cylinder viscometer at 20°C, the fluidity of the paste was taken proportional to 1/μ. Results are shown in Figure 2.26.

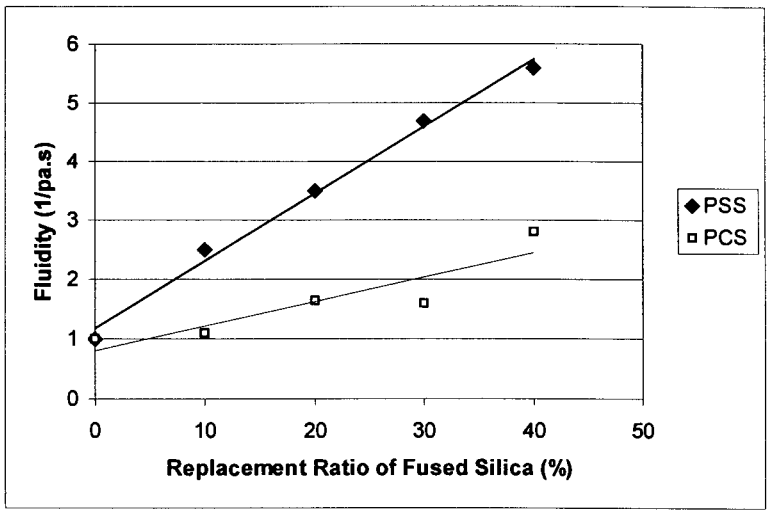

Figure 2.26: The fluidity of pastes with PCS and PSS (Sakai et al, 1997)

From Figure 2.26 we can see that fluidity first increased linearly with increased replacement and secondly that fluidity is the highest with the spherical PSS-replaced pastes. Figure 2.27 shows the effect that the replacement ratio of PSS to PCS in fused silica has on flow at 40% cement replacement by the fused silica.

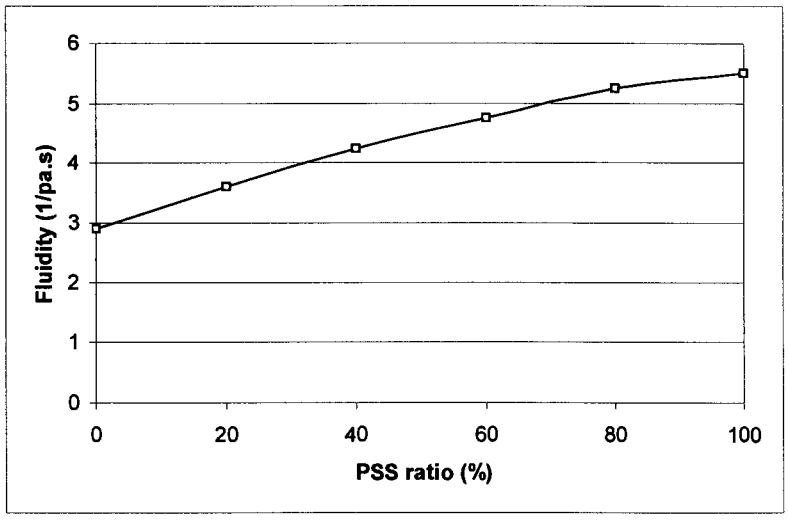

Figure 2.27: Influence of PSS to PCS ratio (%) on the fluidity of the paste (Sakai et al, 1997)

Here we can see that the higher the percentage of spherical PSS in the fused silica, the higher the flow. The packing densities of the different pastes were determined by centrifuging (600rpm, 10min) powder-slurries, made from the individual mixtures, to separate supernatant water. Thereafter the powder-cake height was measured and the height-ratio of powder cake-to-powder slurry (height before/height after) given as the relative packing density in %. Results are shown in Figure 2.28.

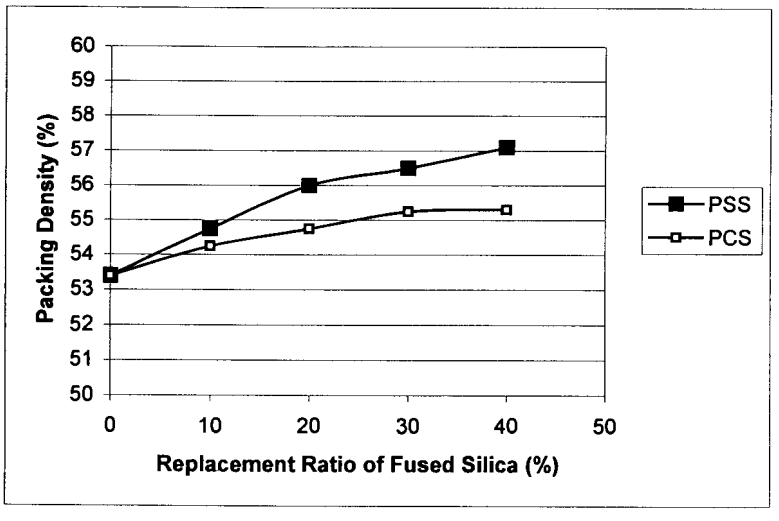

Figure 2.28: Packing density of paste with PCS or PSS (Sakai et al, 1997)

It was found that the packing density of the spherical PSS-containing mixture was higher than that of the irregular shaped PCS. The authors explained that the higher the packing density, the less residual water is entrapped between particles and the more free water is available for lubrication. This effect is illustrated in Figure 2.29.

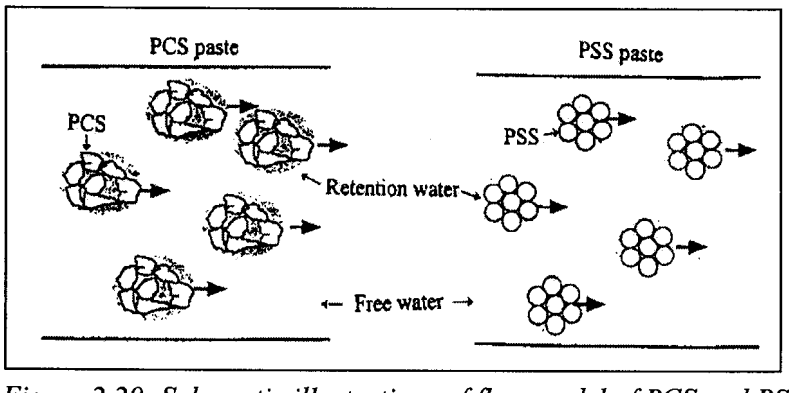

Figure 2.29: Schematic illustrations of flow model of PCS and PSS (Sakai et al, 1997).

Another paste-sample (AWP) was prepared by adding the difference in amount of free water between PSS and PCS to PCS. The fluidity of this paste was measured and compared to those values obtained for PSS and PCS-paste samples. Comparative results are shown in Figure 2.30.

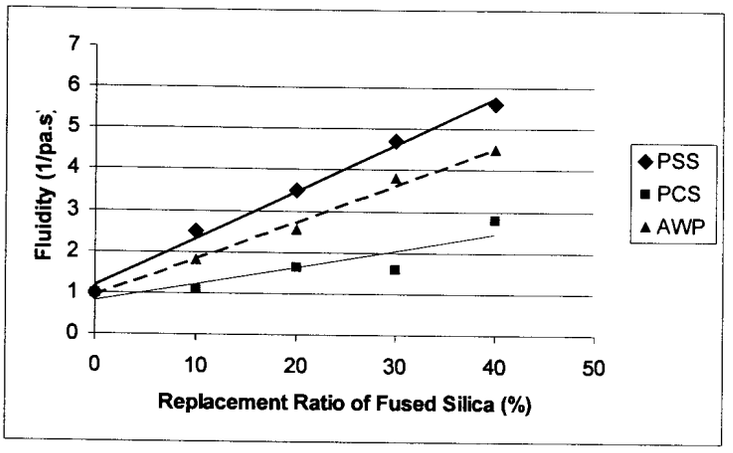

Figure 2.30: Fluidity of pastes containing PSS, PCS and AWP (Sakai et al, 1997).

The authors explain that the difference in fluidity between PCS and AWP-pastes results from the differences in packing and the difference in fluidity of paste with PSS and AWP paste may be contributed to the ball bearing effect as contributed by the round PSS particles.

Another series of flow tests was conducted, this time replacing part of the cement by different inorganic powders. Prepared granulated blast furnace slag, (PBFS), prepared limestone (PLS), prepared fly ash (PFA), PCS and PSS were used and the authors explained that the effect of particle size distribution of powders on the fluidity of paste can be neglected because powders were prepared having the same particle size distribution as the cement. Preparation was done by air separation-method. Table 2.2 shows the chemical composition of the powders and Table 2.3 the packing bulk density and sphericity factor (packing bulk density/specific gravity) of the inorganic powders as well as the fluidity of cement paste prepared by addition of these inorganic powders. The replacement ratio of inorganic powders was 40% and the water/solid ratio 0.9 by volume. 1.6% AE high range water reducing agent was added.

Table 2.2: Chemical composition of inorganic powders (Sakai et al, 1997).

Sample	LOI	SiO_2	Al_2O_3	Fe_2O_3	CaO	MgO	Na_2O	K_2O	Total C
PBSF	0.2	34.5	14.0	0.5	41.0	6.8	0.22	0.29	-
PLS	43.2	0.7	0.2	0.1	55.2	0.4	0	0	-
PFA	1.1	63.4	17.4	4.8	4.3	1.5	0.71	0.8	0.54

Table 2.3: Four inorganic powders and their shape factor (Sakai et al, 1997).

Sample	Specific Gravity	Packing Bulk Density	Sphericity Factor	Fluidity (1/Pa.s)
OPC	3.17	1.639	0.520	1.1
PBSF	2.70	1.563	0.539	2.1
PLS	2.71	1.604	0.592	3.5
PFA	2.32	1.282	0.553	2.6
PCS	2.22	1.282	0.578	2.8
PSS	2.22	1.465	0.660	5.2

It was observed that the sphericity factor positively influenced the fluidity of the pastes. The higher the factor, the higher the content of spherical particles. The authors explained that the presence of unburned carbon in PFA decreased its sphericity factor to below that of PLS and PCS. It was reported by Lea (1996) that the content of irregular shaped carbon in PFA has a negative influence on the fluidity of the paste containing that PFA.

Lastly the influence of particle size distribution were examined. Figure 2.31 shows the particle size distributions of classified limestone powders, which were prepared by hydraulic elutriation to a Blain specific surface area of 440m^2/kg and specific gravity of 2.71. The replacement ratio of limestone powder was 20% by weight and the water to solid ratio again 0.9 by volume. 1.6% High range water reducing agent by weight of powder (cement + limestone) was added. Results of fluidity tests are shown in Figure 2.32.

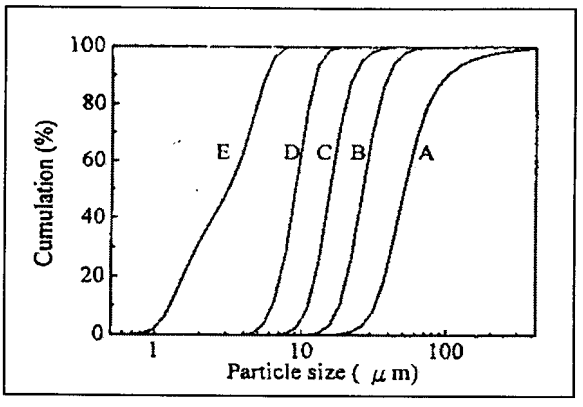

Figure 2.31: Particle size distribution of classified LS (Sakai et al, 1997).

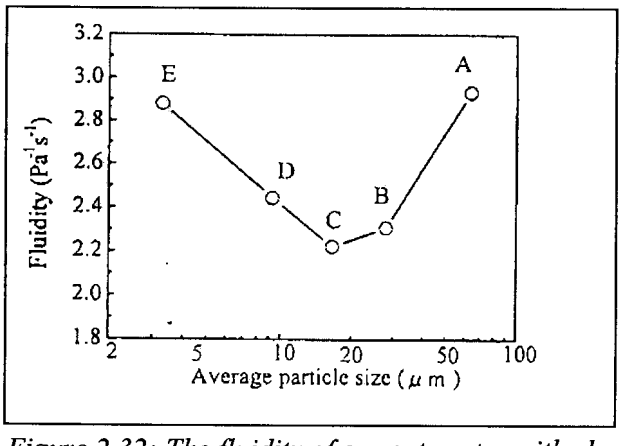

Figure 2.32: The fluidity of cement pastes with classified LS (Sakai et al, 1997).

The average size of the portland cement particles was measured as 18μm. From Figure 2.32 we can see that the fluidity of cement pastes with samples B and C (having average particle size similar to that of the portland cement) were lower than that of cement paste with coarser and finer classified limestone powders (sample A and E).

Figure 2.33 shows the packing density of pastes with classified limestone powders.

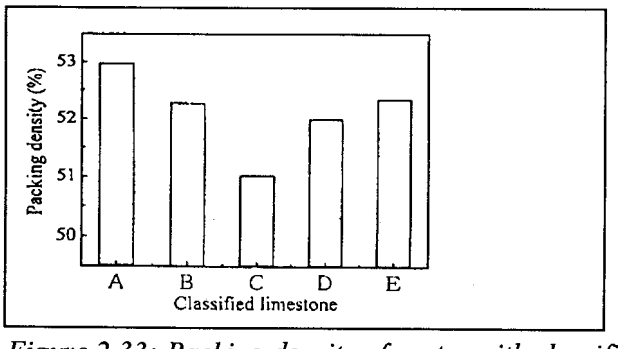

Figure 2.33: Packing density of pastes with classified LS (Sakai et al, 1997).

The packing density of pastes A and E were larger than that of the others, therefore as earlier reported by the authors, resulting in higher fluidity.

The authors thus concluded the following from their tests:

- The shape and particle size distribution of inorganic powders has an influence on the fluidity of cement paste containing these powders. They showed that particles of powders having similar average particle sizes as the cement used result in lower packing density and lower workability. The higher the sphericity of these powders, the higher the fluidity.
- The higher the packing density of a paste, the more free water is available and the higher the fluidity. By incorporating inorganic powders, the particle size distribution of the materials and thus packing density of the paste can be optimized.
- The effects of the shape of inorganic powders on fluidity of cement paste can be related to the packing as well as the ball bearing effect of round spheres.

The results on workability were based on the plastic viscosity measurements alone. It might have been interesting to have seen the effects on the yield value as a relative high water to powder ratio was used. According to Banfill (1994) mixes containing microsilica does indeed tend to result in lower viscosity, but also increased yield value. Thus the mix may "look stiffer" (than the reference containing cement alone) but once shear stress is applied, workability will be better than the reference. Accordingly, if a water reducer or plastisizer is added, the yield value will tend to decrease but the plastic viscosity remain unchanged. Fly ash may cause the mix to show decreases in both yield value as well as plastic viscosity.

A point worth mentioning regarding the final part of the test is the influence of residual carbon within the inorganic powders. The question remains whether the carbon has a physical or a chemical effect on the water demand. Carbon associated with fly ash is irregular in shape due to the combustion-process; therefore it will also have a relatively large surface area. Chemically, carbon repels water and resists being "wetted". Further scope for research is to determine whether more spherical carbon particles in fly ash will have the same effect on water demand than the more irregular "Swiss cheese"-shaped particles.

According to Morat et al, (1993) the ASTM–method (ASTM C-109) of measuring the water requirements of fly ash in slurry containing cement using the flow table is a significant source of errors. According to this method the percentage of water reduction in a fly ash replacing mortar for yielding the same flow as a control mortar without substitution is determined. In their paper a

new simpler method is presented and the effect of fly ash particle distribution on workability of mortars is assessed.

Mixes were made containing 450g P-450 (II – F/35A type) Portland cement (Valenciana de Cementos), 1350g sand (FM=3.56), different water contents (150, 175, 200, 208, 216 and 225 ml) for controlling flow and replacing part of the cement by fly ash (replacement by % weight: 15, 30, 45 and 60%).

Initial fly ash (TO) was separated into four sized fraction samples (T1, T2, T3 and T4), T1 being the coarsest and T4 the finest, using a horizontal air current into an aerodynamic tunnel. Granulomeric data is given in Table 2.4. Particle size distribution was measured using a Sympatec Helos Analyzer. The authors stated that surface area values were calculated however no mathematical reference was given.

Table 2.4: Granulometric data for original (T0) fly ash and sized fractions (T1-T4) (Morat et al, 1993).

Fly Ash	**Percentages of particles with diameter greater than**			**Mean Diameter (μm)**	**Specific Surface (cm^2/g)**
	10μm	**45μm**	**90μm**		
T0	60	20	6	26.8	2841
T1	74	45	20	53.6	1940
T2	71	25	5	30.6	2257
T3	62	6	0	18.1	2782
T4	48	0	0	11.2	3574

Flow table tests were performed to measure workability by placing mortar in a conical mould, centered on the flow table. The mortar was compacted in two layers with a wooden tamper (10 times). Afterwards the mould was removed and the table dropped 15 times (one drop per second). Flow table spreads were given as a mean-value of maximum and minimum diameters of the spread cone. Flow table spreads for T0 – T4 are shown in Table 2.5 and Figures 2.34 and 2.35 (for T0).

Table 2.5: Flow table spread (FTS) values (mm) for control mortars and test T0 fly ash replacing mortars (Morat et al, 1993).

Water (ml)	**150**	**175**	**200**	**208**	**216**	**225**
% Fly Ash						
0	102	101	110	117	123	128
15	106	105	112	117	128	133
30	105	107	118	124	131	147
45	106	112	121	129	139	155
60	108	112	129	142	147	170

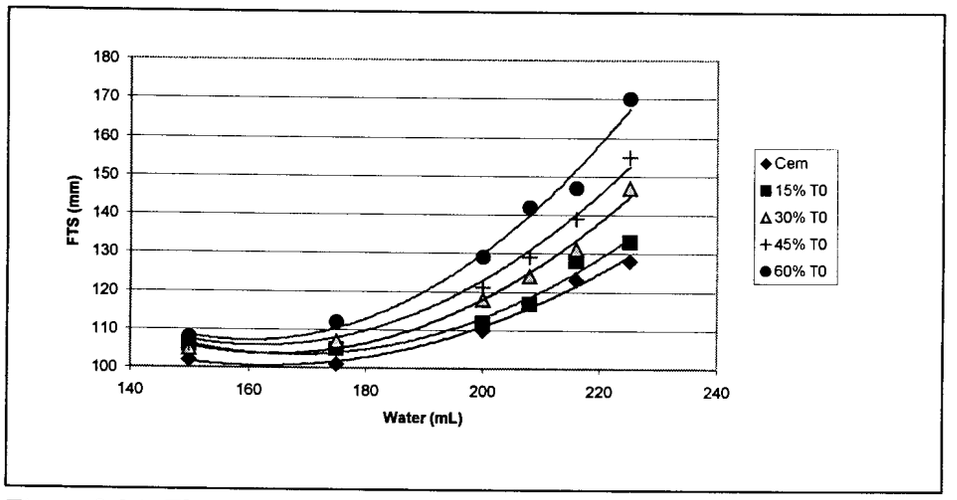

Figure 2.34: Flow table spread values for 0-60% T0 fly ash replacements (Morat et al, 1993).

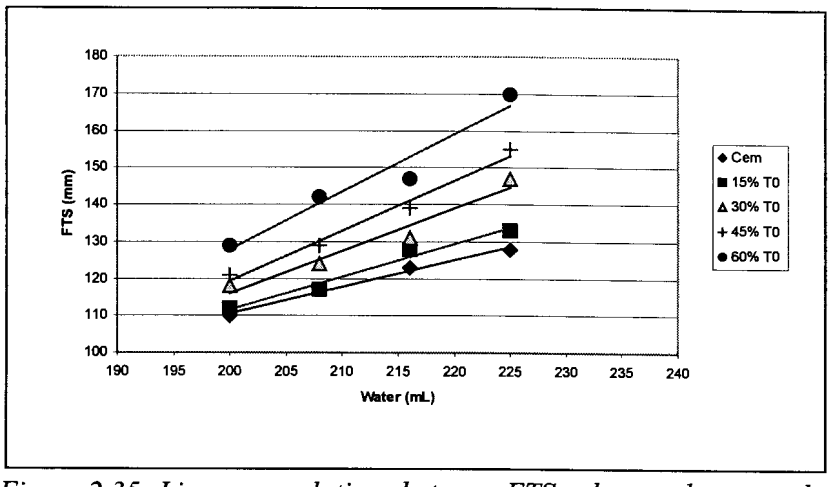

Figure 2.35: Linear correlations between FTS values and water volumes (Morat et al, 1993).

Results proved that increase in spread to be higher for higher water contents in the 216-225 ml range. Increase-rates were also linear only in this range, and it was therefore concluded that the FTS-values of the mortar include crucial errors and do not permit optimum precision for lower water contents, especially in the 150-175 ml range. Greater water contents in mortar imply higher spreads and error measurements become less important. From Figure 2.35, it proved evident that FTS values increased with increased fly ash replacement at constant water content, and that this increase was linear in the 200-225 ml water addition range.

Flow tests were performed on the other fly ash fractions in the 200-225 ml range and results of T1 and T4 are shown in Figure 2.36 and Figure 2.37 respectively with Figure 2.38 showing comparative plots of T0 – T4 at 30% replacement and Figure 2.39 at 225 ml water content.

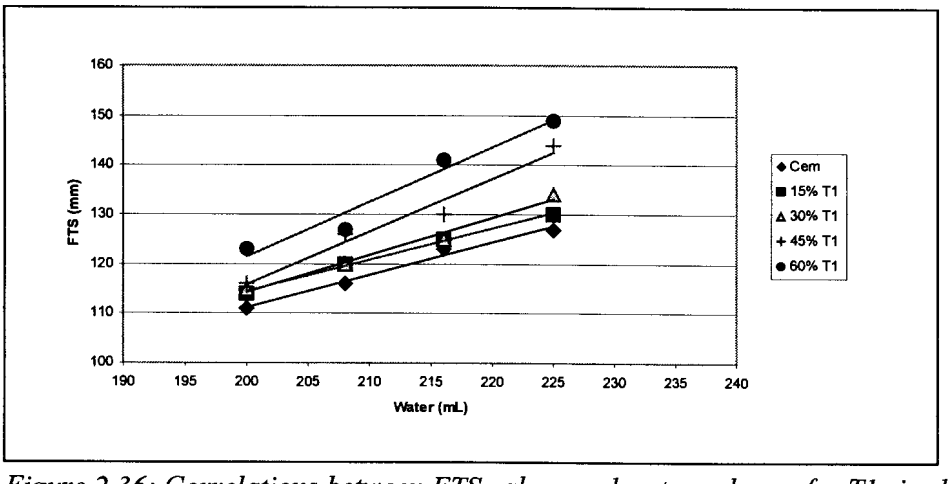

Figure 2.36: Correlations between FTS values and water volumes for T1 sized fly ash (Morat et al, 1993).

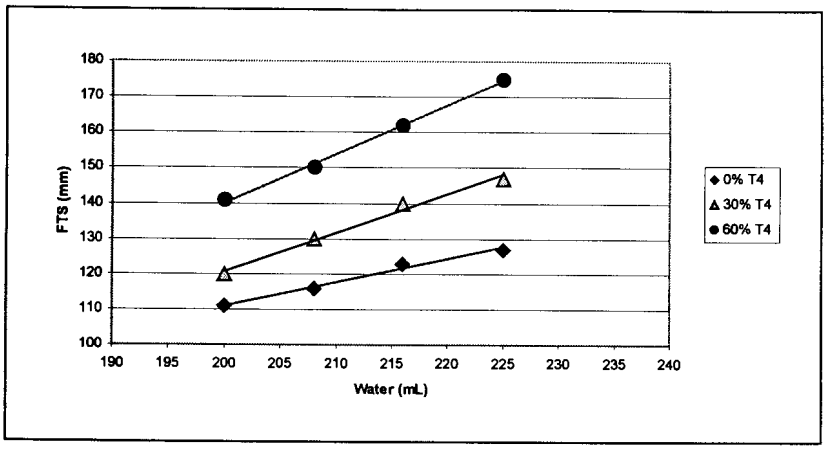

Figure 2.37: Correlations between FTS values and water volumes for T4 sized fly ash (Morat et al, 1993).

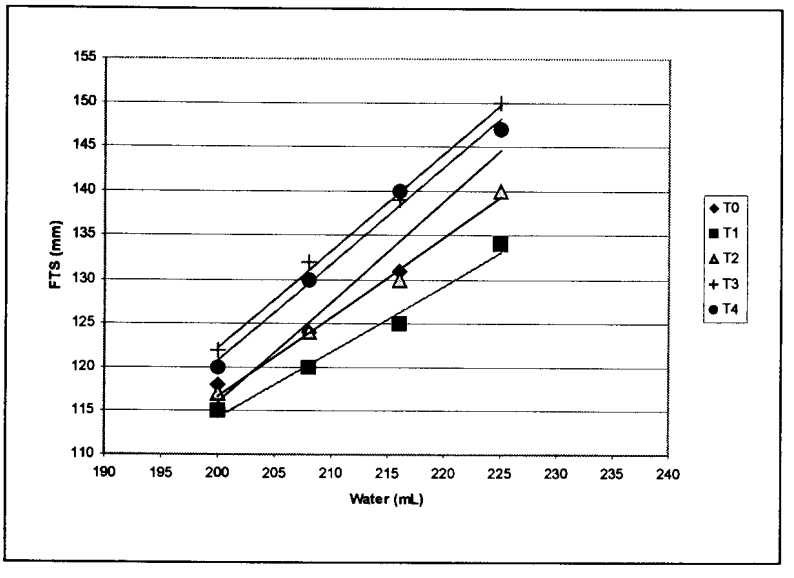

Figure 2.38: Correlation between FTS values for all sized fraction in 30% fly ash replacing mortars (Morat et al, 1993).

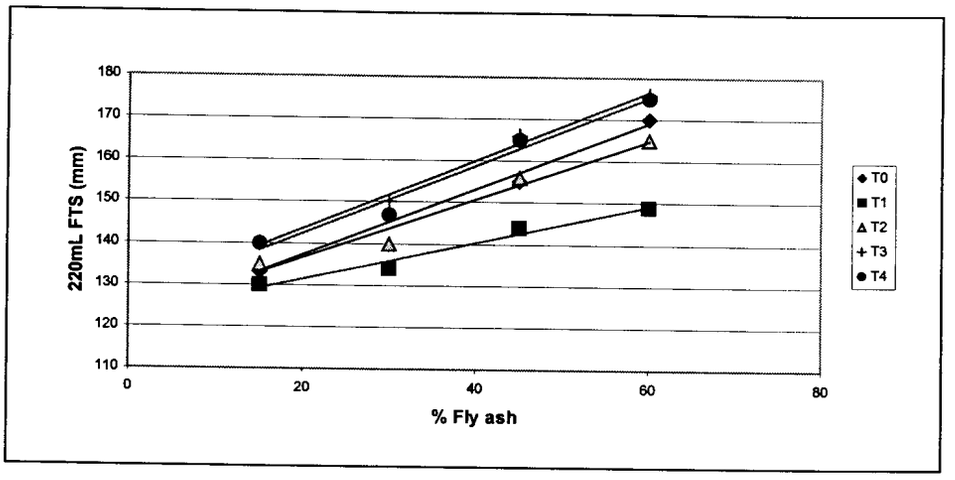

Figure 2.39: Correlation between FTS values for mortars with 225ml water and the replaced percentage of cement (Morat et al, 1993).

Results from T1 and T4 showed the same linear trend than T0. It was also evident that flow increased with increased finess of the fly ash. It seemed that the lubricant effect of fly ash depended on the number of particles per unit mass, with fine fly ash having more particles. However, spreads of T3 and T4 were very similar, indicating that the lubricant effect of the round and smooth surfaces is counteracted by water adsorption onto the surfaces of the fine fly ash particles, however the overall particle size distribution may also have accounted for this.

Lastly particle diameter and calculated surface area were plotted against FTS at 225-ml water addition (Figures. 2.40 and 2.41).

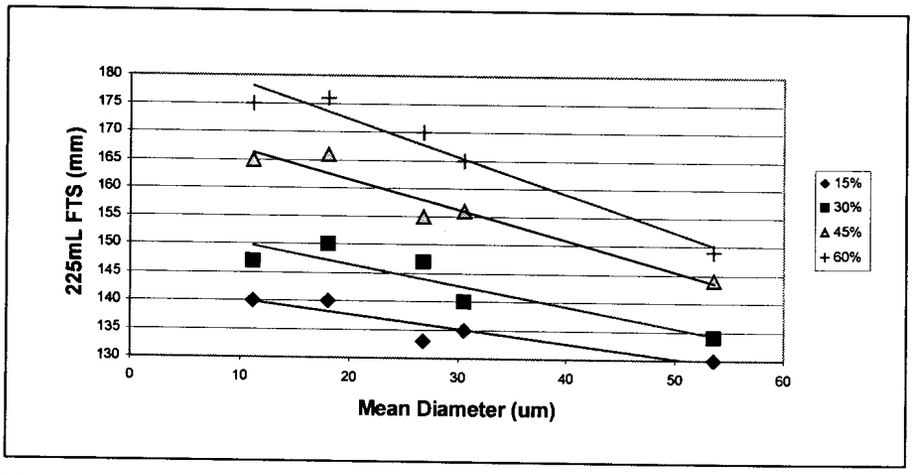

Figure 2.40: The effect of the mean diameter of the fly ash on 225ml – FTS values (Morat et al, 1993).

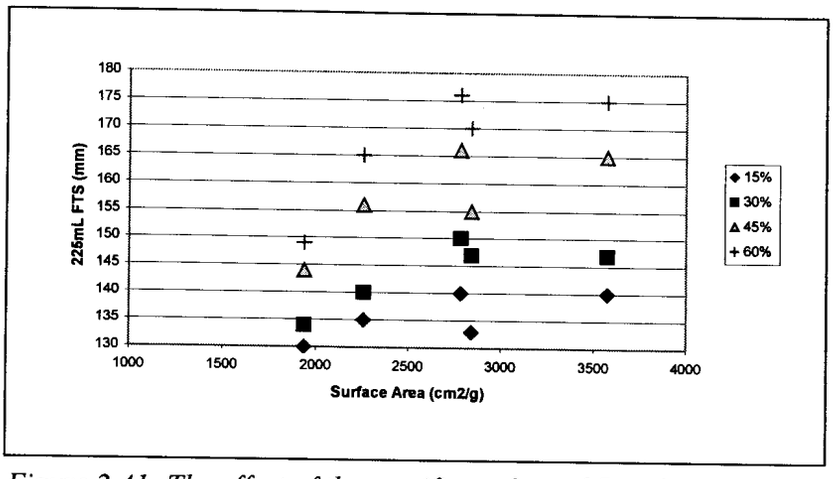

Figure 2.41: The effect of the specific surface of fly ash on the 225ml – FTS samples (Morat et al, 1993).

Figure 2.40 shows the expected trend with flow decreasing linearly with increasing particle diameter and also increasing with increasing % replacement. The trend for the surface area/flow plot in Figure 4.41 is only followed for T1, 2 and 3. It might be that the LOI of the untreated T0 was higher than the treated samples, resulting in a reduction in flow.

The flow table test was originally designed for highly workable mixes where slump measurements would have proved to be inadequate due to collapsing. The "inaccurate range" pointed out by the authors is between water cement ratios of 0.33 and 0.44. This may be an example where the workability range of a test program fell in more than one "one-point testing method" category. However it may also be that the flow values for these specific mixtures only increased linearly with water content from a minimum water content value due to other factors. One possible explanation is that flow increase is linear only once complete or a minimum level of dispersion of particles had taken place.

As described earlier, cement/fly ash mortar is believed to be a Bingham fluid and its workability can be expressed as a function of two properties, namely yield value and plastic viscosity. The flow table as well as the slump test has been reported as good indicators of the yield value but not necessarily of the plastic viscosity. The authors stressed that a better and more comparative idea of the flow changes can be observed at higher water contents, using the flow table. Another solution is maybe to measure the workability in terms of viscosity using a different method.

The authors did not provide references on how the specific surface area was calculated. For the purpose of this dissertation surface areas were calculated from the data given by a derived mathematical equation using the volumes and surface areas of spheres as well as the density of the fly ash. The same equation was also previously derived by (Hopkins, 1983) as well as Iyer and Stanmore (1995) and reads:

$$S = \frac{6}{\rho \times d_{ave}} \qquad \text{(Eq. 2.9)}$$

Where:

S = Surface area

ρ = Density of the fly ash

d_{ave} = Average diameter of particles

It should be noted that the surface area is not a linear function of the diameter but a hyperbolic one. If a typical density of 2.2 is used for fly ash, the equation derives to:

$$S = \frac{2.73}{d_{ave}} \qquad \text{(Eq. 2.10)}$$

This is in the hyperbolic form of $y = \frac{1}{x}$ which is illustrated in Figure 2.42 where sphere diameter is plotted against surface area. This may justify the author's claim for the similarity in flow observed for T3 and T4 as T4 had the highest surface area of all the fly ashes used.

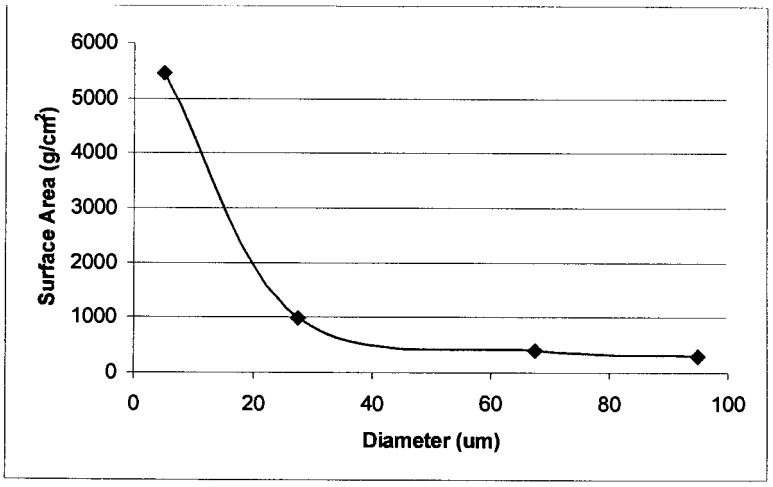

Figure 2.42: Influence of sphere diameter on surface area.

Values for surface area were calculated from the size distribution values given in Table 2.4. Values halfway between given sieve sizes were chosen (5um, 27.5um, 67.5um and 95um) and the fraction of each chosen size of the total sample calculated assuming that the distribution between the given sieve sizes (10um, 45um, 90um) is linear. These chosen diameter sizes was thus taken as the average sizes between given sieve sizes. The surface area for every size was then calculated and multiplied by its fraction of the total sample and these values were added to get the total surface area for each sample. Values are given in Table 2.6. A relatively good correlation was obtained between calculated and published surface areas as can be seen from the calculated/measured ratio, ranging from 0.92 – 0.95.

Table 2.6: Surface area values.

Sample	Calculated Specific Surface (g/cm^2)	Published Specific Surface (g/cm^2)	Calculated / Published
T1	1864	1940	0.96
T2	2133	2257	0.95
T0	2652	2841	0.93
T3	2652	2782	0.95
T4	3312	3574	0.92

The reason sample T0 gave a lower workability than expected (Figure 2.41) may be because of residual carbon present in the original sample. Because of density differences between fly ash and carbon particles, the carbon might have been removed from the fly ash while it was treated in the

aerodynamic tunnel. According to previous researchers such as Lea (Lea, 1980), carbon particles may cause an increase in water demand of cement/fly ash mortars. Another reason may be the combined grading of the cement and fly ash. However no information was given on the grading of the cement used.

Surface area is a significant property because the water demand for dense slurries containing cement or fly ash is believe to be affected by the surface area of the solid particles. The Blaine method has been mostly used to determine surface area values for powders.

With the Blaine-method, a fixed volume of solid is packed into a cylinder and a flow of air passed through the bed. If the flow is laminar, the pressure drop through the bed generated by the skin friction is proportional to the surface area. Thus, the time taken for a fixed volume of air to pass through the bed is recorded, using a manometer to record pressure. By modifying the Kozeny-Karman relationship, the surface area can be calculated using the following equation:

$$S_w = \frac{k(\varepsilon \times \rho_f \times t)^{0.5}}{(1-\varepsilon)\rho \times \mu^{0.5}} \qquad \text{(Eq. 2.11)}$$

Where:

S_w = Surface area = (m^2/kg)

k = Apparatus constant

ε = Bed porosity = 0.51

ρ_f = Density of manometer fluid (kg/m^3)

t = Elapsed time (seconds)

ρ = True density of solid (kg/m^3)

μ = Viscosity of air = 1.825E-0.05 (Pa.s)

Visvanathan (1993) claimed that the Blaine method is only an indirect measuring method, which suffers from a number of weaknesses, including variable particle shape and bed porosity.
When calculating the mass (m) of material to make up the fixed volume, the bed porosity, μ, is taken as 0.51 so that:

$$m = \rho \times V(1-\mu) \qquad \text{(Eq. 2.12)}$$

Iyer and Stanmore (1995) performed tests on two samples of Queensland fly ashes (Curragh and Tarong). They measured the surface areas, firstly using Blaine measurements and secondly by calculation if the average particle diameter is known (see Table 2.7). The particle size diameter was measured by laser diffraction, using the Malvern 2600 apparatus. In the table, a size parameter, $D_{23,}$ is referred to however the authors did not clearly define this. It is unlikely for these values to be the average diameters as they are relatively small. They used the same formula as derived earlier for calculating surface area from diameter if it is assumed that the fly ash is perfect spheres (Eq. 2.10).

Table 2.7: Fly ash slurries flow and surface area (Iyer and Stanmore, 1995).

Ash	Density (kg/m^3)	Air Flow Time (s)	D_{23} (μm)*	Blaine Area (m^2/kg)	Malvern Area (m^2/kg)
Curragh	2290	96	7.9	324	330
Tarong	2110	70	18.4	301	155

* No reference given by the authors.

When measuring the Tarong Blaine surface area, only 75% of the calculated mass (5.07g) could be fitted into the cylinder, as the porosity of the material was greater than 0.51 and the test was therefore carried out with the limited amount filling the cylinder. The staff from the Tarong power station reported that the ash was very cohesive and difficult to handle. As we can see from Table 2.7, measured (Blaine) and calculated (Malvern) surface areas correlated well for the Curragh-ash, which had a relatively small average diameter. For the Tarong-ash, the two areas differed substantially, indicating that the porosity of the bed could not be brought down to 0.51.

The authors concluded firstly that the Blaine and laser diffraction (Malvern) techniques agree well for well-behaved powders. Secondly the operating procedure for the Blaine apparatus needs to be modified to handle cohesive powders, and lastly they concluded that the laser diffraction method should be recommended.

The authors distinguished between two methods, the Blaine-method, which is an indirect way of measurement and a more direct method by measuring particle diameters and mathematically calculating the surface area. The advantage of the latter mentioned method is that it is a more direct method of measuring surface areas. It is however assumed that all particles are spherical in shape, which may not always be the case. Their observation of agglomeration together with the relative low value for the Tarong measured-Blaine confirms the principle of "shape factor", as

defined by Hopkins (1984). According to Hopkins, agglomeration of particles results in a decrease in the measured Blaine-value in comparison to the calculated (Malvern) surface area. Hopkins' work will be discussed in more detail later.

As explained earlier the average diameter cannot be used to calculate surface area due to the non-linear relationship between particle diameter and contribution to total surface area. It has been shown that smaller particles contribute much more to total surface area than larger ones.

Grzeszczyk and Lipowski (1997) performed tests to establish the effect of particle size distribution of high-calcium fly ash on the rheological properties of cement pastes. Their interest was sparked from previous tests performed by Costa and Massazza (1986). These workers reported that the spherical shape of fly ash as well as the presence of glassy phase on the fly ash surface significantly improve the structure of paste by effective densification, and therefore the water content can be reduced while consistency (fluidity) remain constant. The reverse effect however is also possible through dedensification because the density of fly ash is lower than that of cement, thus at higher fly ash contents, the workability may decrease.

The portland cement was produced in the laboratory by intergrinding of clinker and gypsum (5% by weight) to a specific surface of 328 m^2/kg. The chemical composition of powders used is given in Table 2.8.

Table 2.8: Chemical composition of clinker and fly ash (Grzeszczyk and Lipowski, 1997).

Component	Clinker	Fly Ash
	% By weight	
LOI	0.8	1.9
SiO_2	22.7	30.0
Fe_2O_3	3.0	6.0
Al_2O_3	4.6	18.0
CaO	66.5	30.1
MgO	1.4	2.1
SO_3	0.6	10.8
Na_2O	0.2	0.2
K_2O	0.7	0.2
CaO free	0.8	3.0

Furthermore the original fly ash (FA-0) was ground for 7 minutes (FA-1), 15 minutes (FA-2) and 30 minutes (FA-3). Surface areas measured by the Blaine method are given in Table 2.9.

Table 2.9: Specific surface areas of fly ash (Grzsezczyk and Lipowski, 1997).

Fly Ashes	Surface Area of Fly Ashes - Blaine (m^2/kg)
FA-0	261.9
FA-1	393.3
FA-2	430.2
FA-3	471.3

Particle size distributions of fly ashes FA-0 to FA-3 are given in Figures 2.43-46 *(Grzeszczyk and Lipowski, 1997).*

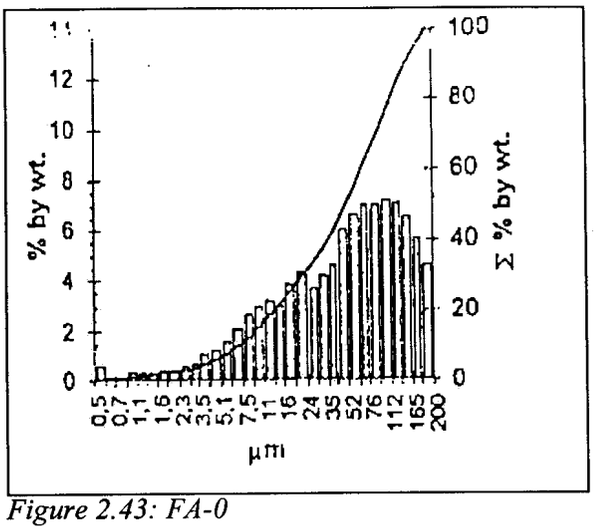

Figure 2.43: FA-0

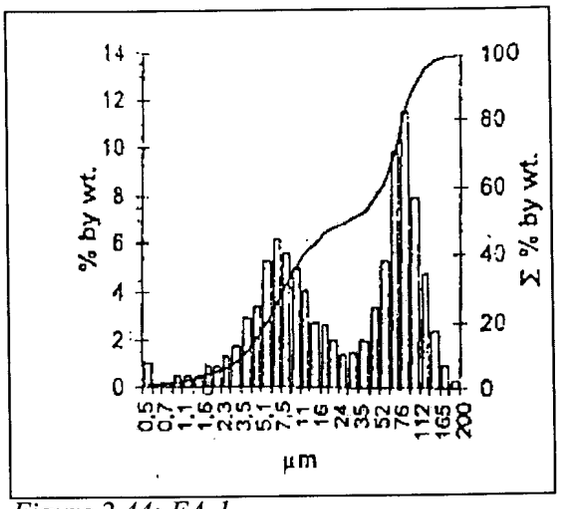

Figure 2.44: FA-1

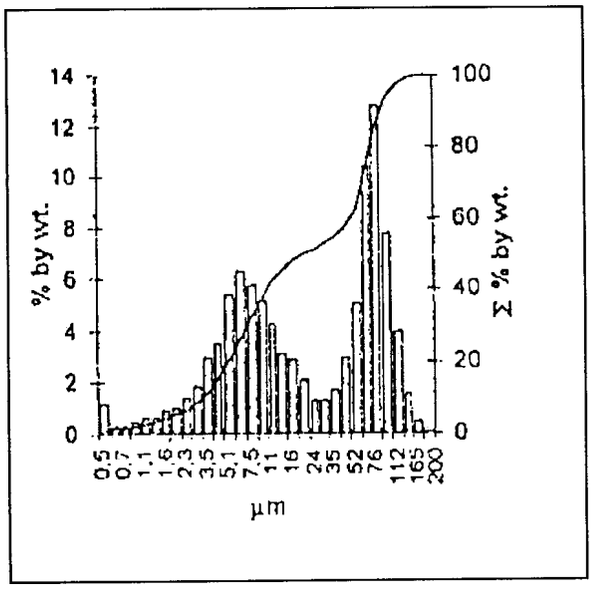

Figure 2.45: FA-2

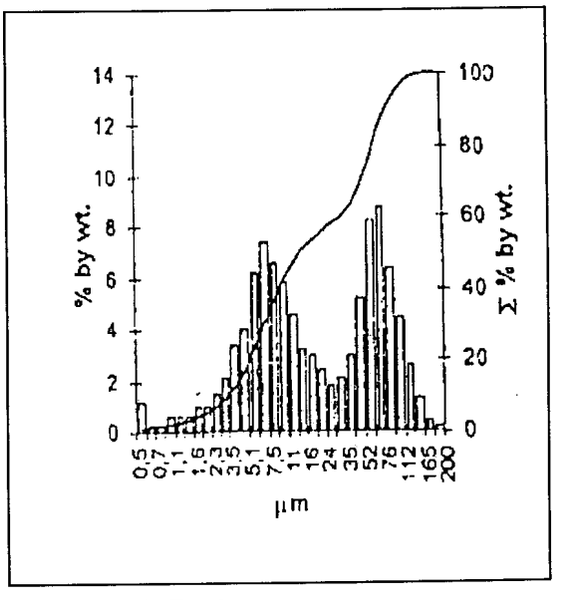

Figure 2.46: FA-3

Cement-fly ash mixes were made containing 20%, 40%, 60% and 80% fly ash (by weight) and were pre-homogenized in a laboratory mill. Water was added at a water/solids ratio of 0.5 and rheological measurements were performed at 21°C using the Rheotest RV-2.1-type viscometer (coaxial cylinder-type). The measurements were performed 10 minutes after mixing with water. Flow curves were drawn and can be seen in Figures 2.47-50 *(Grzeszczyk and Lipowski, 1997).*

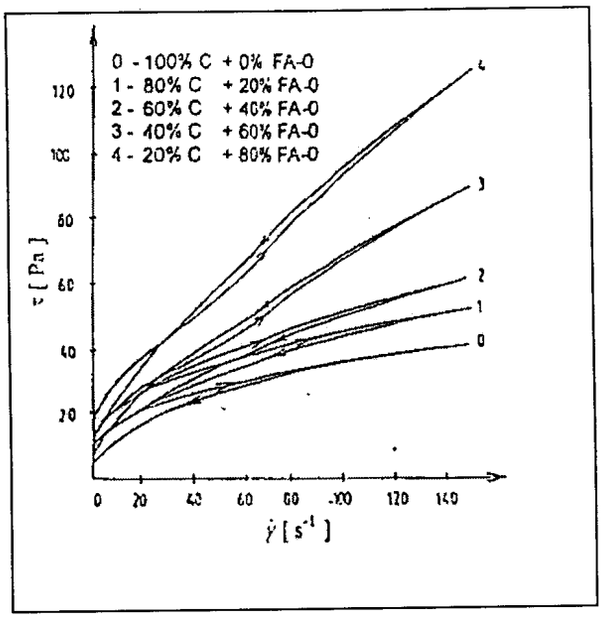

Figure 2.47: FA-0

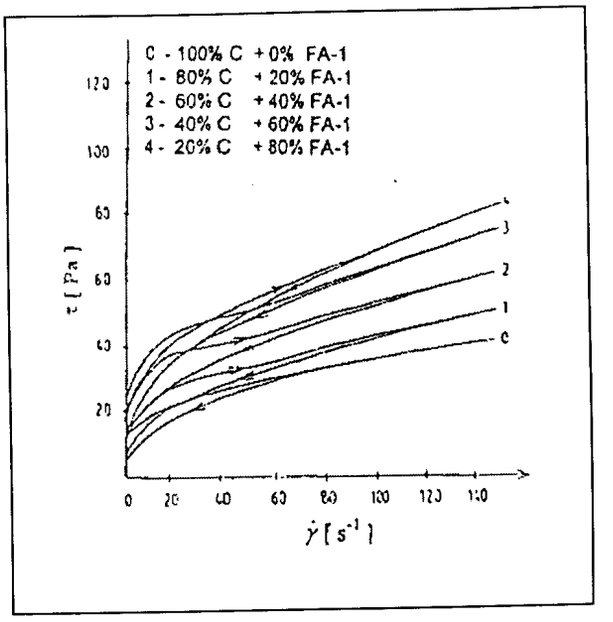

Figure 2.48: FA-1

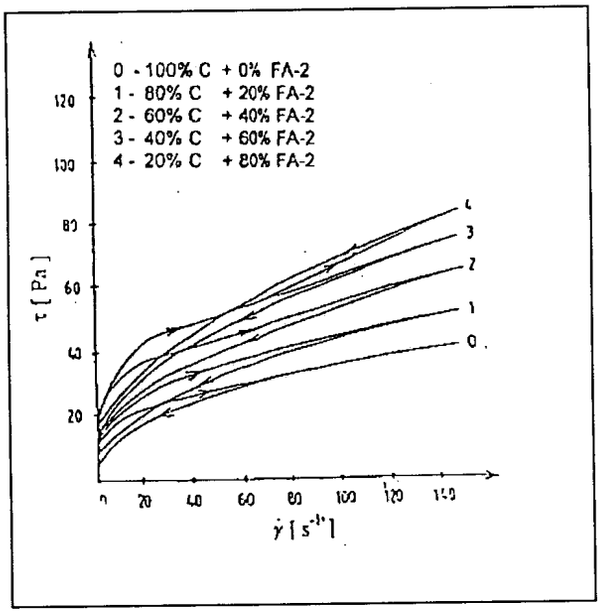

Figure 2.49: FA-2.

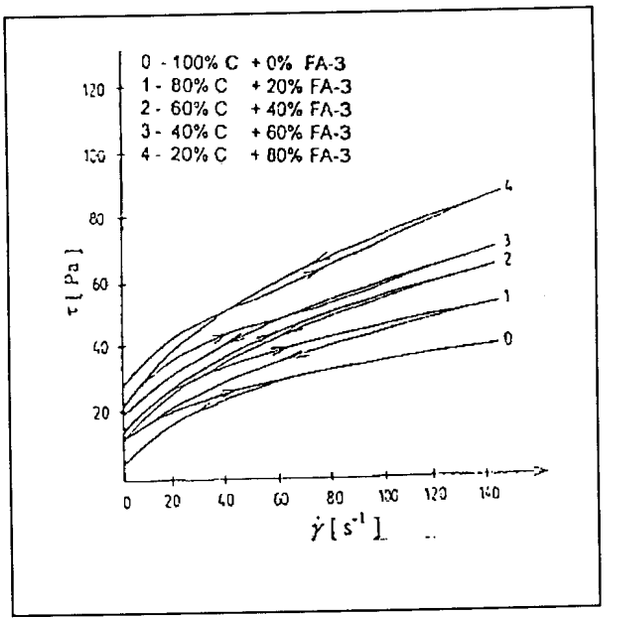

Figure 2.50: FA-3

The yield value and plastic viscosity were determined from the descending parts of the curves, according to Bingham`s model. These values are shown in Table 2.10 and plotted in Figure 2.51

Table 2.10: Yield value and plastic viscosity of cement pastes containing fly ashes (Grzeszczyk and Lipowski, 1997).

No	Composition of cement-fly ash mixtures	FA-0		FA-1		FA-2		FA-3	
		τ_0	η_{pl}	τ_0	η_{pl}	τ_0	η_{pl}	τ_0	η_{pl}
0	100%cem + 0%fa	12.8	0.26	12.8	0.26	12.8	0.26	12.8	0.26
1	80%cem + 20%fa	18.6	0.29	16.4	0.28	15.4	0.30	16.6	0.30
2	60%cem + 40%fa	18.8	0.45	18.9	0.32	20.6	0.35	20.7	0.36
3	40%cem + 60%fa	22.9	0.55	24.4	0.36	25.6	0.39	23.3	0.37
4	20%cem + 80%fa	21.1	0.74	21.5	0.41	24.8	0.47	24.7	0.48

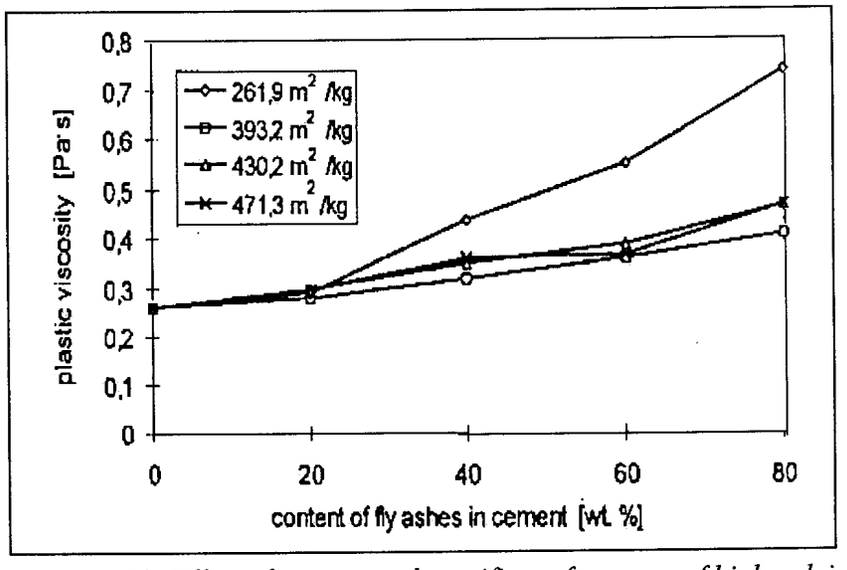

Figure 2.51: Effect of content and specific surface area of high-calcium fly ashes on the plastic viscosity of cement pastes (Grzeszczyk and Lipowski, 1997).

From the figures and table we can see that the plastic viscosity increased with increased amount of fly ash and becomes clearly higher in pastes with 60 wt% and 80 wt% of raw, not ground fly ash. Here the plastic viscosity is two and three times higher than that of the reference cement paste without fly ash. Grinding of the fly ash improved rheological properties (increases fluidity) as compared with paste with conventional raw fly ash, especially at higher fly ash contents.

Scanning electron microscope photos were taken of the two pastes containing low-calcium and high-calcium fly ash after 4 hours and are shown in Figures 2.52 and 2.53.

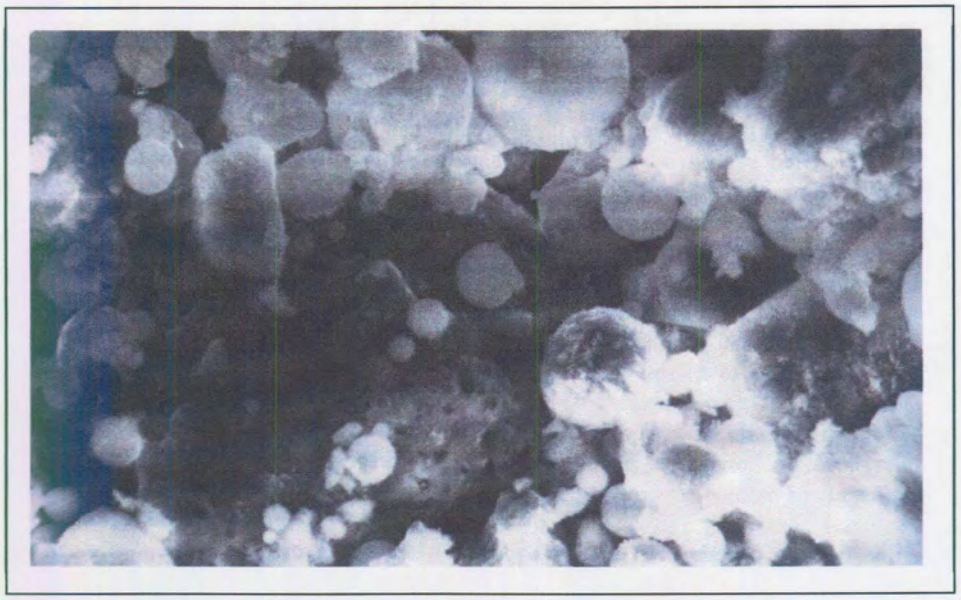

Figure 2.52: SEM micrographic structure of cement paste containing low-calcium fly ash after 4-hours hydration time (Grzeszczyk and Lipowski, 1997).

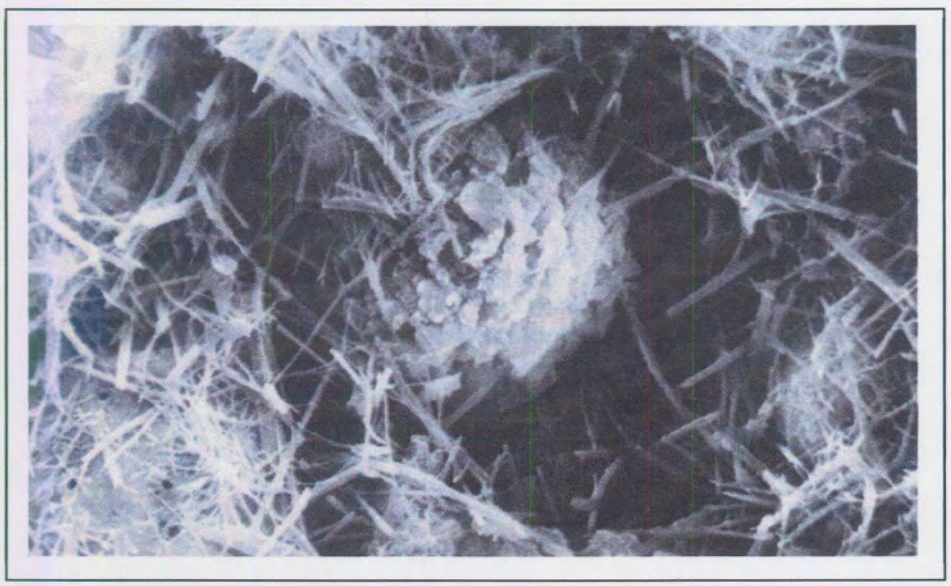

Figure 2.53: SEM micrographic structure of cement paste containing high-calcium fly ash after 4-hours hydration time (Grzeszczyk and Lipowski, 1997).

From these figures one can clearly see that the high-calcium fly ash is much more reactive than the low-calcium fly ash. The exothermic calorimetric peaks are much higher and from the SEM-photos we can see evidence of a much higher degree of hydration with the high-calcium fly ash paste.

The authors concluded that:

- A high-calcium fly ash replacement for cement result in a decrease in fluidity of pastes (higher yield-value and plastic viscosity).
- Additional grinding of the high-calcium fly ash improves the rheological properties of the paste (increase in fluidity).
- The finest fraction content is a better parameter to characterize the rheological properties of cement pastes than the Blaine specific surface.

By looking at Table 2.10 it is interesting to note that for the ungrounded fly ash (FA-0) the yield value did not increase as much as the viscosity with increasing ash content as for the other ashes (FA-1 to FA-3) a slightly higher increase in yield value was observed. Another interesting observation was that for maximum replacement (80%) the yield values for the different ashes were similar, however the viscosity of the FA-0 mixture were nearly double of that for the other mixtures. This shows the importance of using a two-point method as a one-point method relating only to yield value would have indicated that all the mixtures are similar in workability.

The authors proved that the workability of cement paste might not always be improved with fly ash replacement. Another thought is that if the fly ash contains a large percentage of cenospheres, its bulk density may be lower than after it is crushed. This may be another reason why the normal fly ash used in the experiment had a larger influence on the workability than the crushed samples. Previous researchers (Jiang and Roy, 1992; Costa and Massazza, 1986) showed that the workability of a paste containing fly ash may be reduced due to dedensification of the paste. This may happen if the density of the ash proves to be much lower than that of the cement.

Cornelissen and van den Berg (1998) described in their paper the approach for customization of fly ash focusing on the proportioning of concrete mixtures for applications where specific performances like strength, durability and workability are needed. In turn they define the need for "fit for purpose" concrete and distinguish it from high performance concrete as being "defined-performance" concrete. They explain that fine fly ash particles can improve the packing of the

combination of gravel, sand and cement particles, which may result in denser and stronger concrete.

Their work was based on the Grading Modulus (GM), which was introduced by Hughes and Al-Ani (1989). The grading modulus is calculated as follows:

$$GM = \frac{6\left(\frac{1}{d1} - \frac{1}{d2}\right)}{\ln\frac{d2}{d1}} \qquad \text{(Eq. 2.13)}$$

Where *d1* and *d2* represent the diameters of the smallest and the largest size particles of a group between two successive sieves. Table 2.11 shows predetermined grading moduli for 16 bands ranging in total from 1.5 – 188um (Hughes, 1989).

Table 2.11: Grading modulus parameters (Hughes and Al-Ani, 1989).

Size band (μm)	**Grading Modulus (1/mm)**	**Size band (μm)**	**Grading Modulus (1/mm)**
188.0-87.2	48.02	10.1-7.9	673.39
87.2-53.5	88.72	7.9-6.2	859.42
53.5-37.6	134.47	6.2-4.8	1102.86
37.6-28.1	185.24	4.8-3.8	1408.08
28.1-21.5	244.84	3.8-3.0	1781.19
21.5-16.7	317.49	3.0-2.4	2240.70
16.7-13.0	408.28	2.4-1.9	2816.20
13.0-10.1	525.01	1.9-1.5	3562.37

The grading modulus of fly ash with a given particle size distribution can thus be calculated by multiplying the percentage within each band (from the size analyses) by the appropriate value given in the table above. The sum of these products divided by 100 gives the grading modulus.

Thus an increasing weight factor is connected to the finer fractions, which result in an exponential effect of the fine particles on the properties. The authors showed that an increase in GM can results in an increase in compressive strength in terms of the K-value (Figure 2.54).

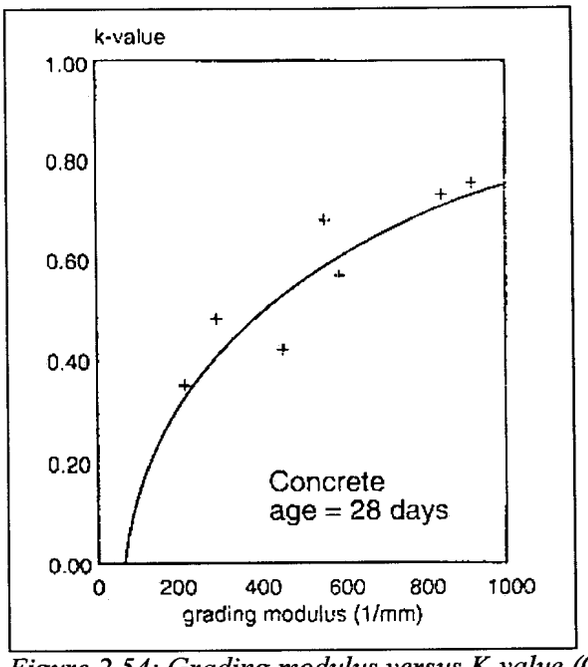

Figure 2.54: Grading modulus versus K-value (Cornelissen and van den Berg, 1998).

The K-value (EN 206) can be defined as that part of fly ash that can be regarded as cement for equal compressive strength as a reference concrete with no fly ash (Cornelissen and Gast, 1992). Like most fly ash activity tests this test is performed at constant workability thus the water content of the concrete mixtures containing fly ash is amended so that the same workability as the reference mix containing no fly ash is obtained.

The authors showed that adding and removing fractions could modify the sieve curve of fly ash. By substituting 11% of coarse particles (> 77.5um) by finer particles (0.5 – 2.6um) the grading modulus will increase from 498 to 1023 (1/mm). Grading curves are shown in Figure 2.55. According to Figure 2.54, a 50% increase in K-value may be expected accordingly.

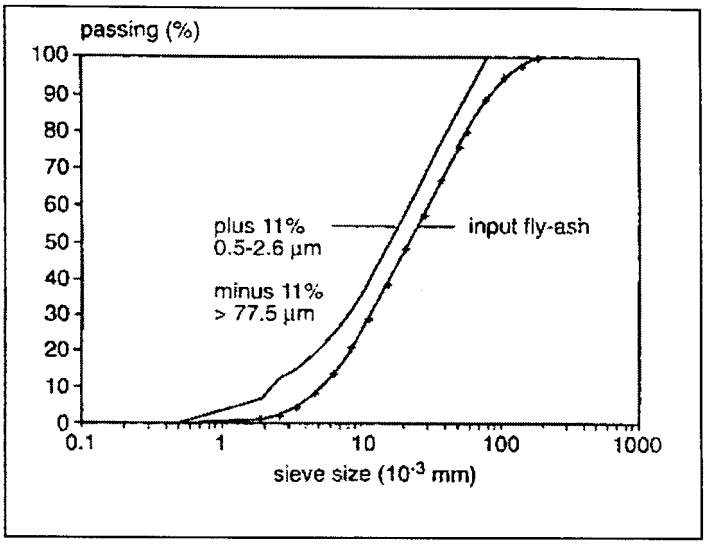

Figure 2.55: Modified sieve curve of fly ash (Cornelissen and van den Berg, 1998).

They emphasized the importance of particle size and grading of the whole system (cement, fly ash, sand, etc.) on packing and subsequently on concrete properties.

The positive effect of dry packing density on the flow properties of mortars and consequently on strength and permeability was also previously confirmed by Cornelissen and Gast (Cornelissen and Gast, 1992). They prepared standard mortars in which 20% of cement was replaced with processed fly ash with various fineness, showing D50 values of 10-80µm. The following model for determining the packing (*Pd*) of the cement, sand and fly ash were used:

$$Pd = 100 \times \frac{V_i - V_c}{V_i} \qquad \text{(Eq. 2.14)}$$

Where:

V_i = Sum of volumes of individual components.
V_c = Volume of components after compaction (Figure 2.56).

Thus improved packing will result in lower V_c and higher dry packing (*Pd*) values.

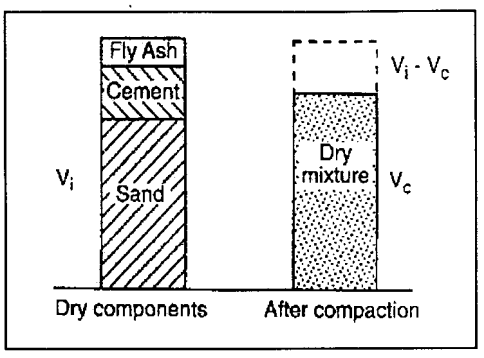

Figure 2.56: Determination of dry packing (Cornelissen and van den Berg, 1998).

A normal hardening (pc-A; D50 = 22um; Blaine = 280 m^2/kg) and a rapid hardening (pc-C; D50 = 15um; Blaine = 550m^2/kg) cement were used in the experiments and the dry packing was measured with mixtures of 5% fly ash, 20% cement and 75% sand. Mortars were made with water/cement ratio of 0.5. Figure 2.57 shows fresh mortar spread (German Hagermann flow) given as a function of dry packing, Pd.

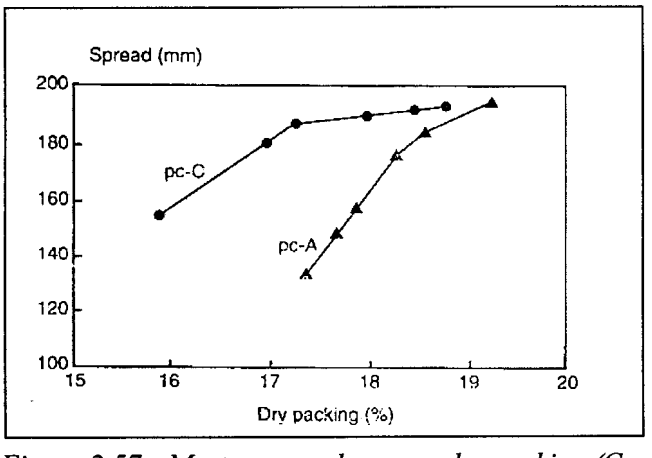

Figure 2.57: Mortar spreads versus dry packing (Cornelissen and van den Berg, 1998).

Higher Pd values were found with coarser cement. Also higher packing densities resulted in higher spread for both types of cement. The authors explained that a wider particle size range is required for dense packing, resulting in a lower total specific surface and more "free" water to facilitate workability.

The authors used two fly ash samples with normal (4.6%; B) and higher (8.3%; M) carbon contents. The original samples were processed in an air classifier and mixed to obtain certain

gradings. Particle size distribution was measured using a Malvern 2600C analyzer and from that, the GM was calculated.

Concrete mixes were made and 150mm cubes were cast by using 320kg/m^3 normal hardening portland cement, which was substituted with 20% fly ash in the case of the fly ash mixtures. The maximum aggregate size range was 16-31.5mm and the actual maximum grain size was 22mm. Water was added until a slump of 70mm + or – 10mm were reached and the amount recorded. Compressive strength tests were performed on cubes at 7 and 28 days. Results are shown in Table 2.12.

Table 2.12: Concrete test results (Cornelissen and van den Berg, 1998).

Sample Code	GM (1/mm)	Water Demand (l/m^3)	Compressive Strength (N/mm^2)	
			7 days	28 days
Reference	-	163	30.5	38.5
B0	225	163	23.0	31.5
B1	456	160	25.0	33.5
B2	462	161	24.0	33.0
B3	850	156	28.0	39.0
M0	299	162	24.5	33.5
M1	563	160	27.0	37.0
M2	600	158	27.5	36.0
M3	919	157	28.0	39.0

It can be seen that the higher the grading modulus, the less water is required and the higher compressive strengths are reached.

After full-scale tests the authors concluded that:

- Higher dry packing resulted in higher workability.
- Grading modulus and dry packing seem to be useful measures to control and adjust particle size for optimal application in concrete and by processing fly ash to increase fine and ultra fine particles, compressive strength of concrete can be enhanced.
- In full-scale tests, the suitability of micronized fly ash for the production of very workable concrete was confirmed.

The authors pointed out the importance of incorporating very fine fly ash into concrete. Finer fractions increase the specific surface area, which in turn may increase water demand but its effect on packing density seems to overshadow that of surface area.

For the purpose of this dissertation the surface area was calculated from the grading curve (as explained earlier) from Figure 2.55 and values of 2363 m^2/kg for the input and 3454 m^2/kg for the modified fly ash were obtained. If the compressive strength or K-value does increase as shown in Figure 2.54 due to lower water demand, it can clearly be seen that the influence of the fly ash is much more pronounced in terms of increased packing density (decrease in water demand) than increased surface area (increase in water demand).

The authors further showed that the grading properties of the whole system (cement, fly ash, etc.) has an influence on the packing density of the dry materials and thus on the water demand as shown in Figure 2.57. From Table 2.12, it is also clear that water demand decreases with increasing grading modulus and therefore compressive strength increases.

Johansen and Anderson (1993) explained the concept of packing density of blended materials according to certain models. They explained that these models could be applied in concrete technology to determine the optimum proportions of the different sized components (cement, sand and large aggregate) to obtain maximum packing densities. By obtaining maximum packing density, minimum porosity and permeability, maximum workability and maximum compressive strength would be obtained. In their work the authors explained the packing density and rheology of paste by means of the Bingham model that is based on measurement of workability with mixer-type equipment, by measuring power consumption at a specific shear rate, as with the Tattersall apparatus.

The authors referred to tests performed by Anderson (1990) mixing sand (0-4mm), rounded coarse aggregate (8-16mm) with different cement contents of 10% and 20%. The water to solids ratio was kept constant. For each mixture, the Bingham flow curve was recorded and the yield value and plastic viscosity calculated by linear regression. Results are shown in Table 2.13 where φ is the relative packing density, η viscosity and τ_0 the yield stress.

Table 2.13: Mix compositions of cement, quartz sand (0-4mm) and coarse aggregate (8-16mm) (Johansen and Anderson, 1993).

Mixture no.	Sand	Stone	Cement	W/c	φ	ηx10 (amp.min)	τ_0
	Volume %						
1	40	40	20	0.5	0.78	4.4	0.13
2	60	20	20	0.5	0.77	8.0	0.27
3	20	60	20	0.5	0.77	8.0	0.15
4	50	30	20	0.5	0.78	4.0	0.15
5	30	50	20	0.5	0.78	7.0	0.08
6	20	70	10	1.0	n.d*	8.5	0.22
7	30	60	10	1.0	0.85	8.0	0.12
8	40	50	10	1.0	n.d	6.2	0.12
9	50	40	10	1.0	0.82	3.7	0.19
10	60	30	10	1.0	n.d	6.3	0.25

* Not documented

The viscosity as a function of the yield value for all mixes is plotted in Figure 2.58.

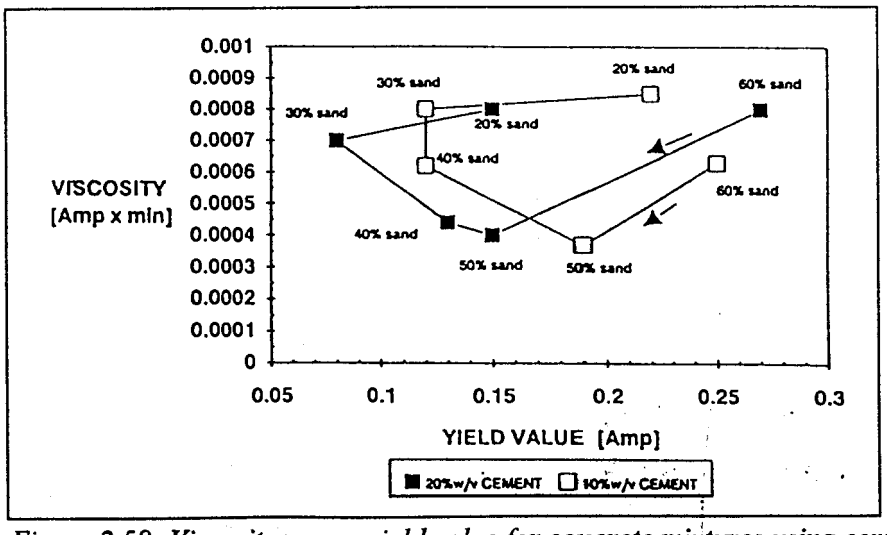

Figure 2.58: Viscosity versus yield value for concrete mixtures using cement, sand (0-4mm) and rounded aggregates (8-16mm) (Johansen and Anderson, 1993).

The figure shows that a minimum yield value is obtained at a sand content of 30 to 40 vol% and that the minimum viscosity is obtained at a sand volume of ~50%.

The authors claimed that the difference in rheology could be attributed to the variations of packing density of the sand and coarse aggregate. By plotting the volume % of coarse aggregate against the yield value (Figure 2.59) and viscosity (Figure 2.60), this was further substantiated.

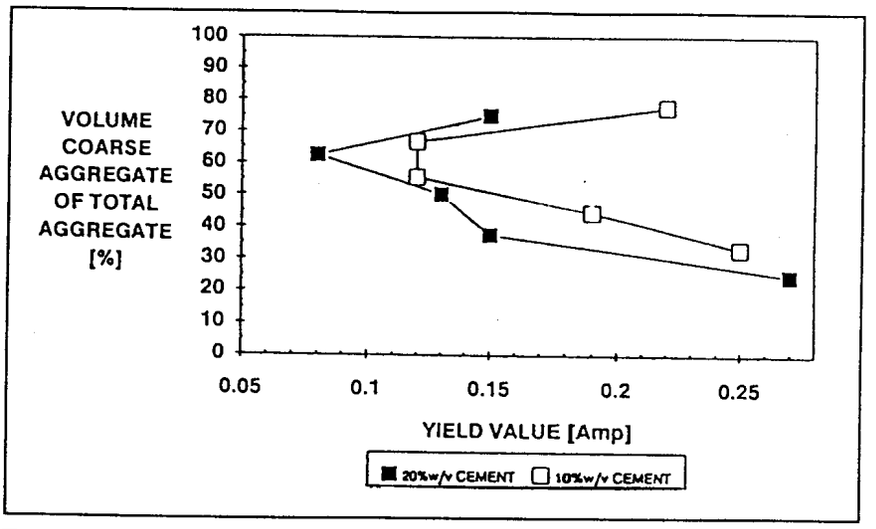

Figure 2.59: Yield value versus the percentage of coarse aggregate of the total amount of aggregates (Johansen and Anderson, 1993).

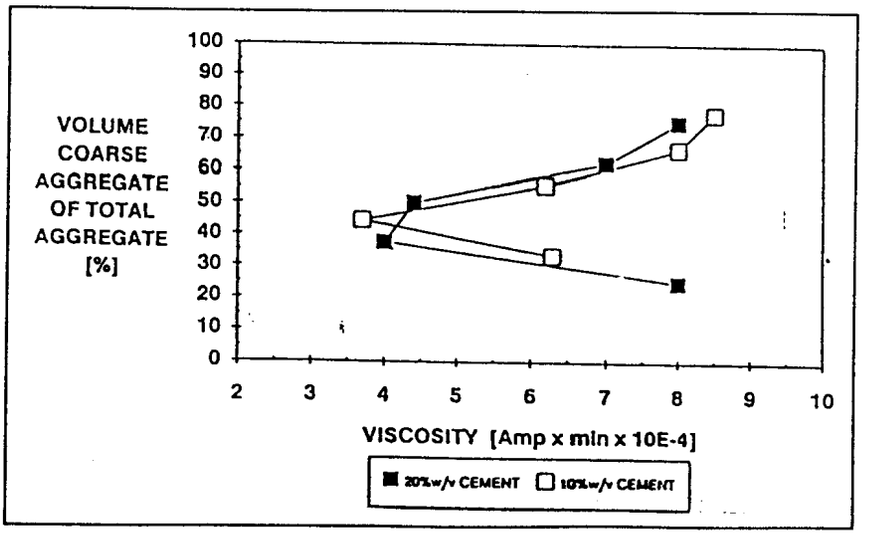

Figure 2.60: Viscosity versus percentage of aggregate of the total amount of aggregates (Johansen and Anderson, 1993).

It is evident from these figures that in terms of yield value the concrete has the highest workability at maximum packing density of sand and coarse aggregate (60:40). The authors explained that above statement is only true for low shear concreting conditions. During these conditions the yield value is decisive for workability measurements. From the Bingham equation:

$$\tau = \tau_0 + \eta \times \gamma \qquad \text{(Eq. 2.15)}$$

It can be seen that at low shear rates $\eta \times \gamma \sim 0$ and hence, $\tau \sim \tau_0$. It can also be assumed that under these conditions a close correlation exists between the yield value and results obtained by the slump or flow table tests. For high shear rate processing like vibrating during casting, the size of $\eta \times \gamma$ may exceed that of τ_0 so that the mixture with lowest plastic viscosity may be the most workable and as we have seen, this may not be the mix with highest packing density.

The authors thus gave a very good explanation why it is important to assess workability by a two-point method, especially when future shear conditions are unknown. As can be seen from their results, the most workable concrete in terms of yield value may be obtained at maximum packing density of coarse and fine aggregate but this is not necessarily true when results are interpreted in terms of plastic viscosity. It is thus again proved that different mix designs may be necessary for concrete processing at different shear stress levels.

By accepting that concrete flow follows the Bingham model, Hobbs (1980) predicted the changes in water demand for paste where part of the cement was replaced by fly ash. His explanations were based on the fact that good quality fly ash, complying with BS 3892 could be regarded as inert and that the amount of water it absorbs is negligible. If this is true, the flow characteristics will change upon replacement because the true water cement ratio will increase. Furthermore if the true water cement ratio were kept constant, the blend would become stiffer because of the increased viscous drag provided by the fly ash particles.

The author previously derived the following equations for calculation of the yield value, $\tau_{oc,}$ and the plastic viscosity, μ_c, of a Bingham suspension (Hobbs, 1980):

$$\tau_{oc} = \tau_{op}\left(1 + \frac{1.5V_{a,m} + V_a^2}{V_{a,m} + V_a}\right) = \tau_{op} f_1(V_a) \qquad \text{(Eq. 2.16)}$$

And:

$$\mu_c = \mu_p\left(1 + \frac{2.5V_{a,m} \times V_a}{(1 - V_a)(V_{a,m} - V_a)}\right) = \mu_p f_2(V_a) \qquad \text{(Eq 2.17)}$$

Where:

τ_{op} = Yield value of the cement paste

μ_p = Plastic viscosity of the cement paste

V_a = Aggregate volume concentration

$V_{a,m}$ = Particle volume concentration for close packing

Accordingly, the Bingham model for a blended cement paste containing fly ash was deduced:

$$\tau_{bc} = \tau_{op}(1 + \frac{1.5V_{fa,m} \times V_{fa} + V_{fa}^2}{V_{fa,m} - V_{fa}}) + \mu_p(1 + \frac{2.5V_{fa,m} \times V_{fa}}{(1 - V_{fa})(V_{fa,m} - V_{fa})})\gamma_{bc} \qquad \text{(Eq. 2.18)}$$

or

$$\tau_{bc} = \tau_{obc} + \mu_{bc} \times \gamma_{bc} \qquad \text{(Eq. 2.19)}$$

Where:

τ_{bc} = Applied shear or viscous stress on the blended paste containing fly ash

γ_{bc} = Shear rate

V_{fa} = Volume concentration of fly ash

$V_{fa,m}$ = Volume concentration of fly ash necessary for close packing

The bulk density of fly ash was taken as between 1120 and 1490 kg/m^3 and its relative density between 2100 and 2400 kg/m^3. Thus

$0.47 < V_{fa,,m} < 0.71$

The factors $(1 + \frac{1.5V_{fa,m}V_{fa} + V_{fa}^2}{V_{fa,m} - V_{fa}})$ and $[1 + \frac{2.5V_{fa,m}V_{fa}}{(1 - V_{fa})(V_{fa,m} - V_{fa})}]$ were replaced by $f_1(V_a)$ and $f_2(V_a)$ respectively.

Plots of $f_1(V_a)$ and $f_2(V_a)$ for V_a-values between 0 and 0.35 were drawn and are shown in Figures 2.61 and 2.62. The author stated that variations in $V_{fa,m}$ when V_{fa} is less than 0.2 would not have a major influence on $f_1(V_a)$ and $f_2(V_a)$.

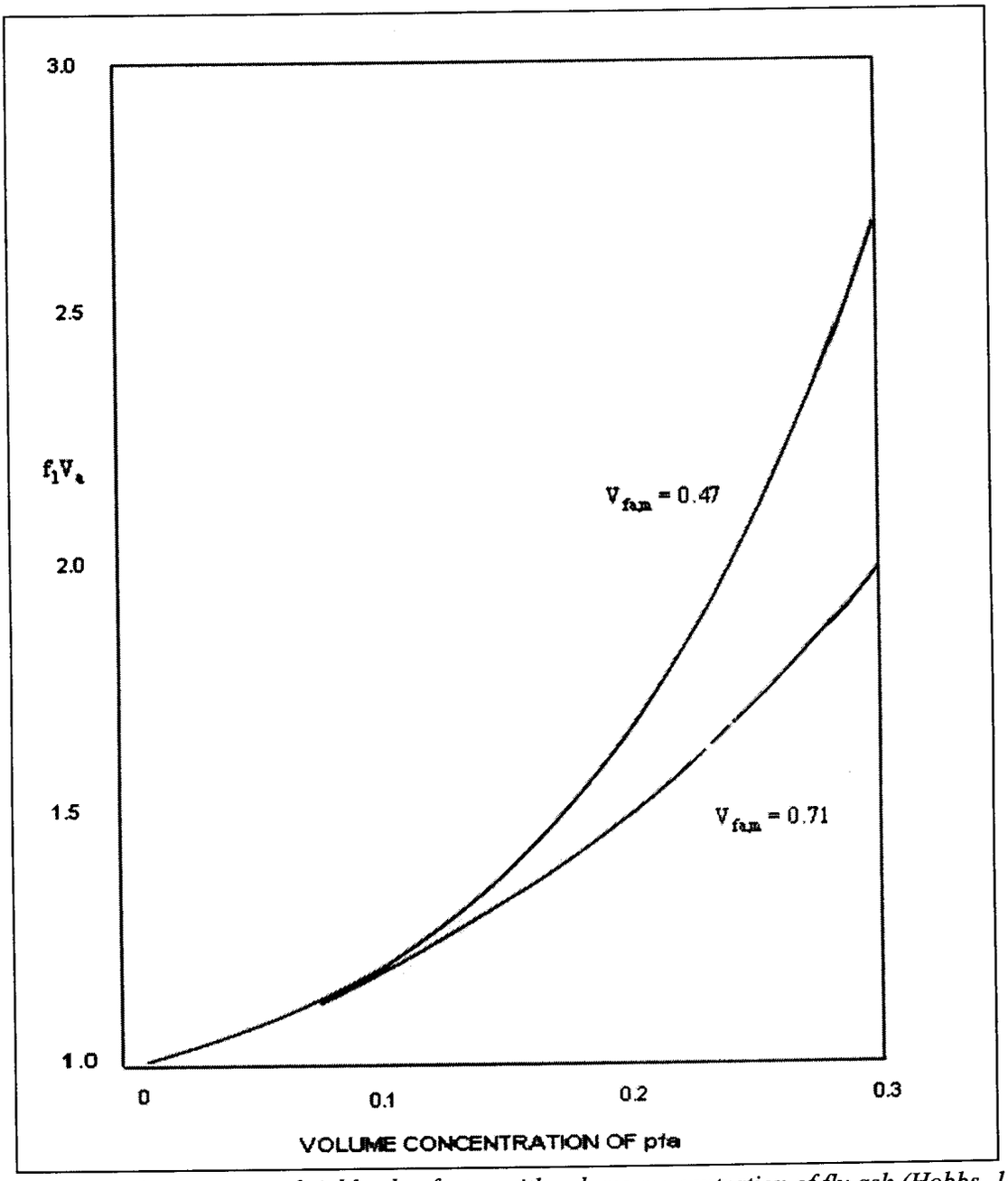

Figure 2.61: Variation of yield value factor with volume concentration of fly ash (Hobbs, 1980).

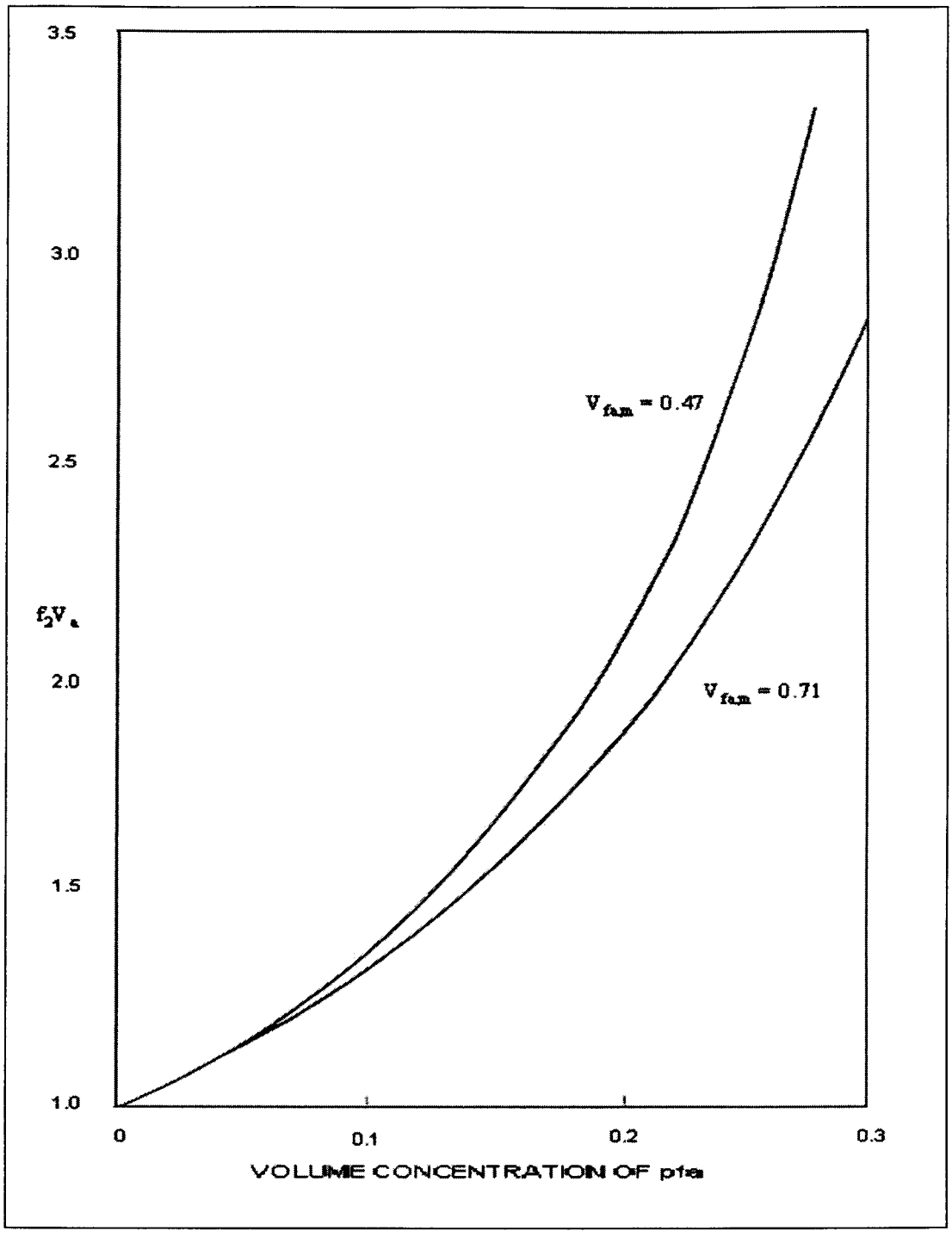

Figure 2.62: Variation of plastic viscosity factor with volume concentration of fly ash (Hobbs, 1980).

For values of yield value and plastic viscosity of cement pastes previously obtained by Vom Berg (1979) the author calculated values for the yield value and plastic viscosity of blended pastes containing fly ash. Vom Berg`s values are shown in Table 2.14:

Table 2.14: Vom Berg Results (Vom Berg, 1979).

Water/Cement	Vom Berg (Age: 10 min, $\gamma < 200s^{-1}$)			
	Yield Value (N/m^2)		Plastic Viscosity ($N\ s/m^2$)	
	SSA = 325	SSA = 450	SSA = 325	SSA = 450
0.40	37	100	0.30	0.62
0.45	-	-	-	-
0.50	10	25	0.12	0.24
0.60	2.8	10	0.045	0.10
0.70	1.6	4.4	0.020	0.047
0.80	1.0	2.7	0.009	0.023

Predicted yield value plastic viscosity-values of blended cement pastes were plotted against water/cement ratio for cement replacements ranging between 0 and 50% by weight and are shown in Figures 2.63 and 2.64:

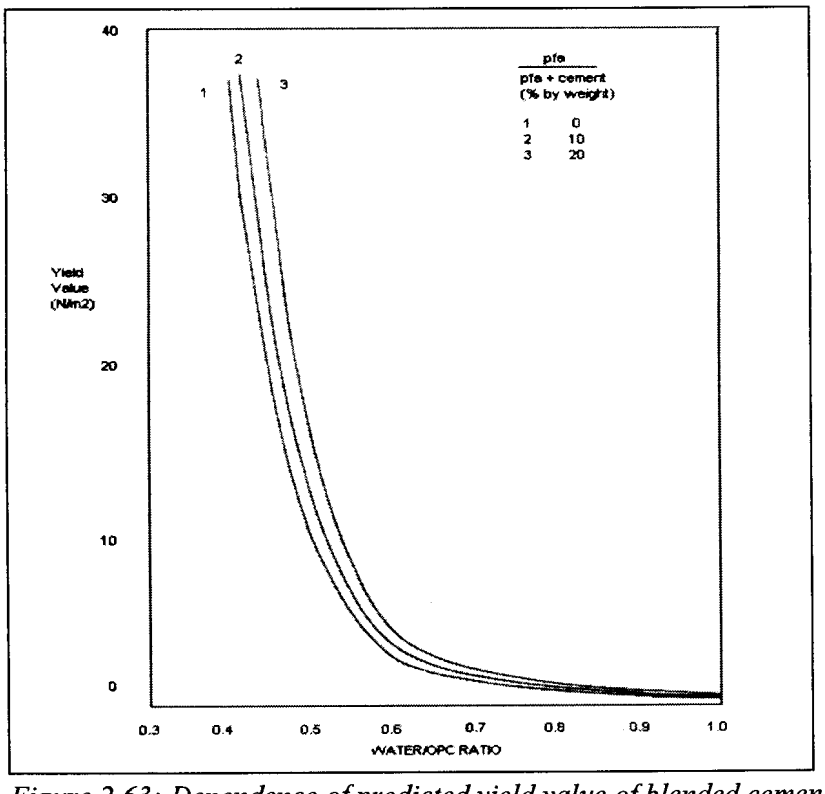

Figure 2.63: Dependence of predicted yield value of blended cement paste on the water/cement ratio (Hobbs, 1980).

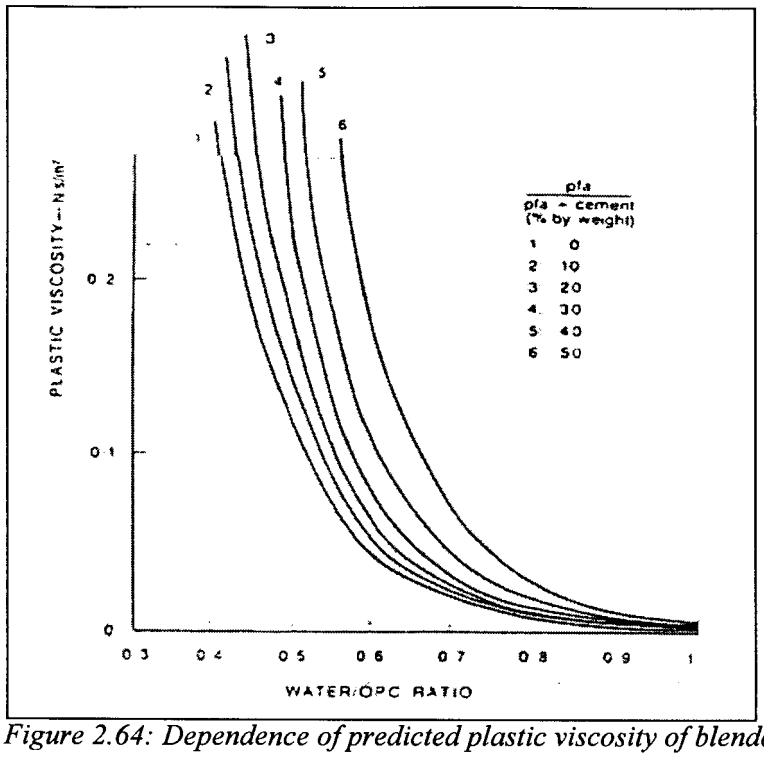

Figure 2.64: Dependence of predicted plastic viscosity of blended cement paste on the water/cement ratio (Hobbs, 1980).

From the above exercise, Hobbs predicted the following:

- The addition of fly ash to concrete has a bigger influence upon the plastic viscosity of the blended cement paste than on its yield value.
- For every 10% **addition** of fly ash, to obtain a constant yield value, the water OPC ratio should be increased by 0.01 ($V_{fa,m} = 0.71$) to 0.02 ($V_{fa,m} = 0.47$) when the water OPC ratio of the normal mix is 0.4 and between 0.1 and 0.3 if the water OPC ratio is 0.6. Further increases will be necessary if the water OPC ratio exceeds 0.6.
- To maintain constant plastic viscosity, the water OPC ratio should be increased between 0.025 and 0.04 for each 10% addition of fly ash.
- The replacement of a portion of OPC by fly ash at constant water content would reduce the plastic viscosity and yield value of a cement paste. The reduction in these factors due to the increase in water OPC ratio will outweigh the increase caused by the presence of fly ash.
- The amount by which the water content could be reduced with replacement of OPC with fly ash to reduce a constant level of workability will depend on the shear rate of the assessment method.

The author then subsequently derived a flow equation for concrete:

$$\tau_c = k_1 \times \tau_{obc} + k_2 \times \mu_{bc} \times \gamma_c \qquad \text{(Eq. 2.20)}$$

Where:

τ_c = Applied shear

τ_{obc} = Average rate of shear

μ_{bc} = Yield value

γ_c = Plastic viscosity

The yield value and plastic viscosity may be obtained from Figure 2.63 and 2.64 and the values for k_1 and k_2 from Equations 2.16 and 2.17 if $V_{a,m}$ is known.

Results from experiments performed by Brown (1980), who measured the effect upon workability of partial replacement of cement by fly ash, were used to test the predictions. In his tests, aggregate volume concentration and grading were kept constant. Results showed that replacement of cement by fly ash increased workability. The magnitude of changes however depended on the mix proportions as well as workability test used. Vebe test results are shown in Figure 2.65.

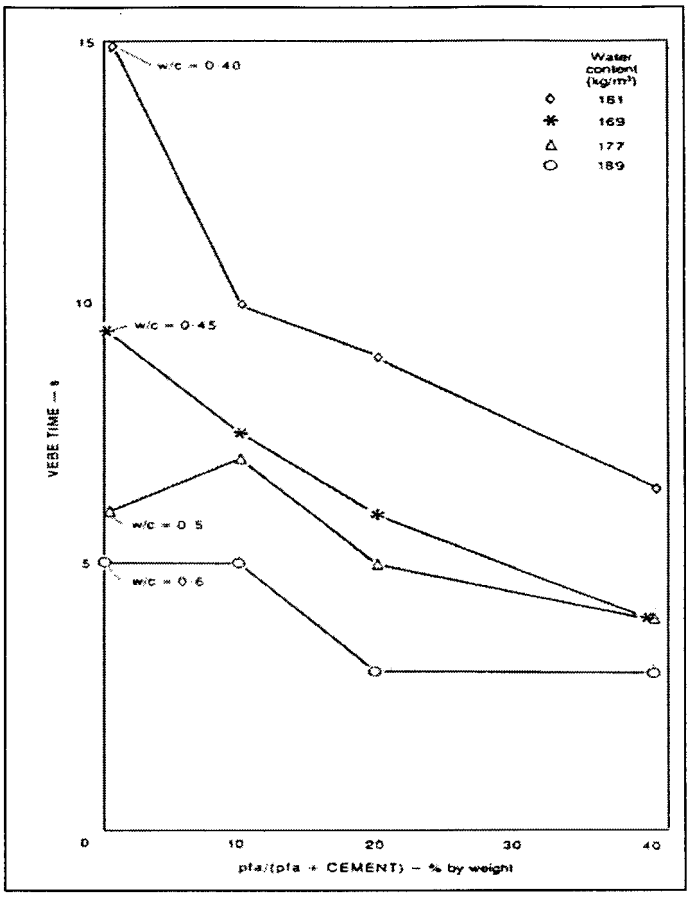

Figure 2.65: Effect of PFA on Vebe-time. Aggregate volume concentration = 0.71, aggregate content = 1880 kg/m^3 (Brown, 1980).

In the case of compacting factor and Vebe test, it was shown that every 10% weight fraction of cement replaced by fly ash had the same effect as increasing the water content of the standard mix by 3.5%. In the case of the slump test, each 10% replacement had the same effect as increasing the water content by 5.5-6%.

The author plotted the predicted yield values and plastic viscosities against the weight ratio of fly ash and fly ash + cement in Brown's mixes. Plots are shown in Figures 2.66 and 2.67.

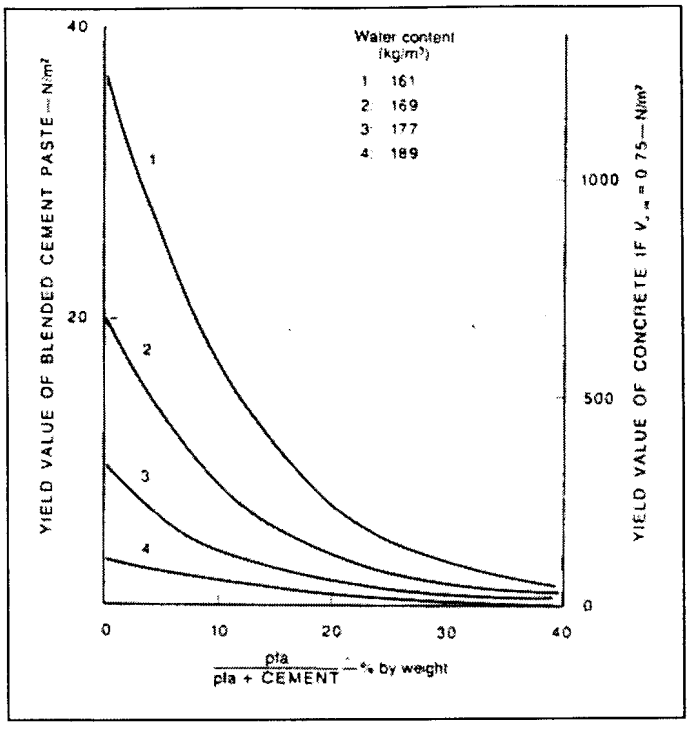

Figure 2.66: Influence of fly ash upon the predicted yield value of the blended cement paste fraction in the concretes tested by Brown. Aggregate volume concentration = 0.71, aggregate content = 1880 kg/m^3 (Hobbs, 1980).

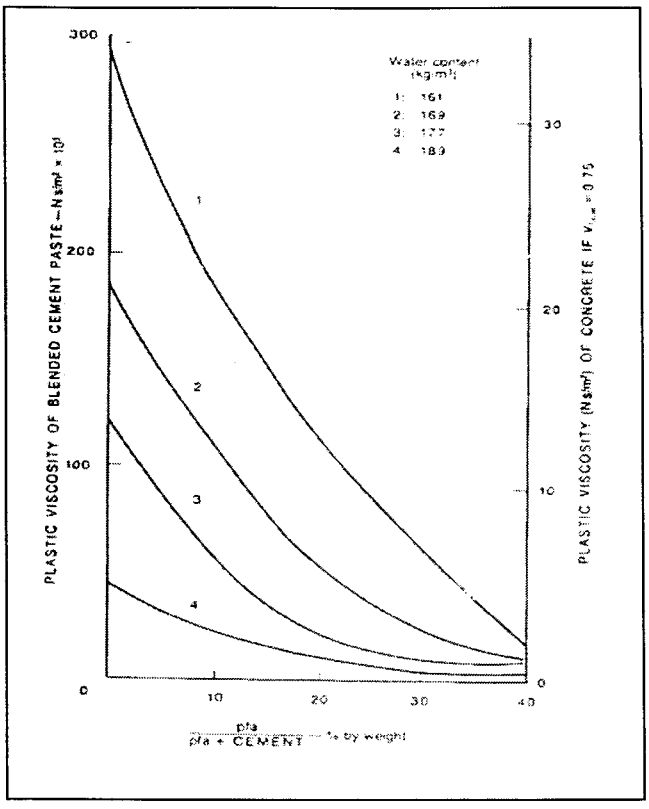

Figure 2.67: Influence of fly ash upon the predicted plastic viscosity of the blended cement paste fraction in the concretes tested by Brown. Aggregate volume concentration = 0.71, aggregate content = 1880 kg/m^3 (Hobbs, 1980).

$V_{fa,m}$ was taken as 0.6 and the density of the fly ash as 2200kg/m^3.

The predicted reductions in water content to maintain constant workability when a portion of cement is replaced by fly ash are shown in Table 2.15 together with the reduction deduced by Brown from measuring slump, compaction factor and Vebe time.

Table 2.15: Reduction in water content necessary to maintain constant workability. The pfa content quoted is the percentage by weight of cement replaced by an equal weight of pfa, namely pfa/(cement + pfa) (Hobbs, 1980).

Water/cement of normal concrete mix	**Predicted reduction in water content (%):**						**Observed reduction in water content (%) to maintain constant:**		
	To maintain constant yield value			**To maintain constant plastic viscosity**			**Slump**	**Compacting factor**	**Vebe**
	10% pfa	**20% pfa**	**40% pfa**	**10% pfa**	**20% pfa**	**40% pfa**			
0.4	5.0-5.5	10.0-11.5	22-25	3-4	6-8	15-20	5.5-6.0 for each 10% substitution of pfa	3.5 for each 10% substitution of pfa	3.5 for each 10% substitution of pfa
0.6	3.5-4.5	7.5-9.0	18-22	3-4	6-8	16-19			

It can be seen that a greater reduction is needed to maintain constant slump than is required for constant compacting factor and Vebe time. According to author, this is exactly what is predicted in that a greater reduction in water content is needed to maintain constant yield value than is required to maintain constant plastic viscosity.

Hopkins (1984) criticized this work by Hobbs in a Ph.D. thesis. She firstly showed that her rheological analyses of cement paste with different substituted fly ashes were based on constant water, cement and fly ash contents. Yet, different results were obtained. The point is that Hobbs discarded the intrinsic properties of fly ash that might have an influence on rheology.

However, his argument that fly ash increases both yield value and plastic viscosity are in context with other researchers (Banfill, 1994). He also explains that effects of a parameter on workability may differ depending on the test used where tests are performed at different shear rate levels.

On the results obtained by Brown, Tattersall commented by saying that different values will be obtained for slump and Vebe-time tests because tests are performed at different levels of shear and the values obtained can thus be related to the two different workability parameters namely yield value (related to slump) and plastic viscosity (related to Vebe-time and compacting factor). He further concluded that it is impossible to adjust water contents with the addition of fly ash so that both yield value and plastic viscosity remain constant. It is thus important to know at which shear rate the concrete will be placed.

In a following article, Hobbs (1993) explained that when coarse or fine particles are added to cement paste, the workability will always decrease due to increased viscous drag provided by the particles and that the concrete will become unworkable if either the cement or aggregate particles come in close contact with one another. For increased workability, sufficient water should be added to keep cement particles apart or decrease the cement volume concentration. There should also be sufficient paste to keep aggregate particles apart and to fill the voids between aggregate particles.

The author also explains that substituting aggregate with fly ash will increase workability because the increase in workability due to the decrease in aggregate concentration in the paste will overshadow the decrease in workability due to viscous drag of fly ash particles. The effect is reversed when more than 5% of aggregate is replaced. The reducing effect of the fly ash on workability then becomes the deciding factor and the concrete becomes unworkable when cement and fly ash particles comes in close contact. This is shown in Figure 2.68 when workability was measured using the slump method. The figure shows the effects of replacement of aggregate with three different fine materials namely fly ash, cement and slag. The figure indicates that the effect is mutual for all fine materials, with cement producing mixes with the lowest workability because it reacts with a proportion of water thus increasing the concentration of solids and decreasing free water content.

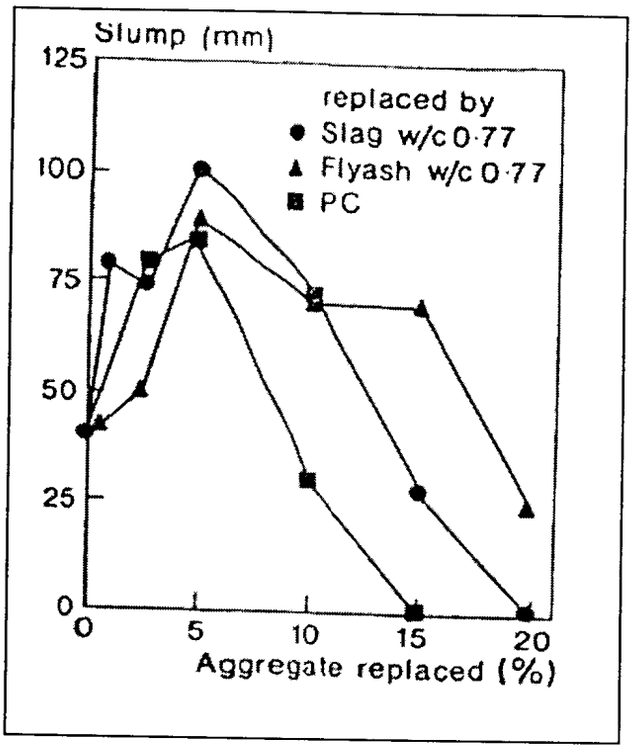

Figure 2.68: Effect on slump (Hobbs, 1993).

Figure 2.69 shows the effect when the compacting factor is used as workability test and Figure 2.70 shows the same for the flow table test.

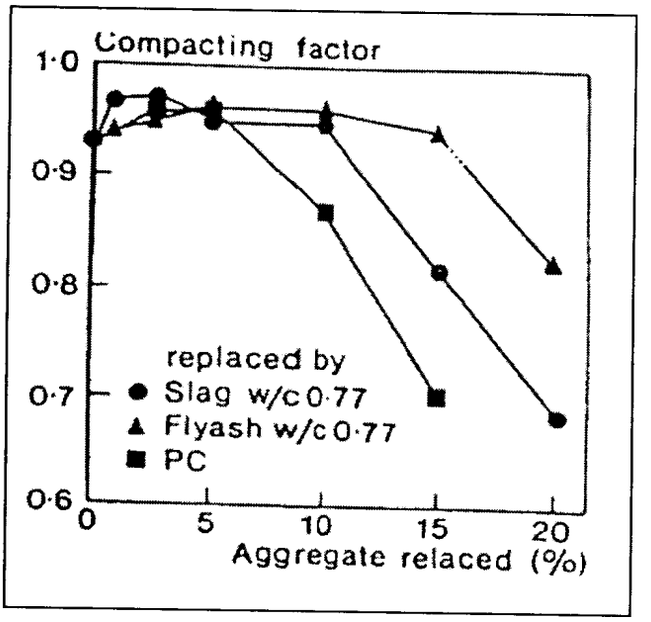

Figure 2.69: Effect on compacting factor (Hobbs, 1993).

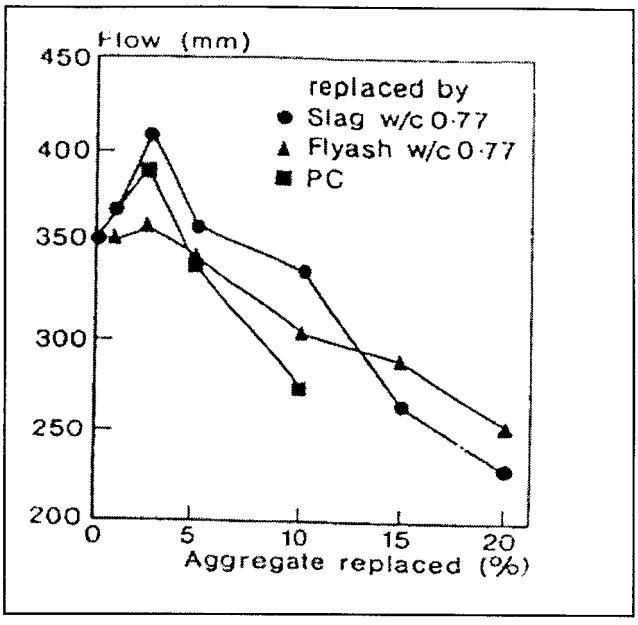

Figure 2.70: Effect on flow (Hobbs, 1993).

From the figures it can be seen that similar trends were observed for slump and flow table tests and this is understandable because both tests are performed under similar shear rate conditions. The compacting factor is performed at higher shear rate conditions.

On the other hand, the author explains as in his previous publication already discussed, that when fly ash is used as replacement material for portland cement, workability may tend to increase due to increasing of the water cement ratio. He explains that the extent of this increase will depend upon the volume concentration of cement in the paste fraction. In Figure 2.71 the author illustrates the boundary between workable and unworkable mixes.

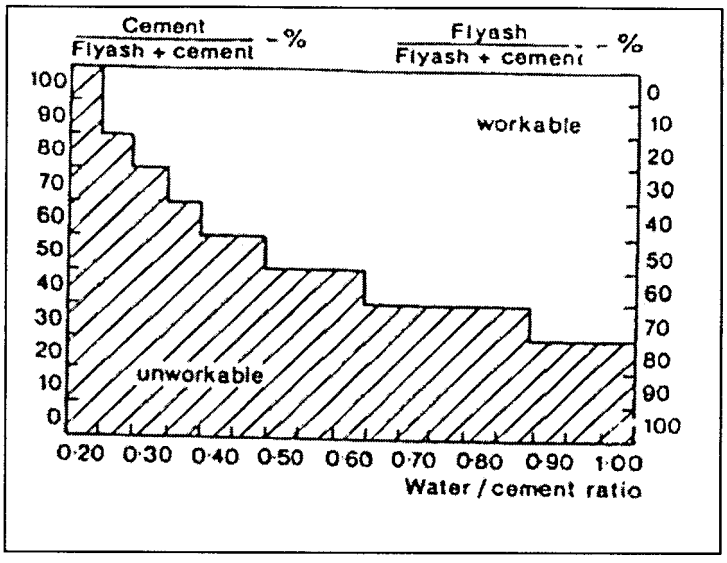

Figure 2.71: Boundary between workable and unworkable mixes (Hobbs, 1993).

The volume concentration of solids (portland cement + fly ash) which produced an unworkable mix was approximately 0.58 which he claims was essentially independent of water cement ratio.

Hopkins and Cabrera (1994) explained in their article that the workability of concrete might be increased or decreased with the addition of fly ash, depending on the particle shape of the fly ash. Each power station produces a different fly ash and the ash produced varies from day to day. Irregular-shaped particles may cause large fluctuations in water demand in cement-fly ash pastes. Another factor that can influence water demand is agglomeration of fly ash particles especially during long storage periods.

In previous publications, Hopkins (1984) identified the "shape factor" of fly ash and the objective was to use this factor as a means to predict the water demand of a paste that contains a certain fly ash. This method is a comparison of the measured specific surface area (MSA) using a Fisher Sub Sieve Sizer and the calculated specific surface area (CSA) derived from the particle size distribution by assuming that the ash consist of discrete spheres.
The interpretation of the shape factor is illustrated by the graph presented in Figure 2.72.

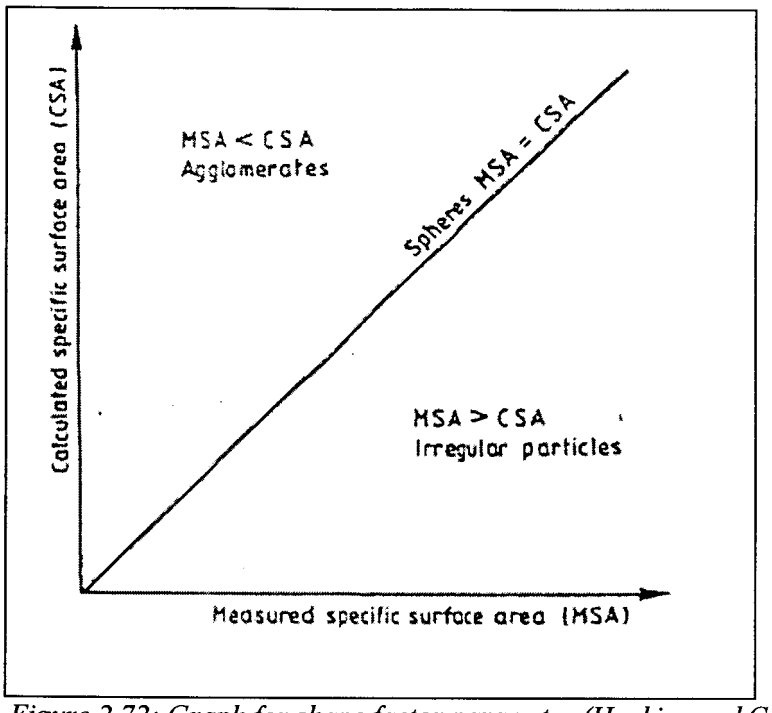

Figure 2.72: Graph for shape factor parameter (Hopkins and Cabrera, 1994).

If the fly ash consists of perfect spheres, the straight line, MSA = CSA, will represent such an ash. Any agglomeration that might occur during storage would cause the MSA to be less than the CSA and the plot would therefore be above the line. In the case of irregular shaped particles, the plot would move below the line, as MSA would be less than CSA. The authors believe that perfectly spherical shaped particles would demand the least water and could produce the most workable concrete.

A two-point test apparatus similar to that of Tattersall was modified by Hopkins and Cabrera and an extensive series of tests measuring the effects of seven fly ashes on concrete workability were performed. The ash properties are listed in Table 2.16.

Table 2.16: Properties of the fly ashes studied (Hopkins and Cabrera, 1994).

Ash	Specific Gravity (g/cm^3)	Measured Specific Surface Area (m^2/g)	% Retained on 45μm sieve	LOI (%)	Mean Particle Diameter (μm)
E	2.30	0.14	19.2	1.5	19.2
D	2.11	0.16	47.7	3.5	17.3
R	2.03	0.19	37.9	2.7	15.3
F	2.40	0.26	5.9	2.5	9.6
T	2.19	0.27	17.3	1.0	10.1
W	2.20	0.31	14.3	2.3	8.9
Y	2.40	0.37	4.0	2.9	6.7

Cement was replaced by fly ash at ratios of 15, 30 and 45% by mass. Sand and coarse aggregate content were kept constant. The amount of water required by each fly ash-concrete to achieve a pre determined workability (that of OPC concrete at w/c = 0.7) was measured.
The speed/torque-plot derived for the fly ash concretes (45% replacement and 0.6 water cement ratio) is shown in Figure 2.73.

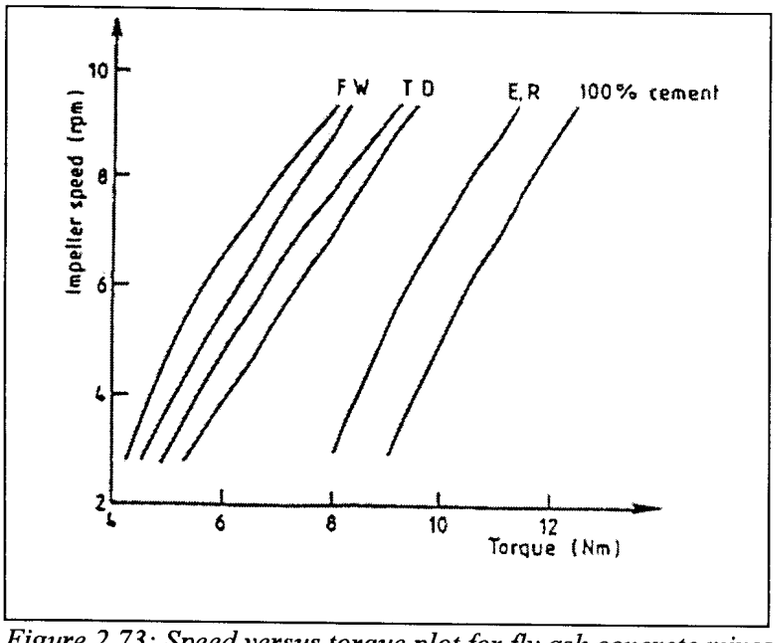

Figure 2.73: Speed versus torque plot for fly ash concrete mixes (45% replacement, 0.6 water/(cement + fly ash) ratio) (Hopkins and Cabrera, 1994).

All replacement mixes showed improvement in workability, some more than others do. The measured surface areas were also determined and the "Shape Factor" graph was drawn and the points plotted (Figure 2.74). Water requirements are shown in Table 2.17.

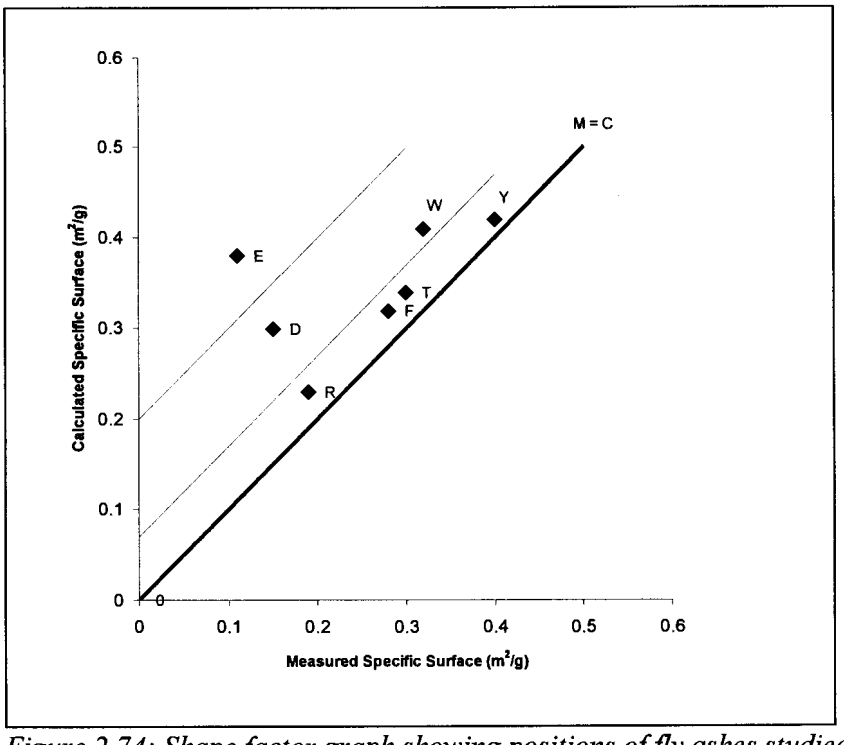

Figure 2.74: Shape factor graph showing positions of fly ashes studied (Hopkins and Cabrera, 1994).

Table 2.17: Water/(cement + fly ash) ratios required by each fly ash concrete to achieve similar workability levels (Hopkins and Cabrera, 1994).

Ash	% Replacement	Water/Binder ratio
E	15	0.675
	30	0.650
	45	0.650
D	15	0.675
	30	0.650
	45	0.612
R	15	0.662
	30	0.650
	45	0.637
F	15	0.650
	30	0.600
	45	0.582
T	15	0.650
	30	0.637
	45	0.612
W	15	0.662
	30	0.637
	45	0.612
Y	15	0.650
	30	0.600
	45	0.600
Cement	100	0.700

The authors claimed that their prediction of workability on the basis of the shape factor is proved by these results. According to them all fly ashes showed some agglomeration and they pointed out that all samples were stored for six weeks before testing. They finally claimed that the ashes closest to the MSA = CSA line proved to contribute the most to good workability (least water needed). Ashes further away had less effect.

The authors concluded by presenting a graph shown in Figure 2.75 showing the overall affect that fly ash with different shape properties have on concrete workability, with:

Zone 1 PFA: Most beneficial for use in concrete and allowing substantial water reductions.
Zone 2 & 3PFA: Producing progressively less improvement in workability
Zone 4 PFA: Unsuitable for use in concrete on account of excessive coarseness or fineness.

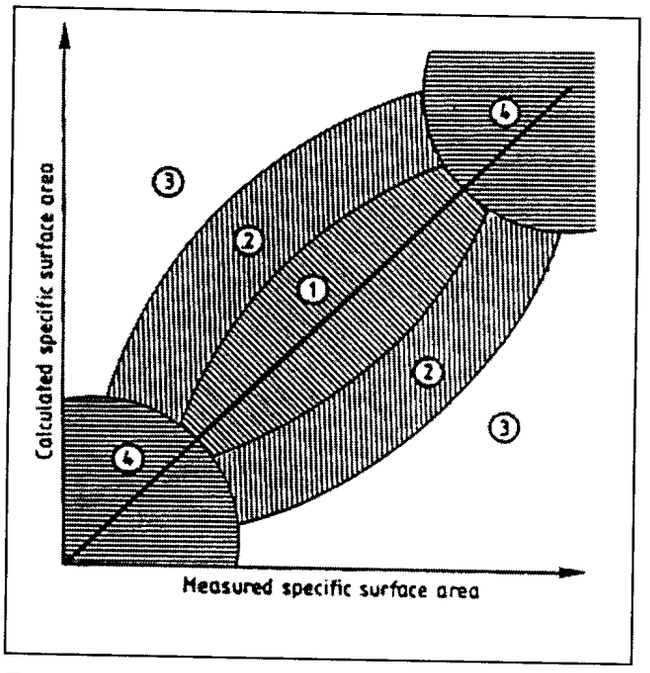

Figure 2.75: Proposed shape factor chart for fly ash classification (Hopkins and Cabrera, 1994).

What is interesting from the torque/speed plots shown in Figure 2.73 for the different fly ashes is the slopes of the different plots remained much the same, indicating that workability only increased in terms of the yield value. Banfill (1994) showed that both yield value as well as plastic viscosity should decrease as a result of fly ash substitution of cement.

Osbeak (1986) investigated the influence of residual carbon in fly ash on the strength development of cement/sand/fly ash mortar. Osbaek explained that the presence of carbon could affect the strength directly by decreasing the pozzolanic reactivity of the fly ash or secondarily by increasing the water demand for constant workability of the paste or by decreasing the air content of the paste. The secondary effects might thus have a negative effect on strength in the former case or a positive in the latter. These two effects might also cancel each other out. By increasing water demand, the water cement ratio is increased thereby resulting in lower strength. By decreasing air content, the density is increased thereby increasing strength.

Tests were performed to assess the pozzolanic activity of fly ash according to ASTM C311. For this test, 35% of cement is replaced by fly ash and the water content is adjusted to obtain constant flow of 100 – 115mm, measured by the flow table technique.

The sand used was ground in a ball mill to fineness of 360 and 720 m^2/kg. For both finesses 4% carbon black was added. The samples were marked SA-1, SA-2, SA-1c (carbon added) and SA-2c, respectively. Fly ash with 10% carbon content was treated at 800°C to burn off carbon. From these two fly ashes (10% carbon and 0% carbon), three further combinations were made containing 2.5% (PFA-2.5), 5.0% (PFA-5.0) and 7.5% (PFA-7.5) carbon. Of the PFA-0 and PFA-10 samples further samples were made by grounding and combining to obtain PFA-0F, PFA-5F and PFA 10F, with Blaine surface increases of about 100 m^2/kg from 360.

To assess the influence on water content on flow, increasing amounts of water were added to all 3 groups of materials. Results are shown in Figures 2.76-78.

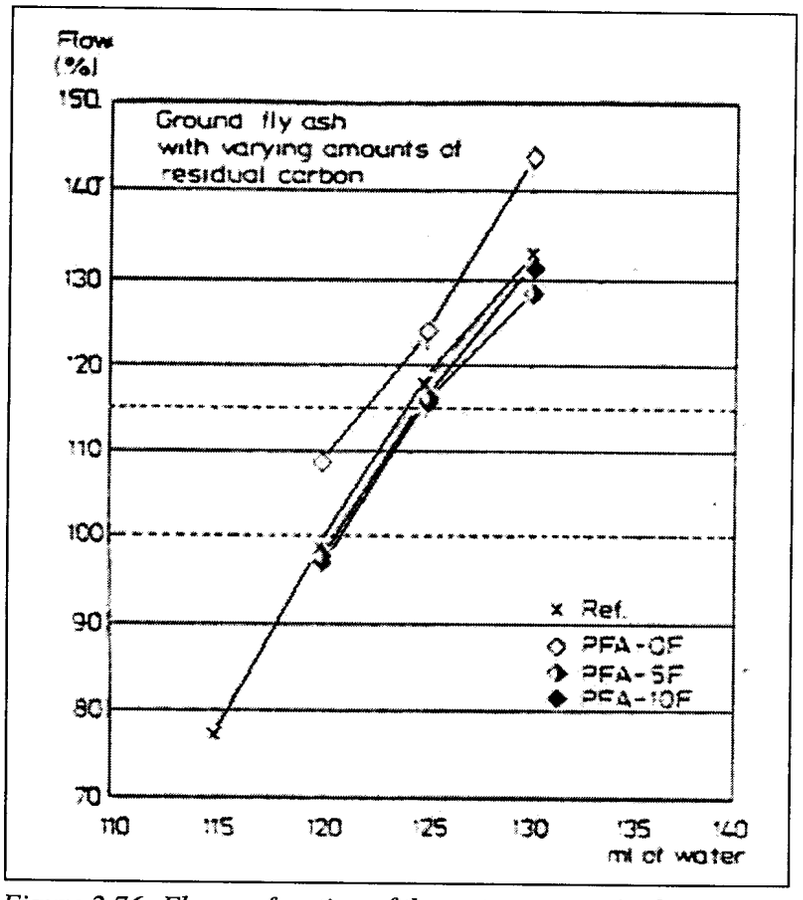

Figure 2.76: Flow as function of the water content in the mortar using ground fly ash with varying amounts of carbon as a 35% cement replacement (Osbeak, 1986).

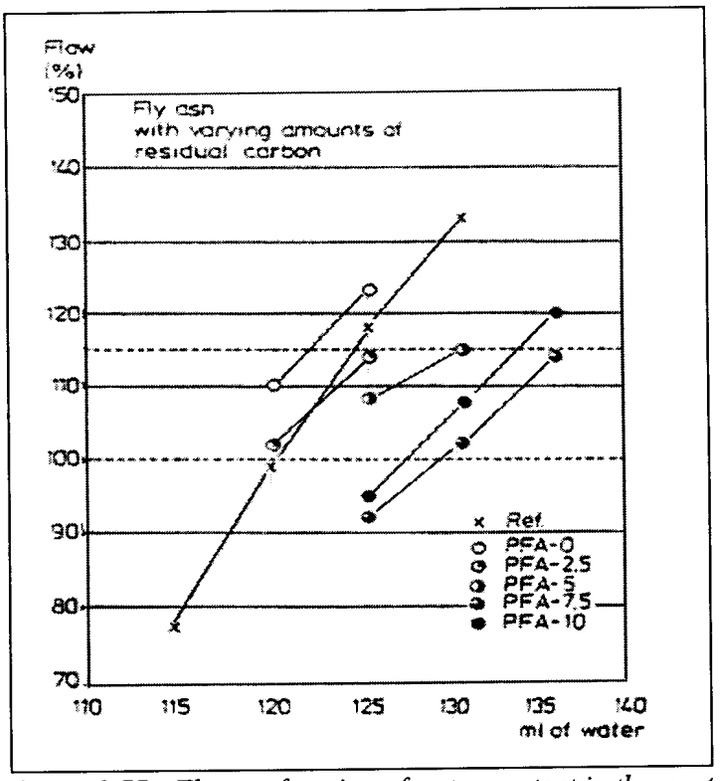

Figure 2.77: Flow as function of water content in the mortar using fly ash with varying carbon contents used at 35% cement replacement (Osbeak, 1986).

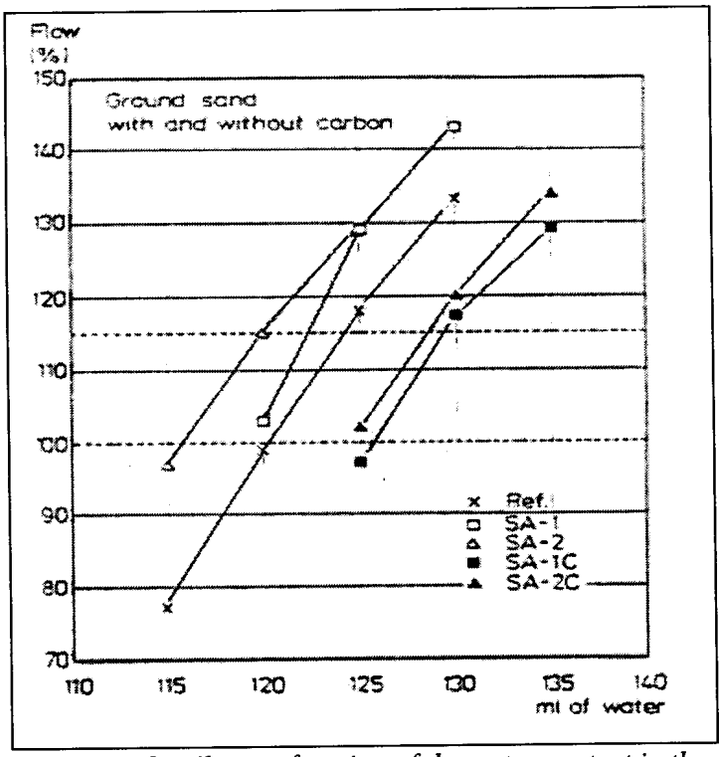

Figure 2.78: Flow as function of the water content in the mortar using ground sand with varying amounts of carbon at 35% cement replacement (Osbeak, 1986).

The results indicate an almost linear relation between water added and flow. Analyses of covariance showed a slope of 3.2% flow per ml of water added. These flow curves were used to estimate the required water demand for the given flow.

Compressive strength (no age was given) values showed little correlation with water demand as shown in Figure 2.79.

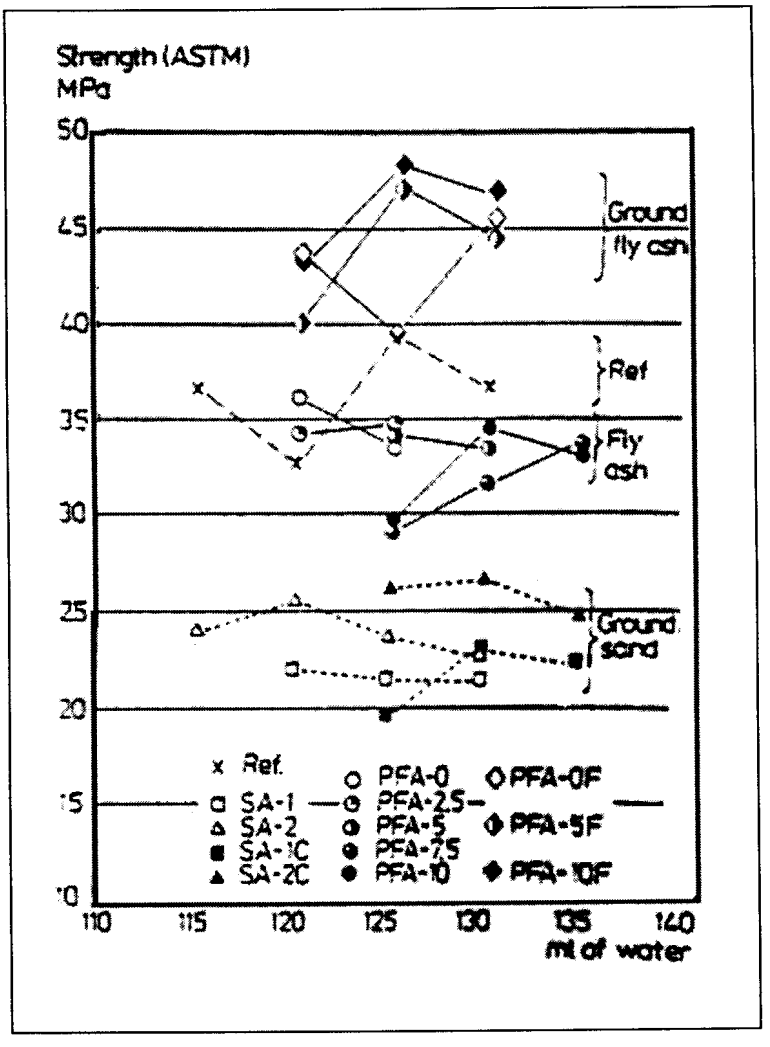

Figure 2.79: Compressive strength as a function of water content in the mortar (Osbeak, 1986).

It is however shown in Figure 2.80 that the water demand does increase with increasing carbon content.

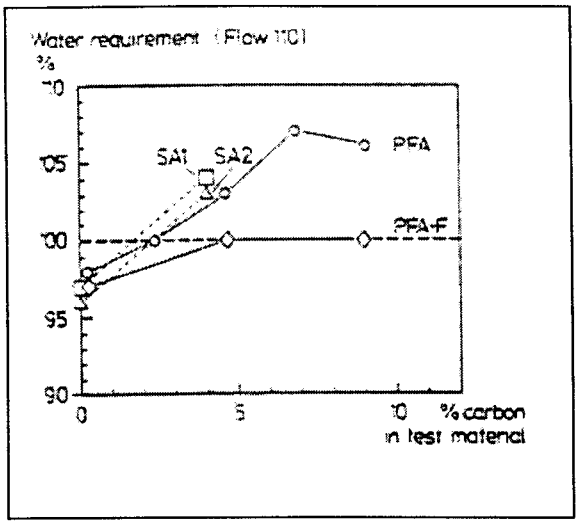

Figure 2.80: Water requirement ratio as a function of carbon content in the replacement materials (Osbeak, 1986).

The strongest influence of carbon on water demand was found for the sand and unground fly ash samples. The author explained that increase fineness of materials tends to decrease water demand, more so for fly ash than for sand.

Figure 2.81 shows the pozzolanic activity index for the different mixtures.

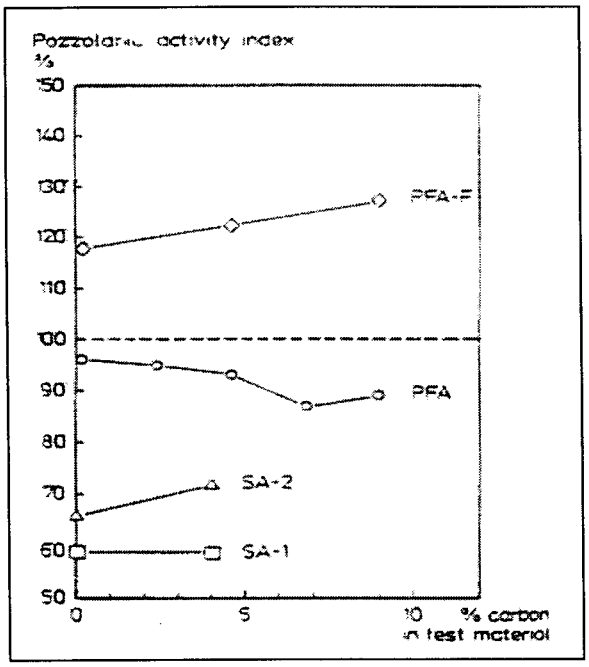

Figure 2.81: Pozzolanic activity index as a function of the carbon content (Osbeak, 1986).

The figure indicates that the pozzolanic index decreased with increasing carbon content only for the normal fly ash. For the ground fly ash and the sand or 'inert fly ash', pozzolanic activity increased with increasing carbon content. The fact that the amount of water added did not correlate with compressive strength proved to be puzzling for the author. He explained that the contribution of the air content factor might explain this as the air content decreased with increased water addition as well as increased carbon content. According to Ferrets `s equation the compressive strength of concrete depends on the water as well as air content:

$$\sigma = F\left(\frac{c}{c + w + a}\right)^2 \qquad \text{(Eq. 2.21)}$$

Where:

σ = Compressive strength
F = Constant relating to the type of cement used
c = Cement content
w = Water content
a = Air content

It is thus shown in this equation that compressive strength should remain constant if the sum of water and air remain constant like is the current case. The author calculated strength values corresponding to Ferret's equation where water and air were given equal values and we can then see in Figure 2.82 that the pozzolanic activity does decrease with increasing carbon content (dotted lines).

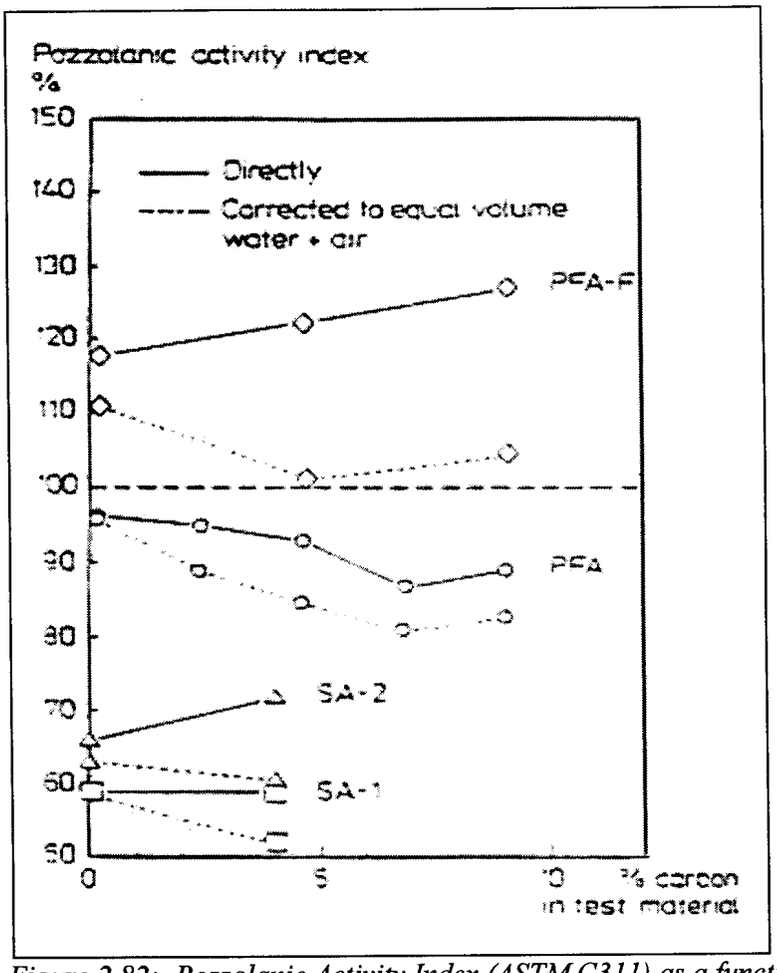

Figure 2.82: Pozzolanic Activity Index (ASTM C311) as a function of the carbon content in the replacement materials (Osbeak, 1986).

The author concluded by saying that carbon in fly ash leads to higher water requirement and changes in strength (or Pozzolanic Activity Index). The effect of carbon on test results can partly be explained by the changes in air content of the mortar caused by the presence of carbon. The air content of mortar is reduced by the presence of carbon, more so if the fly ash has been ground. This reduction in air can have a positive influence on strength, which can reduce or even eliminate the direct effect of carbon on strength (which seems to be a negative one).

In a PhD-thesis, Grieve (Grieve, 1991) investigated the flow properties of concrete containing different South African fly ashes. His methodology included the slump test as well as the coaxial cylinders. For the slump test, concrete mixes containing Matla and Lethabo-fly ash were assessed and compared. Mix-proportions of the different mixes are shown in Table 2.18.

Table 2.18: Mix proportions (kg/m³)

% Fly ash	Materials	w/c = 1.0	w/c = 0.75	w/c = 0.5	w/c = 0.25
0	Water	209	205	203	207
	Cement	209	308	406	518
	Fly ash	0	0	0	0
	Stone	1065	1090	1110	1129
	Sand	979	884	789	675
5	Water	206	201	199	203
	Cement	196	286	378	482
	Fly ash	10	15	20	25
	Stone	1070	1095	1115	1125
	Sand	982	892	797	684
10	Water	203	198	196	199
	Cement	183	267	353	448
	Fly ash	20	30	39	50
	Stone	1075	1100	1120	1130
	Sand	986	895	800	691
15	Water	200	194	193	194
	Cement	170	247	328	412
	Fly ash	30	44	58	73
	Stone	1085	1110	1130	1140
	Sand	985	898	800	701
30	Water	193	188	185	188
	Cement	135	197	259	329
	Fly ash	58	85	111	141
	Stone	1110	1130	1150	1160
	Sand	980	894	803	694
50	Water	186	179	176	179
	Cement	93	134	176	224
	Fly ash	93	134	176	224
	Stone	1135	1160	1180	1190
	Sand	973	890	798	688

Cements from three different sources were used. The amount of water necessary to produce concrete with a slump of 75mm was taken as the test criteria. Figure 2.83 shows the results.

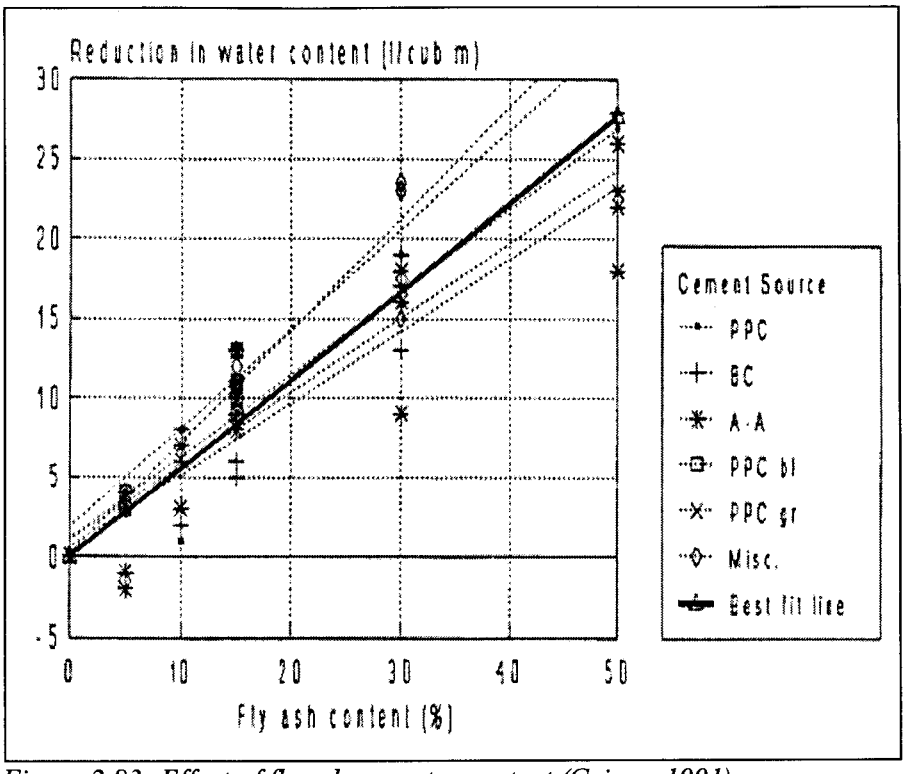

Figure 2.83: Effect of fly ash on water content (Grieve, 1991).

The change in overall grading of the dry materials in the concrete mixture upon introduction of fly ash was also assessed. The overall (including aggregate) grading curves of OPC-cement and a 70:30 OPC/fly ash concrete mixtures are shown in Figure 2.84.

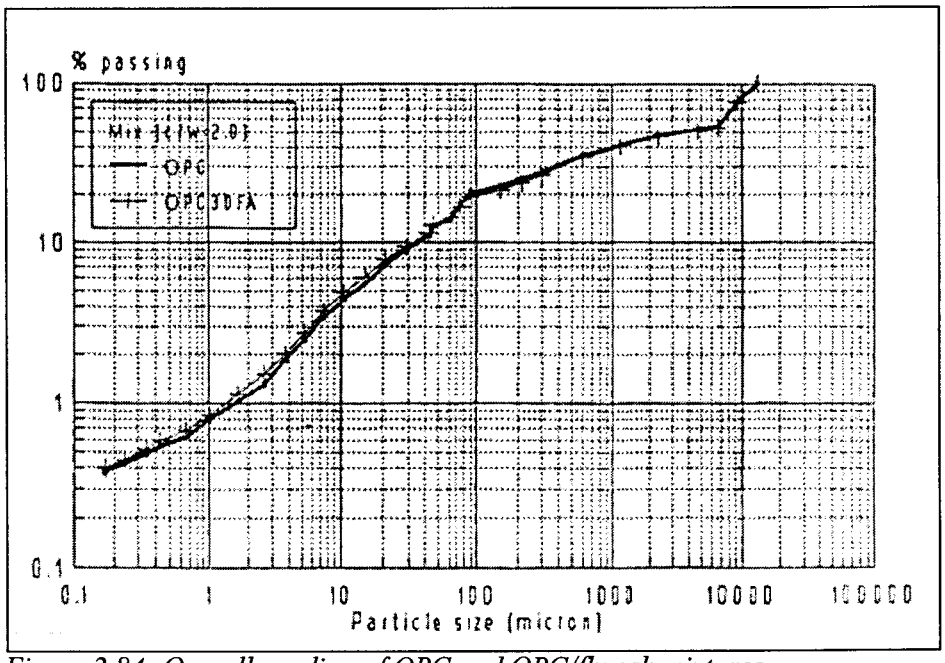

Figure 2.84: Overall grading of OPC and OPC/fly ash mixtures.

It can be seen that there appears to be little difference in the two curves. The author thus suggested that grading of the dry materials does probably not account for the water reduction-effect of fly ash.

The author summarized his findings as follow:

- The partial replacement of cement in a cementitious mix by Matla or Lethabo fly ash improves the flow characteristics of the mix compared to a similar mix without any fly ash in terms of water required to give constant slump.
- Some sources of cement allows for more reduction than others.
- There appears to be no link between the water demand of the type of cement used and the magnitude of water reduction when fly ash is introduced.
- The overall grading of a cement fly ash mixture does not change significantly from that of the cement alone. It is thus not likely that the effect of grading plays a big role in the water reduction phenomenon.
- A first approximation for the magnitude of water reduction which occurs on using Matla fly ash is: Water reduction (l/m^3) = 0.55 x fly ash content (%)
- In the case of Lethabo fly ash the available data suggests that this fly ash is slightly more effective as a water reducer giving a water-reducing constant of 0.59 times the fly ash content (%).

2.5 *Quantification of Particle Size Distribution*

Some researchers have stressed the influence of the particle size distribution or grading of binder materials, filler and aggregate on the workability of fresh binder pastes, grouts and concrete. Schiessl (1990) previously explained that the increased percentage of ultra-fine particles releases water from the interstitial spaces of the bulked particles with a resulting increase in workability. He also found this behavior be more pronounced with coarser cements than for finer ones.

Popovics (Popovics, 1994) proposed the idea that there is an optimum grading for cementitious materials similar to concrete aggregates, so that at a given water content an optimum grading will give optimum consistency. A grading that is significantly finer or coarser than this optimum grading would provide a stiffer mix at the same water content. Popovics concluded from these tests that ground class F fly ash had even more of a plasticizing effect on coarser cements than on finer cements. He claims that this finding proves his hypothesis on optimum grading.

The particle size distribution curve of a material describes two properties of the material namely mean particle size as well as the distribution of other sizes about the mean. The curve is usually drawn as the cumulative percentage-values on the *y*-axis of particles smaller than the corresponding sizes on the *x*-axis. The *x*-axis is drawn to a log scale to accommodate large ranges of particle sizes. The shape of the curve gives an indication of the continuity in size distribution and the slope describes the wideness or range of size-distribution.

Characteristic shapes of curves usually observed describe open graded, gap-graded and continuous-graded materials. Open graded materials consist of mainly single-sized particles. Gap-graded materials consist mainly of a mixture of two sizes of particles with no or very few intermediate-sized particles in between. Continuous-graded materials consist of particles with sizes ranging from a minimum to a maximum size in a normal distribution. The slope of continuous-graded curves decreases with an increase in the difference between the smallest and largest particle sizes. It is generally accepted that a mixture of continuous-graded particles pack denser than mixtures of uniform or gap-graded particles because there are more particles with appropriate sizes to fill gaps between larger particles.

It has been shown by some researchers that parameters for particle size distributions can be quantified. Rosin and Rammler (Rosin and Rammler, 1933) investigated the particle size distribution of crushed coal and found that it can be described by the following function:

$$f(x) = e^{-bx^n} \qquad \text{(Eq. 2.22)}$$

Where b characterizes the fineness of the material and n the slope of the curve. This equation was later modified by Bennett (Bennett, 1936) to:

$$f(x) = e^{\left(\frac{x}{x_0}\right)^n} \qquad \text{(Eq. 2.23)}$$

Where x_0 is known as the absolute size constant. If the weight function, $f(x)$ is denoted R so that

$$R = e^{\left(\frac{x}{x_0}\right)^n} \qquad \text{(Eq. 2.24)}$$

And by substituting x for x_0 gives $R = 1/e$ or R = 0.368 for any value of n. Thus x_0 has a dimension of length and represents 63,2% cumulative passing particles.

Taking the double logarithm of equation 2.24, we obtain:

$$\ln\ln(\frac{1}{R}) = n(\ln x - \ln x_0) \qquad \text{(Eq. 2.25)}$$

This equation describes a straight-line plot with the x-axis made up of values for particle size, x, on a log scale and a y-axis made up of the double logarithm of $1/R$. The slope of the line is described by n. The line intercepts the x-axis at a value describing the particle size x. Sprung (Sprung et al, 1985) has shown that for cements typical values for x_0 and n range from 15μm-30μm and 0.7-1.2 respectively. Hypothetical examples of the diagrammatic representation of the particle size distribution by the Rosin-Rammler distribution function is shown in Figure 2.85 and 2.86.

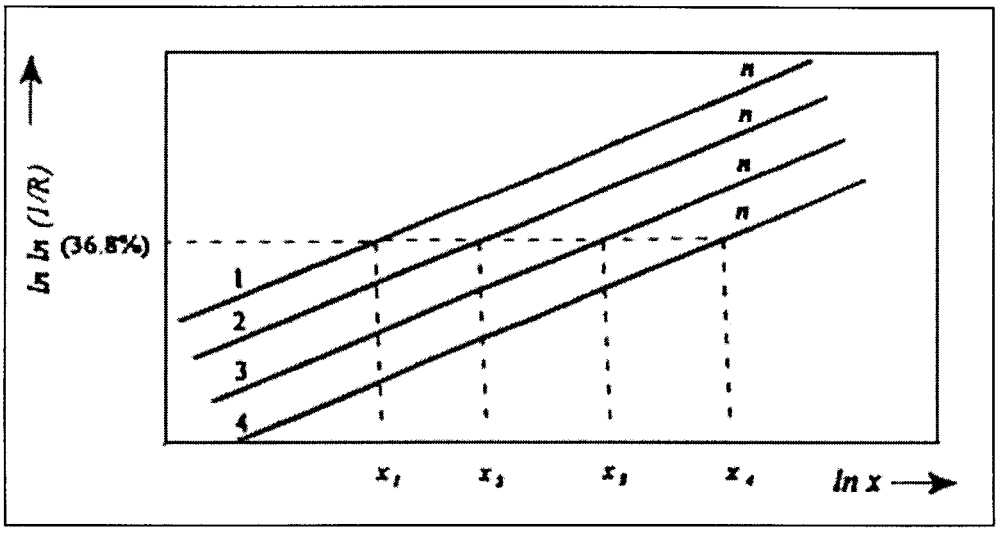

Figure 2.85: Diagrammatic representation of Rosin Rammler distribution function for four samples with constant n and varying x_0 (Wainwright and Olorunsogo, 1999).

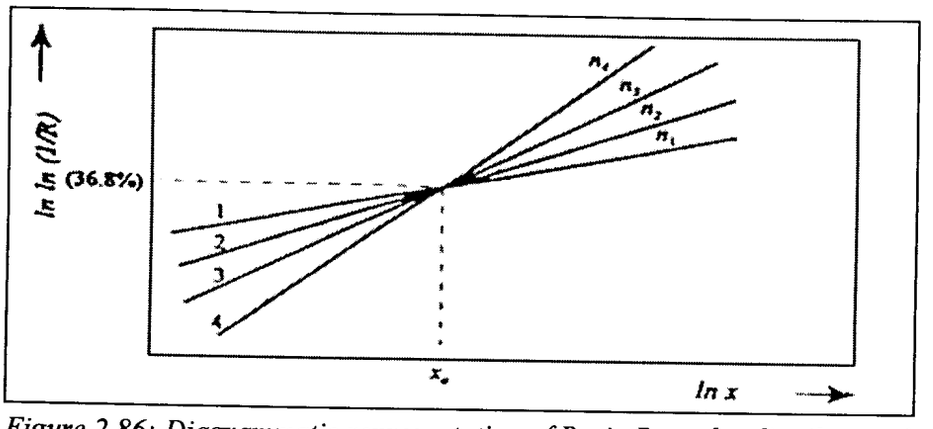

Figure 2.86: Diagrammatic representation of Rosin Rammler distribution function for four samples with constant x_0 and varying n-values (Wainwright and Olorunsogo, 1999).

Figure 2.85 indicates that powders may have similar ranges of size distribution (equal n) but varying degrees of fineness (various x_0). Figure 2.86 indicates a situation whereby the four samples might be of the same fineness (same x_0) but different size ranges.

It was shown by Rendchen (Rendchen, 1985) as well as Sumner (Sumner, 1989) that the mean size of a material, d_p could be calculated if values for x_0 and n are known by using the following equation:

$$d_p = 0.64 \times x_0 \times n \qquad \text{(Eq. 2.26)}$$

Or more accurately by

$$d_p = 1.06 \times e^{(\log_n(x_0) - \frac{0.53}{n})} \qquad \text{(Eq.2.27)}$$

2.6 Fly Ash – Production and variety

Modern thermal power stations normally use powdered (pulverized) coal as fuel. The non-combustible ash leaving the furnaces is called pulverized fuel ash (PFA) and usually consists of bottom and fly ash. Fly ash is the powdery residue that leaves the furnaces with the flue gasses. The fly ash is separated from the flue gasses either by electrostatic precipitators or by filter bags. These precipitators or bags are usually arranged in series of two sections. An example is shown in Figure 2.87.

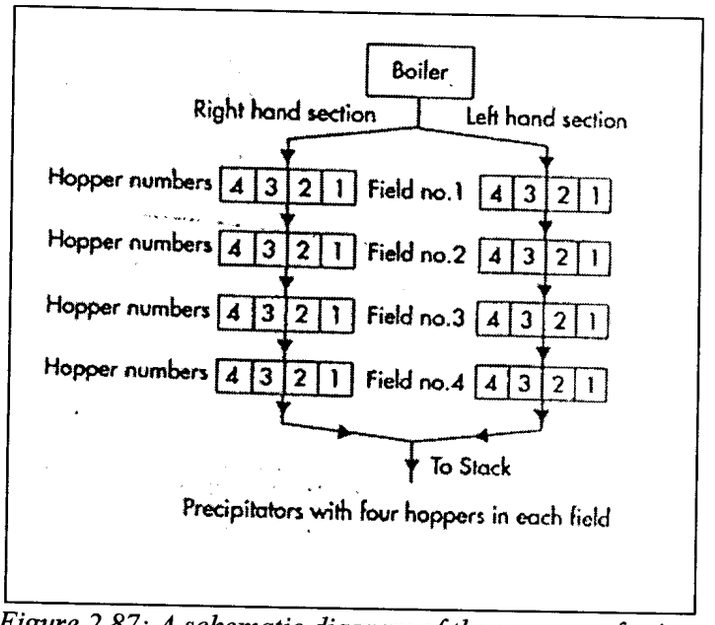

Figure 2.87: A schematic diagram of the passage of exit gases through a four-field electrostatic precipitator arrangement of a thermal power station (Kruger, 1999).

In South Africa, the power stations are situated on the coalfields in the north of the country. Figure 2.88 shows the locations of the major pulverized coal-fired thermal power stations in South Africa.

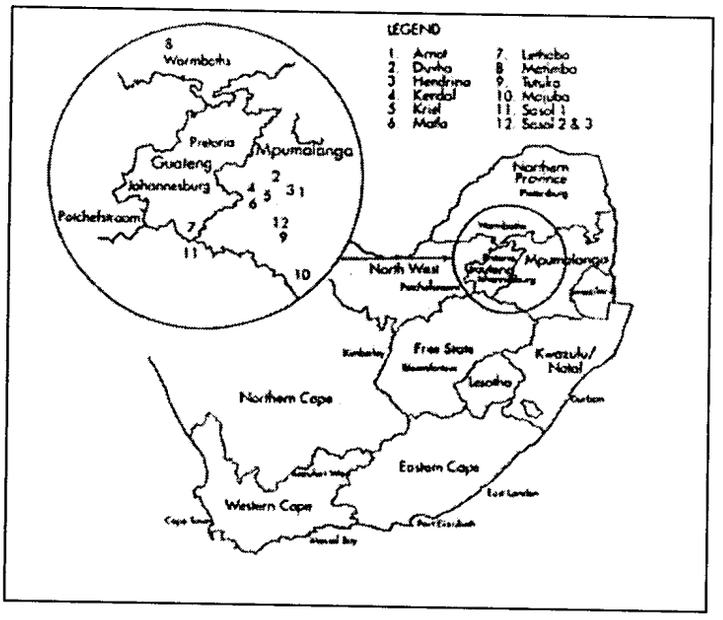

Figure 2.88: Locations of important pulverized coal-fired thermal power stations in South Africa (Kruger, 1999).

Table 2.19 shows the fly ash production output of these power stations.

Table 2.19: The production of fly ash by pulverized coal-fired power stations in South Africa in 1996 (Kruger, 1999).

Power Station	**Locality**	**Production (tons)**
Arnot	Middelburg, Mpumalanga	550 000
Duva	Witbank	400 000
Hendrina	Hendrina	1575 000
Kendal	Witbank	3500 000
Kriel	Bethal	2000 000
Matla	Bethal	2700 000
Lethabo	Sasolburg	5300 000
Matimba	Ellisras	4950 000
Tutuka	Standerton	1765 000
Majuba	Amersfoort	213 000
Sasol 1	Sasolburg	750 000
Sasol 2 &3	Secunda	4000 000
	Total	27703 000

Variations in fly ash can be chemical or physical in nature. These differences can be origin and production related.

Fly ash can chemically be divided into four classes; C, F, N and S. Class C and F are by far the most abundant. Class F fly ash is produced as a result of burning anthracite or bituminous coal. Anthracite is a hard coal with few volatile hydrocarbons. Bituminous coal on the other hand is much more volatile. The fly ash produced usually has a calcium oxide (CaO) content of less than 10% and little or none self-hardening cementitious properties.

Class C fly ash is produced as a result of burning sub-bituminous and lignite coal. Lignite coal is brown with a distinctive woody texture and burning produces a fly ash with a CaO content of 15-30%. Sub bituminous coal has properties intermediate between bituminous and lignite coal and burning produces fly ash with a CaO content of 8-20%. Class C fly ashes are therefore has a CaO

content of larger than 10% and thus has self-hardening cementitious properties in excess of that of class F fly ash (Kruger, 1999).

Fly ash produced in South African power stations mostly fall into the class F-category with CaO content of less than 10%.

Bosch and Willis (1990) performed tests on three South African fly ashes, Lethabo, Matla and Duva fly ash and found the following differences:

- Particle size distribution for Duva field 4 fly ash were slightly coarser than field 4 fly ash of both Lethabo and Matla, which may be due to the coarser particle size of ground Duva pulverized coal.
- The glass content was the highest in Matla and the lowest in Duva
- Mullite was low in Matla but high in Lethabo and Duva
- Quartz was highest in Duva
- Lime was highest in Matla and lowest in Lethabo

Grieve (1991) assessed the properties of concrete made with Lethabo and Matla fly ash. He documented the differences between the two coal sources as well as the two fly ashes as shown in Tables 2.20 and 2.21.

Table 2.20: Analyses of coal samples (Grieve, 1991).

Parameter	Matla (%)	Lethabo (%)
Inherent moisture	4.95	5.90
Ash	23.20	36.45
Carbon	56.49	42.81
Hydrogen	3.46	2.68
Nitrogen	1.35	1.17
Total Sulpher	0.99	0.61
Carbonates (as CO_2)	1.66	1.43
Oxygen (difference)	7.92	8.96
Calorific Value (MJ/kg)	21.87	16.11

Table 2.21: Chemical analyses of fly ash (Grieve, 1991).

Parameter	Matla (%)	Lethabo (%)
SiO_2	50.85	52.55
Al_2O_3	26.40	29.75
Fe_2O_3	4.35	3.95
TiO_2	1.35	1.55
P_2O_5	0.95	0.45
CaO	8.55	5.45
MgO	2.20	1.35
Na_2O	0.50	0.20
K_2O	0.95	0.50
Equiv Sodium (as Na_2O)	1.13	0.53
SO_3	1.95	2.10
MnO	0.04	0.03

It can be seen that Matla coal contains more carbon than Lethabo coal and therefore has a higher calorific value. Matla fly ash also contained a higher CaO content, which is in accordance with findings of the previous researchers already mentioned (Bosch and Willis, 1990).

Variations in properties of fly ash can also occur within one power station using the same source of coal. Two studies by the NBRI (NBRI, 1983) and Bosch (Bosch and Willis, 1990) has concluded that:

- The amount of ash collected decreased from 70% in the first field to 1-2% in the last field
- The amount of SiO_2 decreases in concentration with increasing field number
- The sulfate and alkali contents increased slightly from the first to the last field
- The average particle size decreased as shown in Figure 2.89.

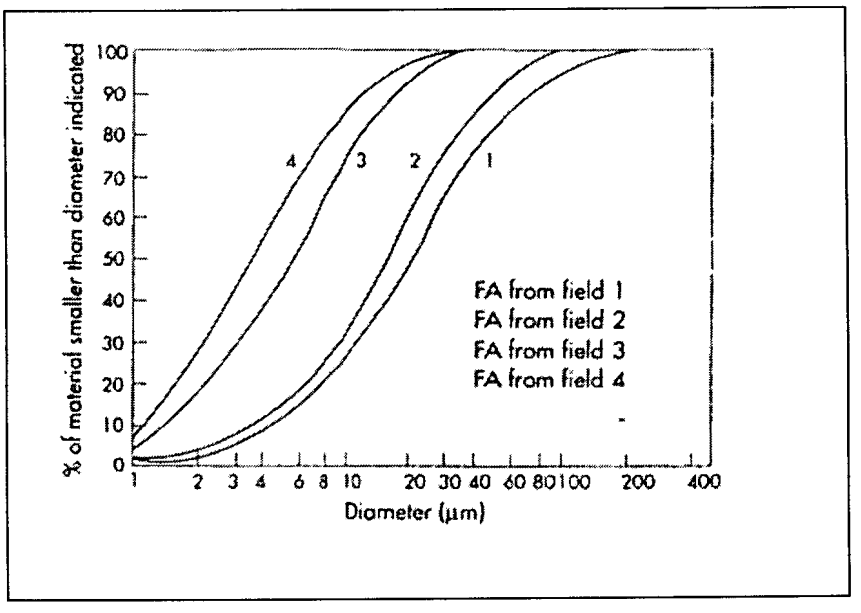

Figure 2.89: Typical particle size distribution curves for fly ash from a pulverized-coal-fired power station (Kruger, 1999).

Lee et al (1999) has also shown that regardless of boiler conditions, the fly ashes collected from three fields increased in fineness, specific gravity and glass content going from the first collector field to the third, but SiO_2 content decreased. He also showed that when the boiler is operated at full-operating load (600MW) in comparison with operating at half load (300MW), the glass content was greater, but the Blaine surface area and carbon content was lower.

2.7 The Assessment of the Quality of Pulverized Fuel Ash

Requirements for fly ash for use in concrete has been developed by countries and is described in standard specifications like BS 3892 (1997), ASTM C618 (1998) as well as SABS. Amongst others, two of the assessment parameters namely the fineness and pozzolanic or strength activity will be reviewed.

The fineness requirement is usually expressed as the weight percentage of particles that is retained on the 45µm sieve after wet-sieved. British (BS 3892, 1997) as well as South African (SABS 1491, 1998) standards require that no more than 12.5% by mass of material may be larger

than 45 μm. USA (ASTM C618, 1998) standards are less strict and require that no more than 34% of material be retained. Some researchers including Hughes (1994) has strongly criticized the fineness specification and argued that fly ash cannot be specified a single size parameter and that the overall size distribution should be taken into account.

Another standard assessment parameter adopted by countries is the pozzolanic or strength activity index with Portland cement. In the USA (ASTM C311, 1998) as well as British Standards (BS 3892, 1997) the cementitious effect of fly ash in concrete when a certain percentage of cement is replaced by fly ash is quantified and defined as the strength or pozzolanic activity index of the fly ash. This factor is determined as the strength ratio of mortar cubes prepared by replacing part of cement by fly ash to that of control-mixture cubes containing no fly ash. For these tests the water reducing effect of the fly ash is also taken into account. This is done by amending the water content of the fly ash-containing mixtures so that the same workability as that of the control mixture is obtained as measured by the flow-table method. The strength ratio can thus be affected by the cementitious contribution of the fly ash as well as the reduction of the water demand for constant workability.

With the ASTM method, the samples is cured in saturated limewater at 23±2°C and compressive strength tests done at either 7 or 28 days. The compressive strength of the test mortars where 20% by mass of cement used for the control mortar has been replaced by fly ash are required to be at least 75% of the control. For the BS-method samples are cured in water at 23±2°C and tested at 28 days with compressive strength required to be at least 80% of the control after replacement of 30% of cement. Helmuth (1994) recommended that the ASTM 311-method should be modified by amending the sand content instead of the water content of mixtures containing fly ash as to obtain constant workability.

South African specifications (SABS 1491, 1998) and test method (SABS TM 1153) describe the reactivity of fly ash with 100% hydrated lime. In the test a mixture is made up of 150 grams of hydrated lime and twice as much PFA by volume. Enough water is added to achieve a flow value of 100-110% as measured by a flow table. The mortar stored in a sealed container, which also serves as the mould, for 6 days at 53-56°C where after compressive strength is measured with a limit of 5 MPa being specified.

SABS 1491 (1998) also specifies a minimum water requirement for fly ash when used as a Portland cement extender. The test is described in SABS TM 1156 (1998) where a control

mixture is made up of 450g of cement, 1350g of standard sand and 225ml water. The workability is measured with a flow table. In the test mixture 292.5g of cement is mixed with 157.5g x ($\rho_{fly\ ash}/\rho_{cement}$) fly ash and 1350g standard sand. The amount of water to achieve the same flow as for the control mix is determined which must be less than 95% of that for the control mixture.

2.8 Summary

The purpose of the literature survey was to gain background knowledge with regards to the workability of cementitious pastes, grouts and concrete. Workability can be defined as the amount of shear strain experienced by a unit volume of a fluid or suspension subjected to a certain level of shear stress. For concrete or cementitious pastes the water content of these mixtures is the main contributing factor to workability. The strength of concrete is a function of the water/cement ratio thus it is inevitable to minimize the water content of a mixture as to conserve strength. However to process concrete a minimum level of workability is usually required for placing, especially in cases where narrow moulds must be filled or where reinforcement bars are closely spaced.

Requirements for workability is usually specified for an application and measurement techniques have been developed over many years. Most standard techniques are termed one-point tests where the amount of shear strain of freshly mixed concrete is measured as a result of standard shear stress at a single level. It has however been shown by researchers like Tattersall (1991) that concrete is a Bingham fluid and that its workability should be measured at more than one shear stress level. This will enable the prediction of the workability of concrete when processed at different levels of shear.

The partial replacement of cement in concrete by pozzolanic extenders like fly ash has proved to be advantageous in terms of workability, economics, late strength and durability. Fly ash is a by-product of coal combustion for the provision of electricity thus its use also makes it environmentally friendly. Its effect on workability has been studied in dept in most cases it was found that it reduces the water demand of concrete mixtures where a certain level of workability is required. In addition its pozzolanic nature results in increased later strength. Many researchers have attributed the water reducing effect of fly ash to surface smoothness and spherical nature as well as to its dispersing effect on cement particles. Other researchers have claimed that fly ash contributes to an optimal particle size distribution of the cement/fly ash binary system in a mix

which in turn improves the packing of particles thus reducing the amount of inter particle spaces.

The use of fly ash in concrete as a replacement and extender for Portland cement has been controlled in countries by development of standard requirements. These requirements have set limits for chemical as well as physical properties; some of these requirements have been questioned and criticized as being arbitrary. The requirements reviewed in this study included requirements for particle size as well as strength or pozzolanic activity. Most size requirements limit the percentage by mass of material that is retained on a 45μm sieve. The requirements for strength activity is based on the ratio of compressive strength obtained for a test sample where part of cement was replaced by fly ash to that of a control sample containing no fly ash, both subjected to the same specified curing regime. The water reducing effect of the fly ash is usually taken into account as tests are performed at constant workability thus the water content of the test mixture is appended so that it has the same workability as the control sample.

2.9 Conclusions

In this literature review the importance of using two-point methods to measure workability was shown and it was decided to use such a method for the experimental part of this dissertation. The aim of this dissertation is to assess the effects of PFA particle size on the workability of cementitious pastes, therefore an accurate and reliable method of measurement had to be established first. After considering mixer-type tests, coaxial cylinders, slump flow and the J-tube test, it was decided to use the latter. Trial tests on pastes using a mixer type apparatus gave insufficient magnitudes of variation between different mixtures where workability was increased by increasing the water content in relatively small increments. An attempt was made to perform the slump flow test on these pastes but apart from the fact that all mixtures showed collapsed slump, the rate of slump was too rapid to measure. Apart from its simplicity, trial tests using the J-tube showed sufficient differences between pastes. It was decided to design a data logging system for the J-tube test by using a load cell, computer and appropriate software. This made it possible to log sufficient data directly during flow thus minimizing the risk of operator errors.

3 EXPERIMENTAL PROCEDURE

3.1 Background

An experimental program was set up to assess the influence of replacing relatively large amounts of cement by different types PFA from one source on paste workability and compressive strength. To assess the effect of PFA particle size, shape and size distribution on paste and mortar properties five different types of PFA with different particle size and distribution properties but similar chemical content were tested. The five PFA-types were produced at the same power station and they all originated from the same stock material. For the experiments, one type of cement was used. This made it possible to relate any differences in workability of mixes to the type of PFA used.

Workability tests were performed on pastes containing the different types of PFA and cement alone as well as blended pastes containing PFA and cement at ratios of 2:1 for PFA and cement.

Several tests were performed on all raw materials as to establish their properties. These properties where then used as parameters to try and explain their influence on paste workability and mortar strength.

3.2 Introduction

Cementitious pastes, containing only cementitious materials and no aggregate, are used for different applications including the production of foamed concrete (Kearsley & Wainright, 1999) and the production of road repair grouts. Relative large amounts of fly ash have been used as a cement replacement material (up to 67% by mass of cement) for the production of foamed concrete (Kearsley & Wainright, 1999), primarily for economical purposes. Fly ash has been used as a sand replacement material for the production of road repair grouts primarily to increase workability and also to eliminate segregation of sand particles. The aim of this dissertation is to assess the influence of PFA particle size on the workability of cementitious pastes containing relative large amounts of PFA as well as cement.

In order to establish an accurate and reliable workability test method a thorough literature survey was conducted related to workability testing and the effects of PFA on concrete and cementitious pastes. It was decided to use both a one-point as well as a two-point method for workability tests. Trial tests were performed using the slump and modified slump test, mixer-type workability test, flow table test and J-tube test. Several trial-mixtures were made and workability was varied by varying the water content in relative small increments. The slump and modified slump tests proved to be inadequate methods because firstly the mixtures showed collapsed slump and secondly the rate of slump was too

rapid to measure. Results obtained with the mixer type workability test did not show clear differences between mixtures, as the magnitude of change in workability was too small. The flow table and J-tube tests proved to be the only adequate one and two-point methods to use, as results were well defined and repeatable.

The effects of PFA size properties on workability was assessed in terms of the water content necessary to produce pastes with constant workability. It was thus decided to vary the water content of mixtures containing each type of PFA as to obtain a relation of viscosity as a function of water content (in terms of water/binder ratio) for each. This made it possible to interpolate and calculate the water/binder ratio necessary for each PFA-type to give a certain level of workability.

It was decided to measure compressive strength of cubes made from each mixture after subjected for 28 days to mild curing conditions. This was done in order to assess the effect of different PFA-types on compressive strength when constant workability is required. Mild curing conditions were employed in order to simulate real conditions and also to limit the pozzolanic contribution of the PFA to strength and thus relate any differences in strength to water demand for constant workability.

3.3 Material Properties

3.3.1 Particle size distribution

The five different types of PFA (A-E) were supplied by Ash Resources and where produced at the Lethabo power station. As the materials were produced from the same source of coal and under the same conditions they differed only in terms of particle size and distribution. The PFA-types are produced and sold by the suppliers as different products thus it was the ideal source of material with regards to the aim of this investigation. Figure 3.1 shows a schematic diagram of their size ranges, as obtained after fractioning. The stock material, PFA-A, was fractioned by electrostatic precipitation into PFA-B, C, D and E. Firstly PFA-A was fractioned into PFA-B and E. This was done in order to obtain a material (PFA-B) that comply to SABS specifications (SABS 1491, 1989) regarding size for PFA which states that no more than 12.5% of particles may be greater than 45μm (R_{45}-value). Thereafter PFA-B was fractioned into PFA-C and D in order to produce an ultra-fine material (PFA-C). The two top-sided fractions produced after fractioning, PFA-D and E, are also referred to in the industry as tailings.

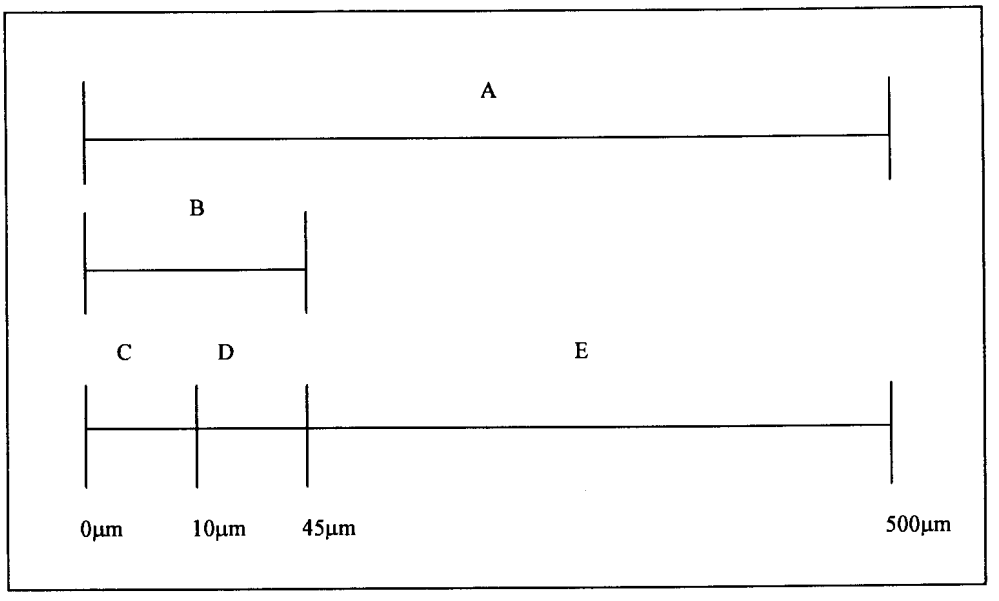

Figure 3.1: Particle size ranges of the types of PFA used.

The Particle size distributions were determined using a Malvern particle size analyzer. Particle size distribution curves are shown in Figure 3.2. The particle size distribution of the PFA-types was used to determine D10, D50, D90 and R_{45}-values as indicated in Table 3.1. D10, D50 and D90-values are the particle sizes where 10%, 50% and 90% respectively of the particles (per mass) are smaller than the given value. The R_{45}-value is the percentage of material larger than 45μm. As explained earlier the latter is used in countries like South Africa, Britain and the USA as a standard classification parameter. From Table 3.1 it can be seen that PFA types B and C complies to the R_{45}-specification with values of 7% and 2% respectively. PFA-A, D and E has R_{45}-values of 36%, 13% and 76% respectively and thus do thus not comply with the R_{45}-specification.

The cement used was supplied by PPC and is a SABS CEMI 42.5R. This is a relatively fine and reactive cement (Blaine surface area of 4500cm^2/g) and is used where high early strength is a requirement.

Table 3.1: Properties of all materials.

Material		PFA-A	PFA-B	PFA-C	PFA-D	PFA-E	CEM I 42.5R
R_{45} (%)		36	7.0	2.0	13	76	7.0
D10 (μm)		2.8	2.2	1.8	5.8	11	3.3
D50 (μm)		26	10	5.5	18	92	12
D90 (μm)		143	38.0	12.0	53.0	225	40.0
GM (1/mm)		527	711	942	457	274	616
RD		2.18	2.12	2.32	2.16	2.11	3.11
Grading Slope (*n*)		0.74	0.97	1.67	1.27	0.91	1.1
Surface Area (cm^2/g)	CSA	2737	4299	5708	2378	1241	3589
	BSA	2850	3600	5500	2500	ND*	4500

* Not Determined. The material was too coarse for Blaine-measurement.

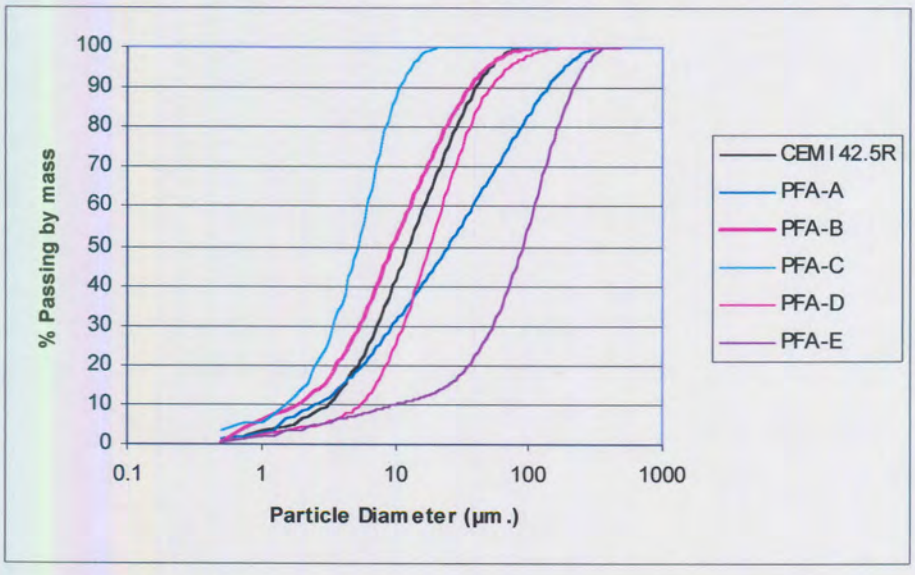

Figure 3.2: Particle size distributions for materials used.

3.3.2 *Relative Density*

Relative Density (RD) measurements were performed with an Accupyc picnometer-apparatus. These values were used for further calculation of surface area. Values for RD can be seen in Table 3.1.

3.3.3 Surface Area

The surface area of the different PFA-types as well as the cement used was determined according to the Blaine-method. A theoretical surface area was also calculated using sphere-geometry in order to calculate shape factor-values as described by Hopkins and Cabrera (1994). The shape factor is an indication of the proportion of the particles that are spherical and is determined as the ratio of the measured surface area to the calculated surface area. A value of one indicates that all particles are spherical in shape.

The Blaine surface area was determined by measuring the air flow-rate through a bed of material with a porosity of 0.51 compacted in a cylinder. To perform the test the relative density of the material must be determined. When the relative density is known the mass of material needed to result in a porosity of 0.51 given the cylinder-tube volume can be then be calculated.
The following equation is then used to calculate the surface area:

$$S \approx \frac{C}{\rho} \times \sqrt{t} \qquad (3.1)$$

Where:

S = Blaine Surface Area (cm^2/g)
C = Instrument constant
ρ = Density of material (g/cm^3)
t = Average time in seconds for the fixed volume of air to pass through the compacted bed.

The theoretical surface area, referred to as the Calculated Surface Area (CSA) was calculated by multiplying the proportion of particles between two successive sieve sizes by the surface area calculated for the average of the two sieve sizes using the following equation:

$$SA_x \approx \frac{6}{\rho \times \frac{D}{10000}} \qquad (3.2)$$

Where:

SA_x = Surface area of particles with a diameter of χ µm

ρ = Density of material (g/cm^3)

D = Average diameter of particles between the two successive sizes.

It was assumed that the particle size distribution between the two sizes vary linear to a log scale. The measured and calculated surface areas for the materials are listed in Table 3.1.

3.3.4 *Grading Modulus*

The Grading Modulus (GM) of the materials was calculated as described by Hughes (1989; 1996) and Cornelissen (1998). The procedure is similar as for the calculation of CSA. The following equation is used:

$$GM = \frac{6(\frac{1}{D1} - \frac{1}{D2})}{\ln \frac{D_2}{D_1}} \tag{3.3}$$

In the formula, D1 and D2 represent the diameters of the smallest and largest size particles of a group between two successive sieve sizes. Between these two sieves the size distribution is assumed to vary linear to a log scale. The GM-values for each of the materials used in this study can be seen in Table 3.1.

3.3.5 *Particle Size Distribution*

In order to quantify the effect of particle size distribution, two values for the slope of the grading curve was calculated. The first is an empirical value based on the Rosin-Rammler distribution theory. The distribution index, n, was calculated using the following equation:

$$n = \frac{\ln \ln \left(\frac{1}{R}\right)}{\ln x - \ln x_0} \tag{3.4}$$

Where: R = % Retained at sieve size x

x_0 = Size where 63.2% passes

The parameter n is thus the slope of the line described by:

$$\ln\ln\left(\frac{1}{R}\right) = n(\ln x - \ln x_0) \tag{3.5}$$

The second parameter, the G10/90, is the calculated grading slope by regression analyses of the particle size distribution (grading) curve between D10 and D90 on a log scale. This value was determined only for comparative purposes, current technology and the development of mathematical software programs has made it possible to perform regression analyses in the matter of seconds.

3.3.6 Chemical analyses

Chemical analyses were performed on the materials used by means of X-ray fluorescence. Chemical compositions are shown in Table 3.2. The results indicate that the chemical compositions of the PFA samples tested are substantially the same. PFA-C does seem to have less SIO_2 and more Al_2O_3 than the others four PFA samples.

Table 3.2: Chemical analyses of materials.

%	CEM I 42.5R	PFA-A	PFA-B	PFA-C	PFA-D	PFA-E
SiO_2	21.25	54.93	54.1	50.99	55.85	55.58
TiO_2	0.29	1.55	1.6	1.74	1.54	1.47
Al_2O_3	4.07	31.51	32.37	34.24	31.19	29.93
Fe_2O_3	1.96	3.34	3.13	3.11	3.07	4.0
MnO	0.21	0.03	0.03	0.03	0.03	0.03
MgO	1.82	1.16	1.18	1.39	1.06	1.17
CaO	65.17	4.69	4.52	4.88	4.2	5.33
Na_2O	0.27	0.24	0.26	0.25	0.27	0.22
K_2O	0.42	0.63	0.68	0.72	0.65	0.60
P_2O_5	0.05	0.37	0.43	0.68	0.3	0.31
Cr_2O_3	<0.01	0.03	0.04	0.04	0.04	0.03
NiO	<0.01	<0.01	<0.01	<0.01	<0.01	<0.01
V_2O_5	<0.01	0.03	0.03	0.03	0.02	0.02
ZrO_2	<0.01	0.05	0.06	0.05	0.05	0.05
LOI	2.57	0.21	0.1	0.24	-0.22	0.22
TOTAL	98.11	98.78	98.53	98.41	98.07	98.98

3.4 Test Methods

3.4.1 Standard workability tests

Standard tests conducted included the slump as well as flow table tests. A standard slump cone and plate was used for the slump test. The cone had base and top diameters of 200mm and 100mm respectively and height of 300mm. Procedures was carried out according to SABS Method 862-1 (1994). Materials were compacted in three layers, tamping each layer 25 times with a tamping rod. Measurements were taken to the highest point of the specimen tested.

Flow table tests were performed according to BS. 1881: Part 105: 1984 using a standard flow table test-apparatus. The flow plate had a diameter of 255mm. The form-cone of the apparatus was 50mm high. The top and bottom diameters were 70mm and 100mm respectively. The plate was lifted and dropped by means of a built-in device. This enabled the lift-and-drop procedure to be uniform for every repeat. The flow diameter was calculated as the slurry-cone diameter after 15 drops.

3.4.2 J-tube tests

The j-tube was made from 67mm diameter PVC pipe and bend-fittings. Figure 3.3 shows a schematic diagram of the tube.

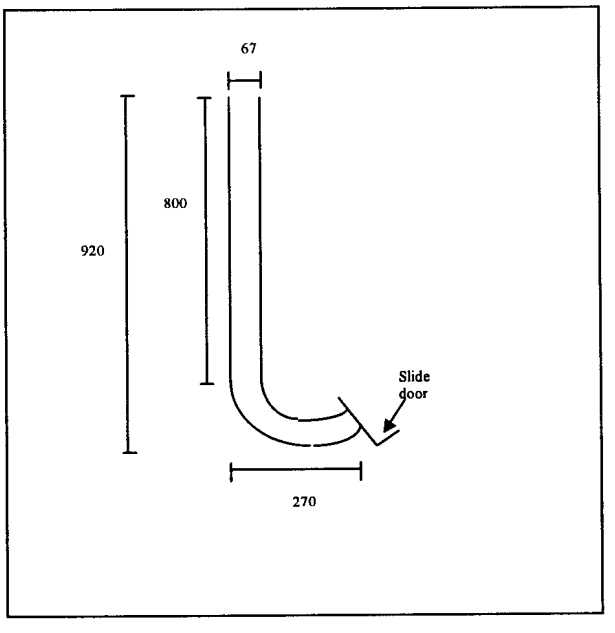

Figure 3.3: The j-tube-apparatus with dimensions in mm.

Figure 3.4 shows the j-tube apparatus set-up. The tube was mounted onto a load cell connected to a signal amplifier and computer. By using software, it was thus possible to log the mass loss of the

slurry-filled j-tube over time (every 0.1 seconds) as the flow proceeded. A shallow bin was put under the lower mouth of the tube to catch the out-flowing slurry.

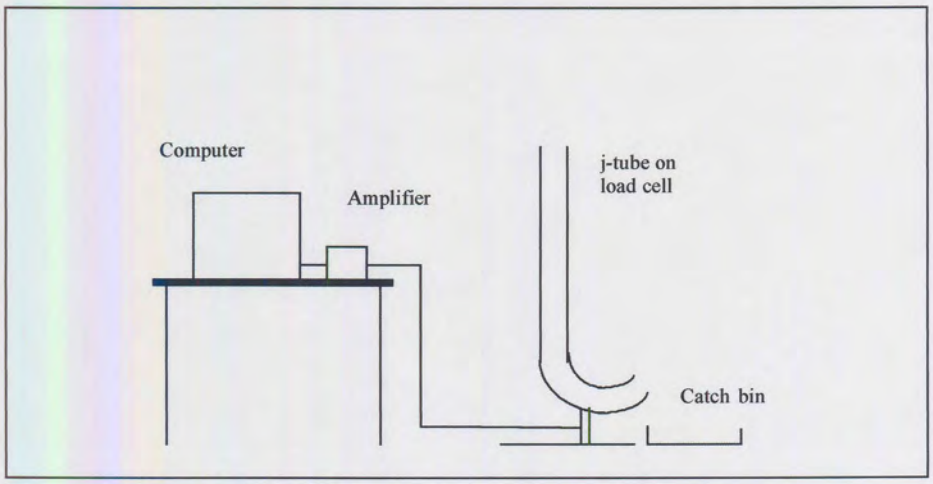

Figure 3.4: Set-up of the j-tube tests.

Calculation of yield stress and plastic viscosity was done as described by Govier (Govier, 1972) for laminar flow in capillary tubes. A typical flow curve is shown in Figure 3.5. The results in this graph are for mixtures that differed only in water/binder ratio. As the water/binder ratio of the mixtures is increased, their flow rate also increased resulting in a steeper slope for the mass/time-graph. This relates to a decrease in viscosity. The end height of the slurry in the tube when flow seizes relates to the yield stress of the slurry. The higher the end height the higher the yield stress.

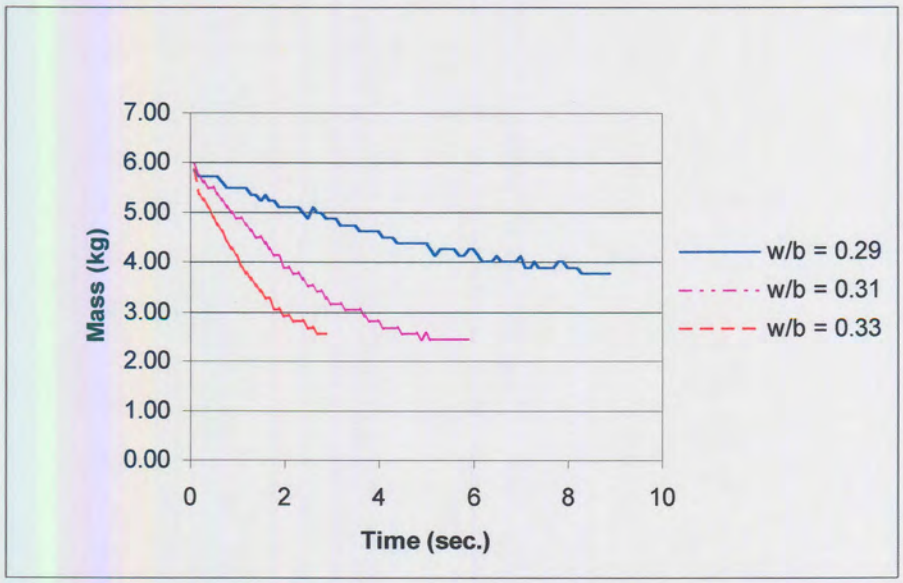

Figure 3.5: Typical flow curves for slurries.

The average fluid velocity (V) was calculated using the following equation:

$$V = \frac{4Q}{\pi D^2} \tag{3.5}$$

Where:

V = Average fluid velocity (m/s)
Q = Volumetric flow rate (m^3/s)
D = Inside diameter of tube (m)

The shear stress at the tube wall was calculated using the following equation:

$$\tau_w = \frac{D\Delta P}{4L} \tag{3.6}$$

Where:

τ_w = Shear stress (Pa)
L = Effective length of tube (m)
ΔP = Pressure drop due to elevation (Pa)

The rate of shear at the tube wall was calculated from the following equations:

$$S = \frac{1+3n}{4n} \times \frac{8V}{D} \tag{3.7}$$

Where S = Rate of shear (1/s) and;

$$n = \frac{\partial \ln \frac{D\Delta P}{4L}}{\partial \ln \frac{8V}{D}} \tag{3.8}$$

Cementitious pastes are a believed to be Bingham fluids, thus a τ_w versus S plot should be linear with the τ_w-axes intercept value being the yield stress and the slope of the plot the viscosity. Shear stress

and shear rate values was calculated and plotted. Figure 3.6 shows the shear stress versus shear rate plot for the same mixtures shown in Figure 3.5.

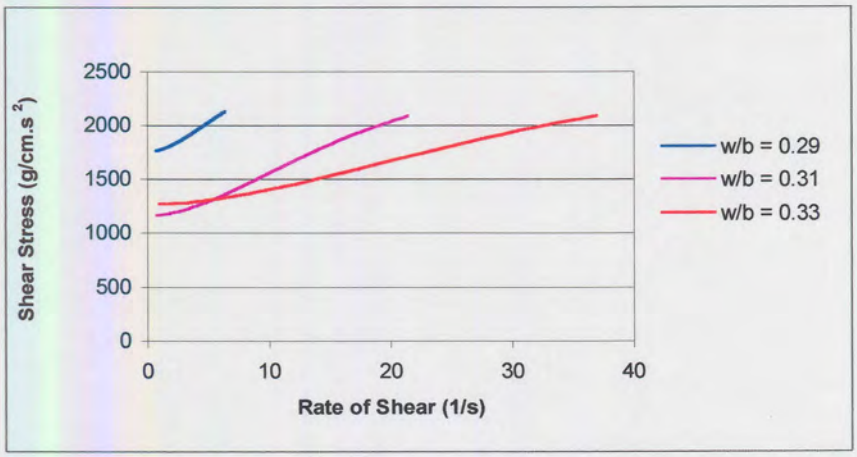

Figure 3.6: Shear stress versus rate of shear graph.

The yield stress (in Pa) was calculated from equation 3.6 using values for ΔP and L when flow had stopped. The viscosity (in Pa.s) was calculated as the slope of the shear stress/rate of shear plot.

The workability range for which the test can be used is relatively small. The lower range limit is set by initiation of flow and the upper by maximum shear velocity for transition from laminar to turbulent flow, as the test is only valid for laminar shear flow. By calculating the Reynolds number at maximum flow viscosity, it was possible to estimate whether the flow was laminar or turbulent. This number must be below 2000. This is believed to be the transition value between laminar and turbulent flow, (Benedict, 1969). This value increases with increasing flow velocity and increasing pipe diameter. It decreases with increasing viscosity. The Reynolds number was calculated as follows:

$$\mathrm{Re} \approx \frac{\rho V D}{\mu} \qquad (3.9)$$

Where:

Re = Reynolds number

ρ = Specific Gravity of fluid

V = Flow velocity (m/s)

D = Tube diameter (mm)

μ = Measured viscosity (N.s/m^2)

The Re number thus sets the higher flow velocity limit and thus the higher workability range limit of the apparatus, which in turn is dependent on the water content. This limit can however be easily modified by changing the tube diameter as shown in Equation 3.9.

The lower flow velocity limit and thus the lower range limit for the test is governed by firstly the motion of flow (too dry mixes will not flow) and secondly the ability to accurately measure the flow rate. This measurement of flow rate becomes difficult when flow is so slow that the slurry exits the pipe opening in a drag-before-drip manner, resulting in a step-like flow curve.

The water demand required for different mixes to fall within this workability range differed, thus different water/binder ratios were used.

3.4.3 Compressive Strength

Compressive strength values were determined at 28 days after casting cubes. Cubes were wrapped in plastic after demoulding and stored at 22°C. The cubes were not cured in water because the water/cement ratios of the cement slurries were below that of the minimum water/cement ratio for complete hydration, namely 0.36. The water/binder range used was 0.31 to 0.34, thus if extra water was absorbed it would have affect compressive strength values obtained. Three cubes were crushed for each mix and the average strength was calculated.

3.5 Preliminary workability tests

Preliminary tests were performed to assess the suitability of the j-tube test apparatus as a two-point paste-workability test. Cement/ PFA-mixtures were made and the water content of the mixtures was progressively increased as to obtain varying workability. The sensitivity of the method was tested by increasing water/binder ratios in relatively small increments.

Mortars were mixed containing SABS CEM I 45,2R cement and one type of PFA at a weight ratio of 1:2. The water/binder ratio was increased in five increments from 0.26 to 0.30. Mix proportions are shown in Table 3.1 together with workability results. Graphs of shear stress and shear strain are included in Appendix A. After the results were analyzed it was decided that the test is satisfactory for further use. The only modification made was by cutting the discharge end opening of the tube to an angle of 30° as to prevent accumulation of paste before it falls into the catch bin.

Table 3.1: Mix proportions and results for preliminary tests.

Mix no.	Cement (kg/m^3)	PFA-A (kg/m^3)	Water (L/m^3)	Water/ Binder ratio	Yield stress (Pa.)	Viscosity (Pa.s.)
1	501	992	387	0.26	181	8.5
2	488	977	395	0.27	142	8.0
3	482	964	404	0.28	106	6.7
4	476	948	412	0.29	106	5.7
5	473	944	427	0.30	104	4.1

3.6 Mix Proportions

Mixes were prepared in 2 parts, one with pastes containing relatively high volumes of PFA and the other with pastes containing only PFA or cement and water. The five types of PFA were tested at three different water/binder ratios for each. These different water contents were chosen by trial for each PFA as the ranges for each differed so as to fit into the flow velocity range of the test.

Mix proportions are shown in Table 3.4.

Table 3.4: Mix proportions.

Mix	Type PFA	Water/ Binder	Cement (kg)	Cement (kg/m^3)	PFA (kg)	PFA (kg/m^3)	Water (l)	Water (l/m^3)
1	A	0.19	0	0	22.5	1541	4.28	293
2	A	0.21	0	0	22.5	1495	4.73	314
3	A	0.23	0	0	22.5	1452	5.18	334
4	A	0.27	7.5	489	15	977	6.08	396
5	A	0.28	7.5	482	15	963	6.30	404
6	A	0.29	7.5	475	15	949	6.60	413
7	B	0.22	0	0	22.5	1482	6.53	326
8	B	0.24	0	0	22.5	1440	6.98	346
9	B	0.27	0	0	22.5	1380	7.43	373
10	B	0.28	7.5	484	15	967	6.75	406
11	B	0.29	7.5	477	15	953	7.00	414
12	B	0.31	7.5	463	15	926	7.50	431
13	C	0.23	0	0	22.5	1513	4.95	348
14	C	0.25	0	0	22.5	1468	5.40	367
15	C	0.29	0	0	22.5	1387	6.08	402
16	C	0.34	7.5	455	15	908	6.30	463
17	C	0.36	7.5	443	15	884	6.53	477
18	C	0.38	7.5	431	15	861	6.9	491
19	D	0.29	0	0	22.5	1328	5.18	385
20	D	0.31	0	0	22.5	1294	5.63	401
21	D	0.33	0	0	22.5	1261	6.53	406
22	D	0.3	7.5	467	15	931	7.60	419
23	D	0.31	7.5	460	15	917	8.20	428
24	D	0.33	7.5	446	15	891	8.60	445
25	E	0.28	0	0	22.5	1326	6.30	371
26	E	0.3	0	0	22.5	1292	6.75	388
27	E	0.33	0	0	22.5	1244	7.43	410
28	E	0.28	7.5	475	15	949	6.30	399
29	E	0.29	7.5	469	15	936	6.60	407
30	E	0.3	7.5	462	15	923	6.80	415
31	CEM 42.5R	0.31	22.5	1599	0	0	6.91	492
32	CEM 42.5R	0.32	22.5	1564	0	0	7.30	500
33	CEM 42.5R	0.33	22.5	1516	0	0	7.50	515

4 TEST RESULTS

4.1 Introduction

Tests were performed as set out in chapter 3. In chapter 4, test results are given and the effects of water content in terms of water/binder ratio on paste workability and compressive strength are determined. It is also determined whether the physical differences of the different PFA-types affect the paste and mortar properties tested and if so to what extent. Results obtained for the different workability tests are also compared.

Table 4.1 shows a summary of paste test results. A short discussion of the results of each test follows the table. Actual test results are attached in Appendix B.

Table 4.1: Paste test-results.

Mix	Binder type	Water/ Binder Ratio	Flow Radius (mm)	Yield Stress (Pa)	Viscosity (Pa.s)	Reynolds No.	Paste Density (kg/m^3)	28 day Cube Density (kg/m^3)	28 Day Compressive Strength (MPa)
1	PFA A	0.19	-	112	7.9	2.5	1768	-	-
2	PFA A	0.21	-	48	4.6	8.6	1781	-	-
3	PFA A	0.23	-	8	1.3	107	1742	-	-
4	PFA A & CEM I 42.5R	0.27	88	183	7.5	2.6	1977	1815	40
5	PFA A & CEM I 42.5R	0.28	92	116	5.2	6.5	1838	1809	39
6	PFA A & CEM I 42.5R	0.29	97	92	3.4	13	1834	1795	35
7	PFA B	0.22	-	113	8.3	2.4	1813	-	-
8	PFA B	0.24	-	80	4	9.7	1833	-	-
9	PFA B	0.27	-	8	1.2	249	1739	-	-
10	PFA B & CEM I 42.5R	0.28	96	200	13	0.23	1890	1839	35
11	PFA B & CEM I 42.5R	0.29	97	149	9.7	0.93	1880	1827	34
12	PFA B & CEM I 42.5R	0.31	104	124	6.9	2.31	1849	1809	29
13	PFA C	0.23	-	139	7.9	1.5	1840	-	-
14	PFA C	0.25	-	138	7.1	2	1818	-	-
15	PFA C	0.29	-	102	0.6	301	1803	-	-
16	PFA C & CEM I 42.5R	0.34	100	189	11.6	0.26	1823	1816	27
17	PFA C & CEM I 42.5R	0.36	106	105	6.5	2.6	1853	1778	18
18	PFA C & CEM I 42.5R	0.38	107	104	4.9	4.8	1793	1739	17
19	PFA D	0.29	-	169	6.5	1.1	1697	-	-
20	PFA D	0.31	-	89	4.6	7.1	1647	-	-
21	PFA D	0.33	-	90	2.3	20.7	1679	-	-
	PFA D & CEM I 42.5R	0.30	82	N.M*	N.M*	N.M*	1865	1770	30
22	PFA D & CEM I 42.5R	0.31	96	152	6.9	1.6	1844	1767	29
23	PFA D & CEM I 42.5R	0.33	104	93	4.4	7.5	1822	1755	25
25	PFA E	0.28	-	90	8.4	1.6	1666	-	-
26	PFA E	0.30	-	29	4.6	9.2	1655	-	-
27	PFA E	0.33	-	8	1.7	115	1655	-	-
28	PFA E & CEM I 42.5R	0.28	95	93	5.4	5.0	1844	1795	35
29	PFA E & CEM I 42.5R	0.29	97	93	4.5	9.2	1803	1736	27
30	PFA E & CEM I 42.5R	0.30	110	79	2.4	24	1793	1734	29
31	CEM I 42.5R	0.31	90	197	5.9	1.3	2089	2037	69
32	CEM I 42.5R	0.32	86	197	4.9	1.5	2087	2039	69
33	CEM I 42.5R	0.33	93	130	4.0	5.7	2065	1993	63

* Not Measurable due to insufficient fluidity.

4.2 Standard workability tests

Slump tests performed on pastes all showed collapsed slump thus no results were taken. Flow table tests were performed on cement and cement/PFA-blend pastes, results are graphically shown in Figure 4.1. As expected the flow radius increased with increasing water/binder ratio for each PFA-type. However, it seems that different PFA-types gave different flow radius-values for cement/PFA-blend pastes at similar water/binder ratios. Cement pastes showed low flow radius-values in comparison with cement/PFA-blend pastes.

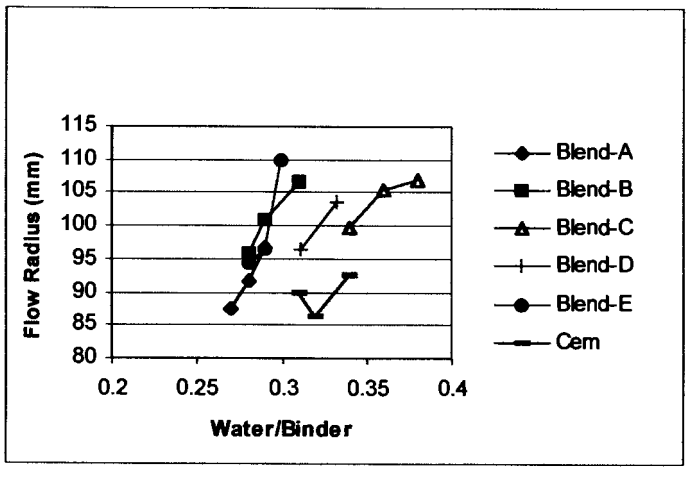

Figure 4.1: Flow table results.

4.3 J-Tube tests

J-tube tests were performed prior to slump flow tests. After shear stress vs. shear strain graphs were plotted values for yield stress and plastic viscosity was calculated. Values for cement and PFA-pastes are plotted in Figures 4.2 and for cement/PFA-blend pastes in Figure 4.3. Figure 4.2 indicates that cement pastes have a higher water demand for a given viscosity than any of the PFA-pastes. The yield stress obtained for cement pastes were also higher than that obtained for any of the PFA-pastes.

Yield stress and viscosity values decreased with increases in water/binder ratio as expected for mixes containing the same type of materials. For both raw materials as well as blend-mixtures the water demand to obtain constant viscosity vary for the types of PFA used. The figures indicate that the viscosity and yield stress are not only a function of the water/binder ratio but also of the PFA-type used.

Figure 4.3 shows that for a given water/binder ratio the viscosities of blends containing PFA-A and E are similar to the viscosities of blends containing PFA-B and D at a higher water/binder ratio. PFA-C

requires significantly more water than any of the other PFA-types to produce similar viscosity and yield stress.

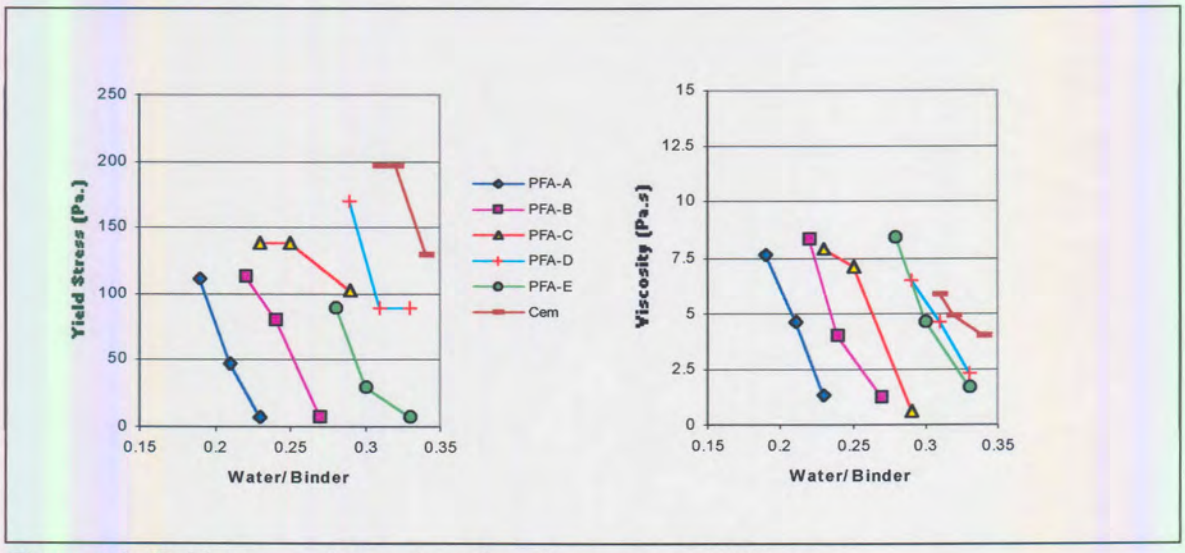

Figure 4.2: Yield stress and viscosity-values for cement and PFA-pastes.

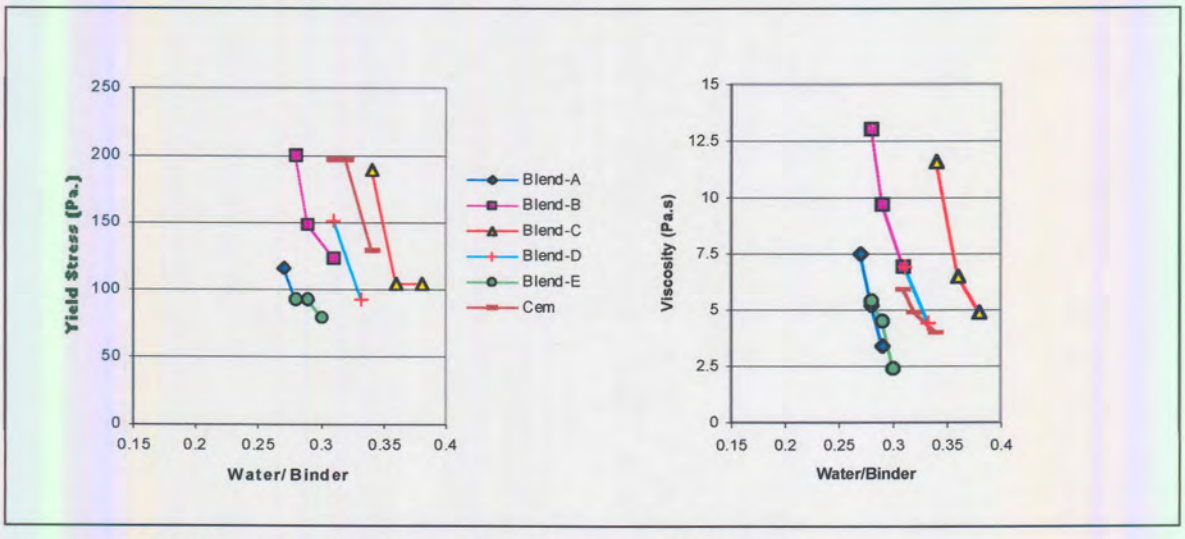

Figure 4.3: Yield stress and viscosity values for cement/PFA-blend pastes.

Values for viscosity and yield stress was plotted against flow diameter and is shown in Figure 4.4. For all blended mixture, the viscosity as well as the yield stress decreased with increasing flow radius. Mixtures containing PFA-B and C seemed to follow the same pattern for both viscosity as well as yield stress as did mixtures containing PFA-types A and E.

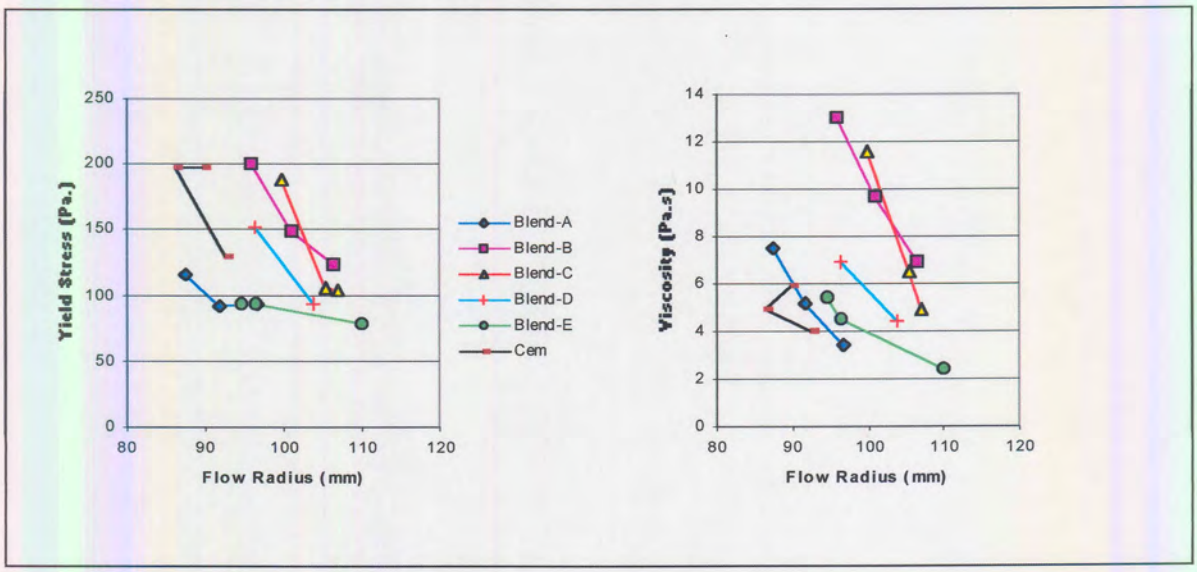

Figure 4.4: Relation of viscosity and yield stress with flow radius.

Figure 4.5 shows the relation between yield stress and viscosity as measured by the j-tube. A good correlation between yield stress and viscosity was observed only for blend-pastes.

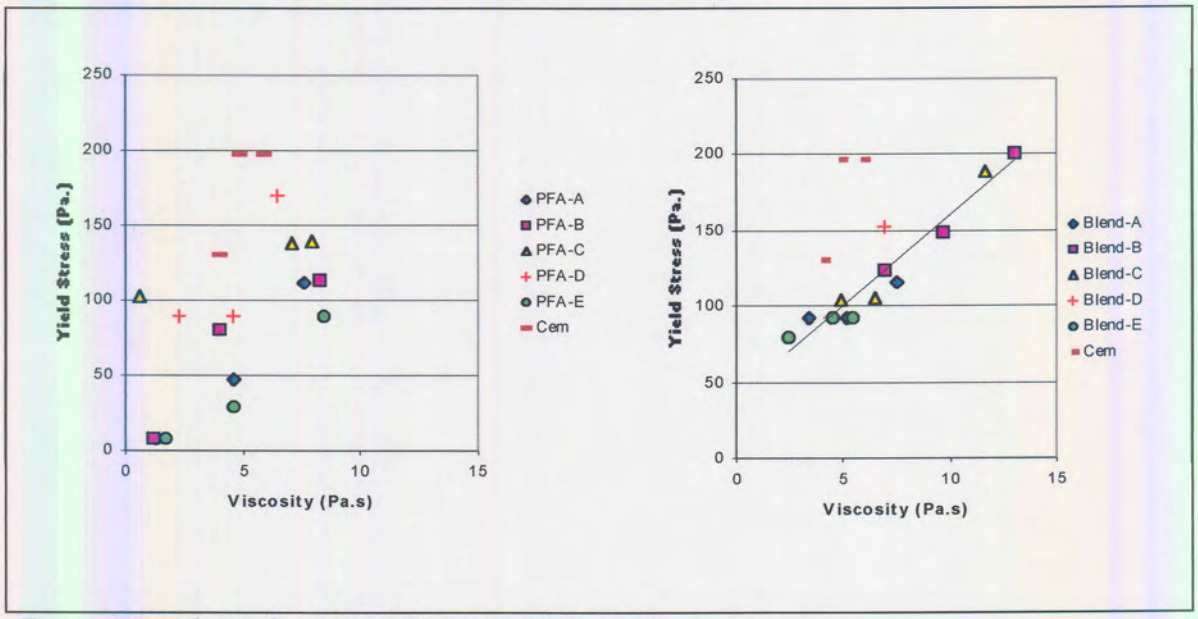

Figure 4.5: Relation between yield stress and viscosity.

4.4 Compressive Strength Tests

Figure 4.6 shows 28-day compressive strength values for cement as well as cement/PFA-blend mortars in terms of water/binder ratio and also water content per cubic meter. As expected high replacement of cement with PFA resulted in a decrease of early strength. The compressive strength-values of cement/PFA-blend mortars decreased with increase in water/binder ratio as expected.

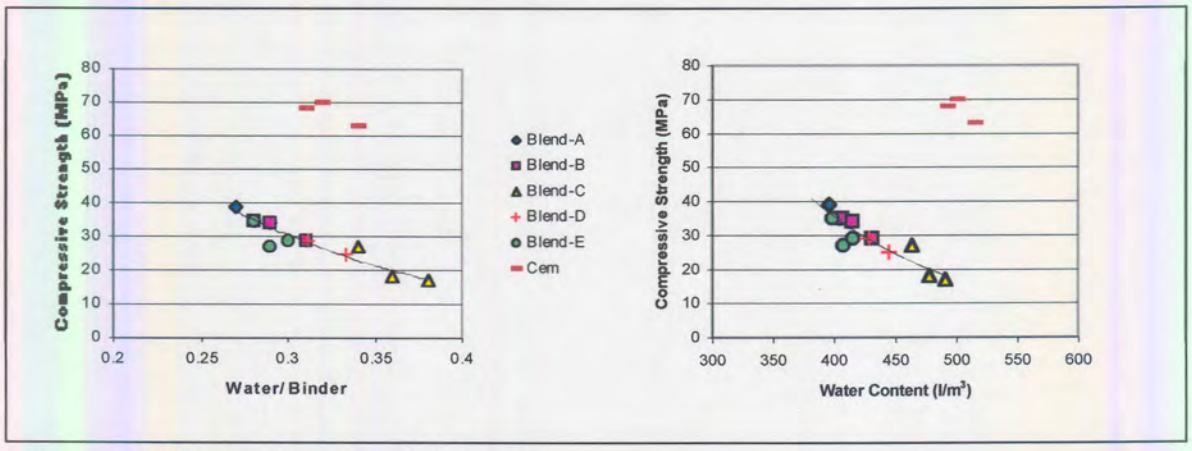

Figure 4.6: Compressive Strength Values.

The regression line for the best fit to the data plotted in Figure 4.6 for water/binder ratio was used to calculate theoretical strength values. The equation calculated for the line was:

$$y = 248.8e^{-7.0039x}$$

With: y = Compressive Strength (MPa)

x = Water/Binder Ratio and,

$R^2 = 0.90$

The error for each measured value was calculated as the measured value minus the calculated theoretical value. These errors were plotted against water/binder ratio and are shown in Figure 4.7. The figures indicate that only the water/binder ratio has a significant effect on compressive strength. Only mortar made with PFA-E showed measured compressive strength values lower than that of calculated values for all 3 mixtures with the highest error being –6MPa being 17% less than the calculated value.

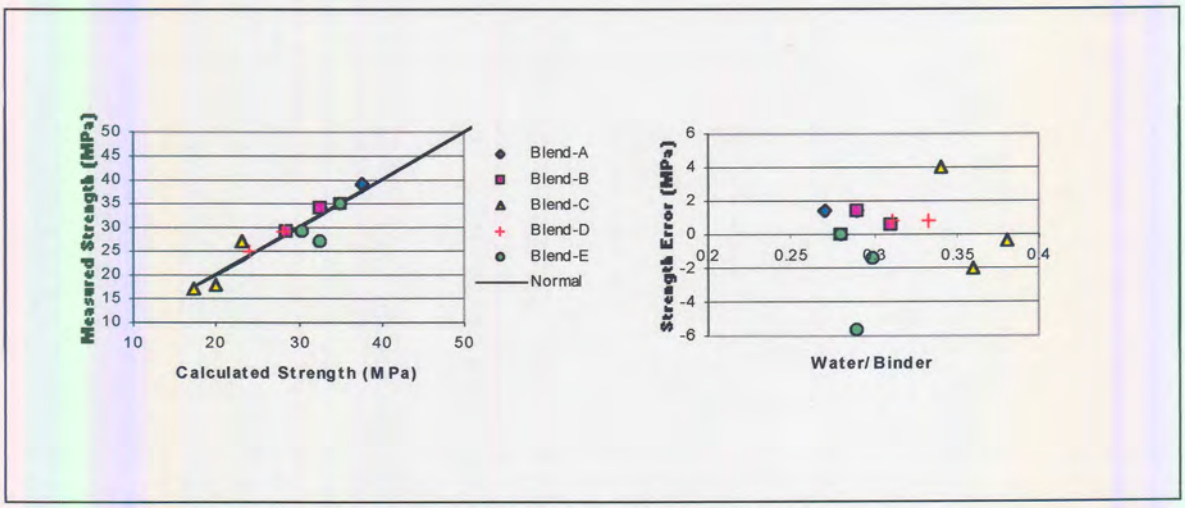

Figure 4.7: Relation between Measured and calculated strength values.

The type of PFA used in the pastes had a significant influence on the workability of the paste but no significant influence on compressive strength. The compressive strength of the mortars was mainly a function of the water/binder ratio. The type of PFA will have an effect on compressive strength when constant workability is required.

4.5 Conclusions

In this chapter results of tests performed on cement and PFA-pastes as well cement/PFA-blend pastes were compared with water/binder ratio and type of PFA used. It was found that the water demand per mass of cement pastes is higher than that for PFA-pastes to obtain constant workability and that the workability of paste improves when large volumes of cement is replaced by PFA.

Different PFA-types significantly affect the workability of pastes where high proportions of cement were replaced with PFA and the effects was observed in terms of both yield stress as well as viscosity. It was found that only the water/binder ratio significantly affects the compressive strength of cement/PFA-mortars where large volumes of cement are replaced by PFA. This may however only be true as for the curing conditions used in this study. Curing was performed at room temperature without storing the samples in water.

5 THE EFFECT OF PFA PROPERTIES ON PASTE WORKABILITY

5.1 Introduction

In chapter 4 it was concluded that the different types of PFA significantly affect workability and only secondarily affect compressive strength. It was therefore decided to investigate the effect of different PFA-properties on the workability of PFA-containing pastes for the remainder of this dissertation. For mixtures of cement and PFA the size properties were proportionally corrected. The PFA-types used were produced at the same source and from the same stock material; the chemical compositions of the different types were thus similar. The loss on ignition was found to be relatively low for all PFA-types and it was assumed that this factor had no significant effect on workability. The types of PFA thus only differed significantly in terms of particle size and distribution as was seen in Figures 3.1 and 3.2.

5.2 Effect of PFA-properties on Water Demand of Pastes

Table 5.1 shows the water demand (water/binder ratio) of pastes tested in chapter 4 to obtain a viscosity of 5.0Pa.s. These values were derived from Figures 4.2 and 4.3 by interpolation.

Table 5.1: Water Demand for Pastes.

PFA-type	Water Demand (w/b)	
	PFA Pastes	**CEM I 42.5R/PFA-blend Pastes**
A	0.21	0.28
B	0.24	0.32
C	0.27	0.38
D	0.31	0.33
E	0.30	0.29
Cement	0.32	

5.2.1 *Effect of Particle Size*

Figure 5.1 shows the effect of D10, D50, D90 and R_{45} of pastes on the water demand to obtain a viscosity of 5.0Pa.s. From the figures it seems that for high PFA-replacement pastes the D10 values have no measurable effect on water demand while increases in D50-value seems to result in decreases in water demand. For the D90-values there is an optimum of 150μm where optimum workability in terms of viscosity is obtained. The same trend is observed for R_{45} with an optimum value being in the region of 40%. PFA-specifications in certain countries specify typical R_{45}-values of 12.5%, however Figure 5.1 suggests that the PFA-types that conform to this specification (types B and C) did not result in optimal workability. In fact it can be seen that for cement/PFA-pastes, the two PFA-types with the highest R_{45}-values (A and E) had the lowest water demands. It was already shown that for the type of cement and curing conditions used in this study water/binder ratio is the main governing parameter affecting strength and the PFA-types conforming to the R_{45}-specification would thus not produce mortars with the highest strengths when a given workability is required.

The trend found in this investigation does not necessarily hold true for other mix compositions and curing conditions and different minimum values may be obtained for different mixtures.

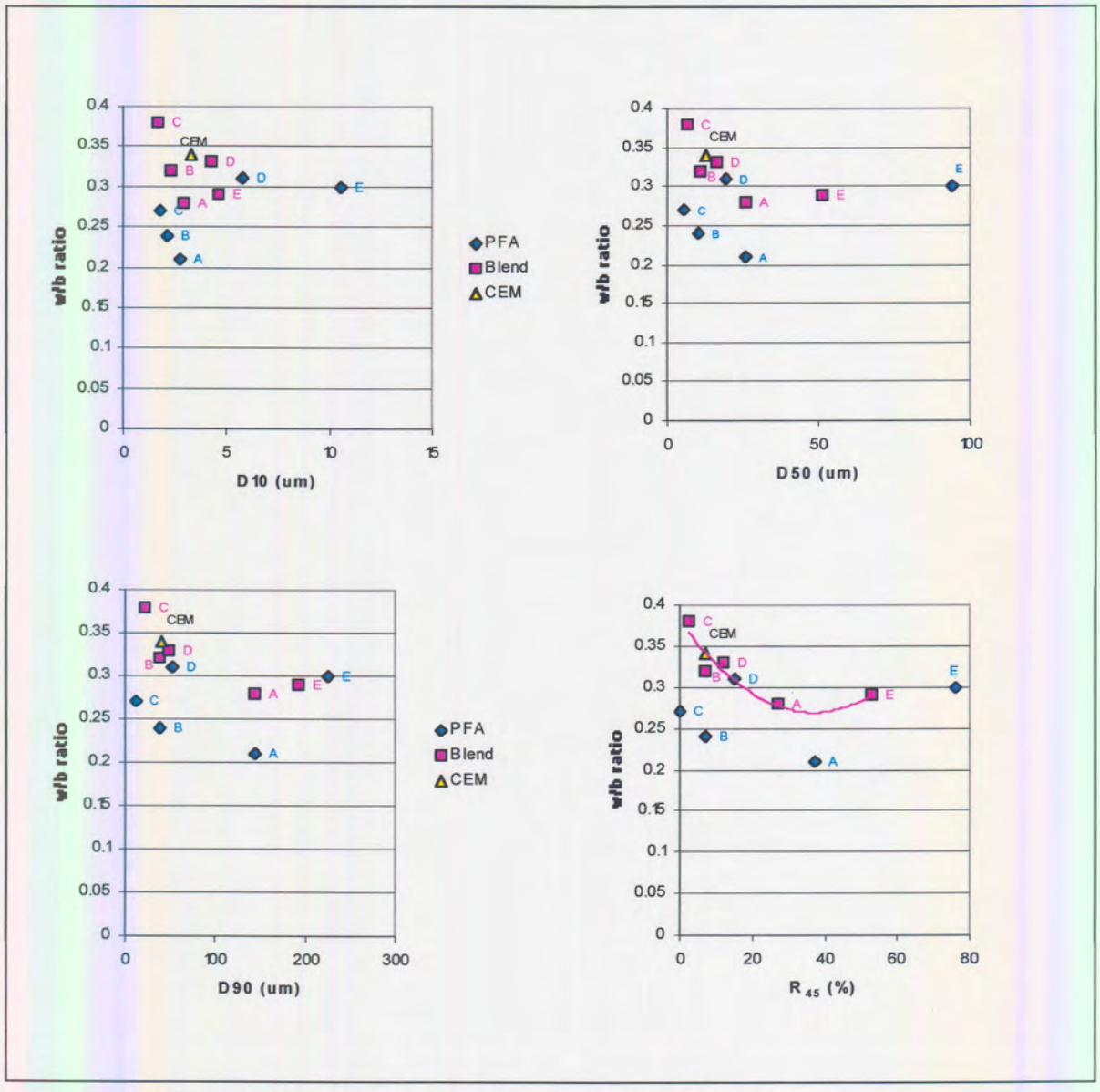

Figure 5.1: Effect of particle size on paste water demand for viscosity of 5,0Pa.s.

5.2.2 *Effect of Grading Modulus*

Hughes (Hughes, 1994) suggested that a single-size parameter like the R_{45} is not appropriate to classify PFA but that other size fractions should also be taken into account. He introduced a new term, the Grading Modulus (GM) for PFA and the value is determined by all size fractions, with smaller fractions contributing more than the larger ones. This is because smaller sizes contribute more to surface area than larger sizes. Cornelissen and van den Berg (Cornelissen and van den Berg, 1998) showed that for concrete where 20% of cements were replaced by fly ash with different GM-values the water demand for constant

workability decreased with an increase in fly ash-GM thus also causing increased strength. Hughes (1994) also suggested that the quality of PFA as a replacement for cement improves as the GM increases.

The effect of grading modulus on water demand is shown in Figure 5.2.

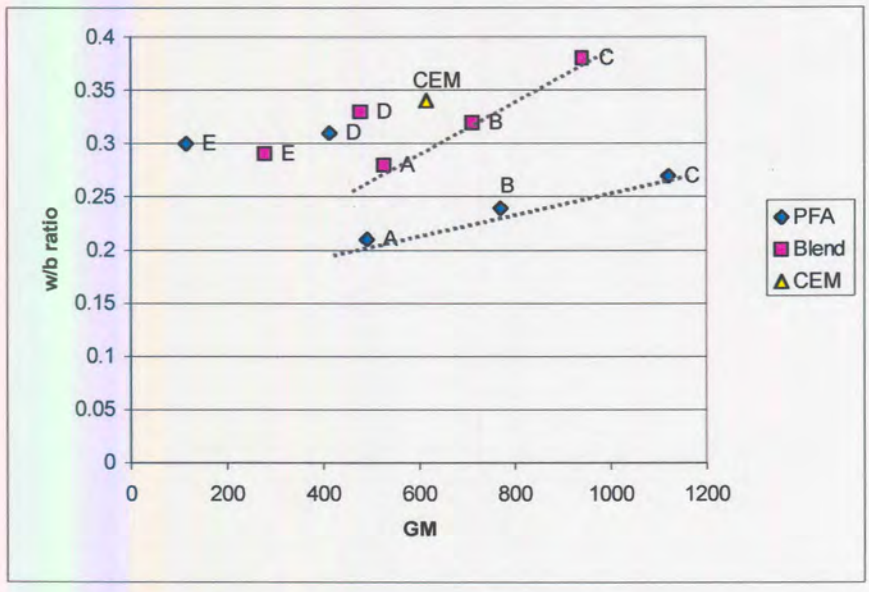

Figure 5.2: Effect of Grading Modulus on water demand for viscosity of 5.0 Pa.s.

The figure indicates that in general the water demand increases with increasing GM. This effect seems to become more pronounce for PFA-types with a GM of larger than 500, thus Types A, B and C. It can thus be seen that an increase in PFA-GM does not always result in increased workability (as claimed by Cornellisen and Gast, 1998). The effect of GM seems to be specific for different types of mixtures and the factor cannot be used as a universal specification parameter.

The difference in water demand for PFA and blended paste seems to increase with increase in GM. Plots for types A, B and C seems to follow the same pattern as does plots for types D and E. These two trends represent PFA-types with similar smallest size fractions.

5.2.3 *Effect of Surface Area*

Surface area-values were measured using the Blaine-method and the values were compared to the theoretical calculated surface area values using sphere-geometry. Shape Factor values were calculated as the ratio of measured values and calculated values as described by Hopkins and Cabrera (Hopkins and Cabrera, 1994) and explained in Chapter 3. These values are shown in Table 5.2.

Table 5.2: Surface area-values for PFA-types.

PFA-type	Surface Area (g/cm^2)		Shape Factor
	CSA	MSA	
A	2737	2850	0.96
B	4299	3600	1.19
C	5708	5500	1.04
D	2378	2500	0.95
E	1241	*ND	

*Not Determined – Material too coarse.

As explained in Chapter 3, the surface area of a sphere bears much resemblance to the Grading Modulus and the magnitude of change with decreasing diameter is similar. The effect of surface area, both calculated as well as measured on water demand is shown in Figure 5.3.

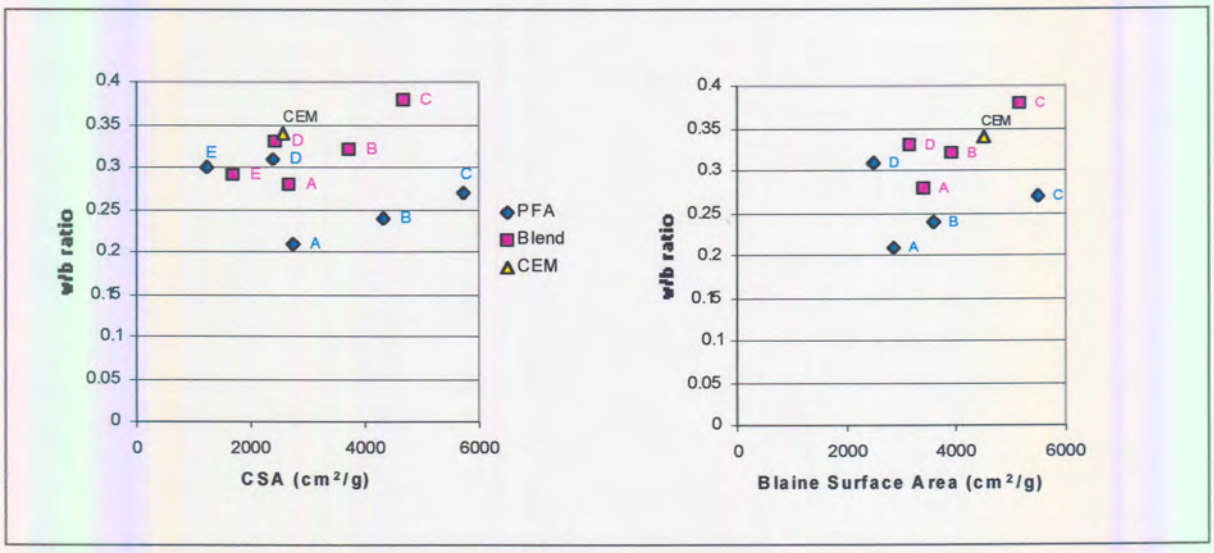

Figure 5.3: Effect of surface area on water demand.

The surface area (measured as well as calculated) had the same effect on water demand as the GM. It seems that the water demand increases with surface area when the surface area exceeds 2500g/cm^2. This trend is also observed for PFA-types D and E. These two types had lower surface area-values because of lower finest fraction particles (<10μm). It seems that the trend of increasing water demand with increasing GM and surface area is followed for PFA-types with similar original finest fractions. If we look back at

Figure 3.1, which illustrates the size ranges of the PFA-types after fractioning, it can be seen that PFA-E was produced from PFA-A by removing finer fractions (<45μm). The process thus fractioned PFA-A into PFA-B and PFA-E. PFA-C was produced by removing finer fraction particles (<10μm) from PFA-B. If the finest fractions contribute the most to surface area of powders it can thus be seen why PFA-types B and E have the lower surface areas. The water demand increases with increasing surface area of the PFA only for PFA-types containing the same original finest fractions.

Figure 5.4 shows the effect of Shape Factor on water demand. For PFA-pastes the mixture with the lowest water demand did not necessarily contain the PFA-types with the best Shape Factor (closest to 1) as suggested by Hopkins and Cabrera (1994). However blended mixtures all had lower shape factors than PFA-mixtures due to the presence of cement and the fact that cement particles are not spherical in shape. Blended pastes thus had higher water demands than PFA pastes containing the same PFA-type. All blended mixtures, except the one containing PFA-C, had lower water demands than the mixture containing cement alone indicating only a partial contribution of the spherical PFA-shape to workability. In general the Shape Factor had the expected effect on water demand, with mixtures containing cement particles having higher water demands than those who does not contain cement.

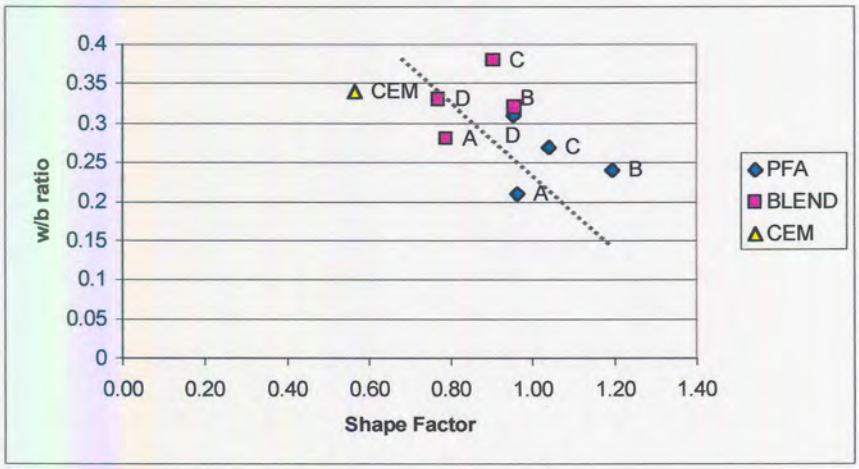

Figure 5.4: Effect of Shape Factor on Water Demand.

5.2.4 Effect of Particle Size Distribution

Values for grading slope of PFA as well as the PFA/cement mixtures are shown in Table 5.3. Again the values for the blended mixtures were calculated proportionally.

Table 5.3: Particle Size Distribution Parameters.

PFA-type	*Distribution Index (n)*		Calculated Grading Slope (G10/90)	
	PFA	Blend	PFA	Blend
A	0.74	0.78	0.49	0.55
B	0.97	1.03	0.72	0.73
C	1.67	1.34	1.11	0.90
D	1.27	1.14	0.91	0.83
E	0.91	0.75	0.62	0.48

The values for PFA grading slope in Table 5.3 were plotted against water demand for both PFA as well as blended pastes and plots are shown in Figure 5.5.

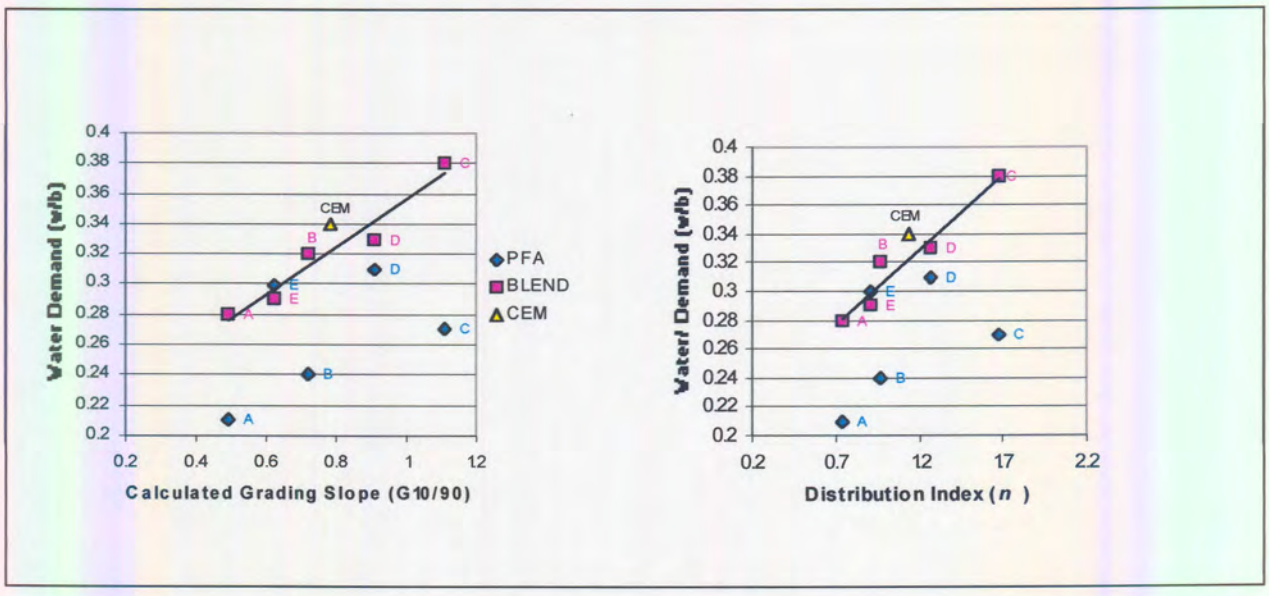

Figure 5.5: Effect of PFA-Grading Slope on water demand.

The two plots are nearly identical thus showing that the distribution index is just as good an indication of the grading slope than the theoretical slope calculated directly from the grading curves via regression analyses between D10 and D90.

The plots show that the PFA-Grading Slope has a significant effect on the water demand of cement/PFA-pastes. As expected, the lower the value of the Grading Slope, the less water is required for constant workability. The same pattern was not found for PFA-pastes. Here the water demand increased

accordingly for pastes containing PFA-types A, B and C as well as for D and E. Again it seems that the same trend is only followed for PFA-types containing the same original finest fractions but once cement is added, its effect on the overall particle size distribution over-rules this effect because now all the cement/PFA-pastes contain the finest fractions of the cement.

In Figure 5.6 water demand for the blended pastes is plotted as a function of the blend-grading slope in terms of both *n* as well as G10/90. This time however the particle size distribution of the whole system is taken into account and again it is shown that the lower the distribution index, the lower the water demand.

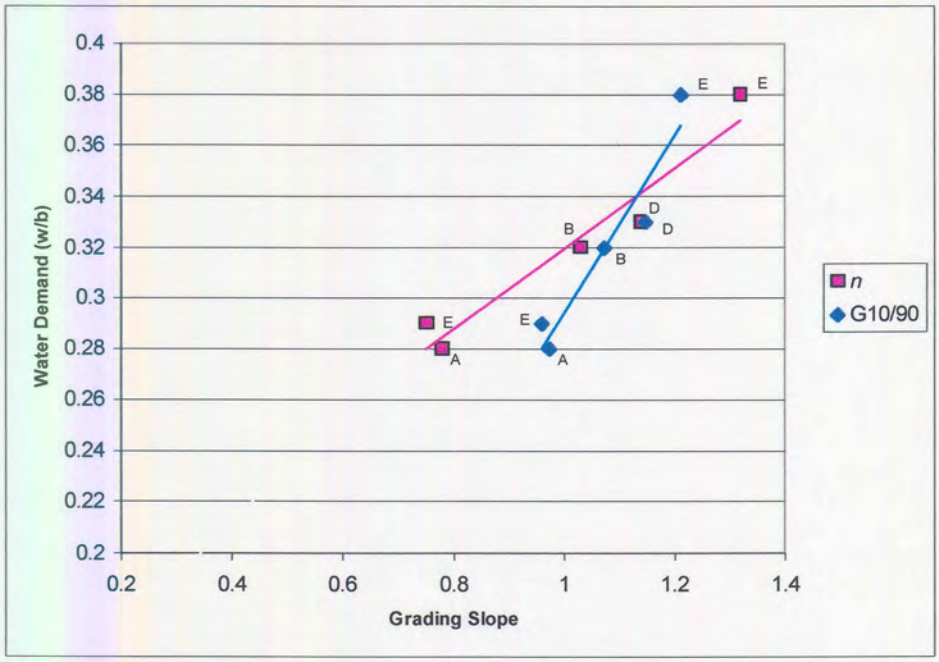

Figure 5.6: Effect of blend distribution index on water demand for blended pastes.

The trend is similar than that of the PFA-grading slope for both parameters indicating that the contribution of the cement distribution index was proportional for all PFA-types. The linear fit to the curves seems to be better probably because the particle size distribution of the whole system is now taken into account.

5.3 Conclusions

The follow conclusions can be drawn for PFA-pastes investigated:

- No clear trend could be found to explain the effect of PFA-particle size properties on the water demand of PFA-pastes for constant workability. However for PFA-types containing similar finest fractions (types-A, B, C and types-D, E) it can be concluded that the coarser the PFA (higher R_{45}-value), the lower the water demand. The pastes containing PFA that comply to the SABS-specification for particle size did not have the lowest water demands.
- The GM and surface area-values of the PFA-types are a measure of their fineness and these parameters also showed that increased PFA-fineness resulted in increased water demand for PFA-pastes. Linier trends were observed for PFA-types containing similar finest fractions.
- No clear relationship exists between Shape Factor and water demand.
- The PFA-grading slope had a similar effect on water demand as particle size. It was found (for PFA-types with similar finest fractions) that the water demand decreased with decrease in grading slope (or increased particle size range).

The following can be concluded for blended pastes investigated:

- In terms of D50, D90 and R_{45}-values, it was found that the water demand for constant workability increased with increase in fineness and that there seem to be an optimum value. Again the pastes containing PFA that comply with the SABS-specification for particle size did not have the lowest water demands.
- The GM and surface area showed similar trends than those observed for PFA-pastes, with increased fineness for blends containing PFA-types of similar finest fraction material resulting in increased water demand.
- Again no trend was found for the effect of Shape factor on water demand. However and overall trend was found for PFA-pastes, blended pastes and cement pastes indicating that the higher the Shape Factor (more round particles in mixture) the lower the water demand. It can be concluded that Shape Factor only contributes partially to workability.
- In terms of grading slope it was found that the broader the combined particle size distribution of the blended materials the lower the water demand.

6 CONCLUSIONS AND RECOMMENDATIONS FOR FURTHER RESEARCH

A two-point method for measuring the workability of cement and cement/PFA paste has been established. The method is sensitive enough so that relative small changes in workability can be assessed. The method is applicable where the minimum water contents for cement and cement/PFA pastes are crucial to obtain satisfactory workability and also conserve strength. The J-tube apparatus designed is satisfactory for laboratory tests; more work is however needed to find a design that will be practical and user friendly on construction or production sites. This is possible because the design is based on that for capillary viscometers already used in the industry, however not for cement pastes yet.

The method was used to assess the effect of different types of PFA with similar chemical content but different size and size-distribution properties on pastes where 67% of cement was replaced by PFA. It was found that for the curing regime used, the compressive strength of the mortars was not affected by the type of PFA used but only by the water/binder ratio. The type of PFA however significantly affected workability of the pastes. This caused variations in compressive strength when constant workability was required due to different water demands.

Standard specifications in South Africa, Britain and the USA specify PFA in terms of particle size and the R_{45}-value has been accepted with a minimum value, usually in the order of 12.5%. This means that not more than 12.5% by mass of the particles may have a diameter in excess of 45μm. In this study it was found that the PFA-types with the lowest R_{45}-values did not result in pastes with the lowest water demand for constant workability. This may be as result of using a relatively fine cement for the purpose of this dissertation as apposed to a coarser OPC used for standard specification test methods. The cement used had a particle size distribution with a range intermediate between the ranges of the different PFA-types while a typical OPC has a range on the coarse side of most PFA-types.

Other size parameters like Grading Modulus (GM) that describes PFA in terms of more than one particle size were assessed, trends were found only for PFA-types containing the same original finest-fraction material. This is probably due to the relatively large effect that the finest fraction has on GM. These trends were however not consistent with those concluded by previous researchers (Cornelissen and van den Berg, 1998) as the water demand increased with decreasing GM. Again a possible reason may be the fact that relatively fine cement was used instead of a typical OPC, thus resulting in a different overall particle size distribution.

Effects of surface area proved to be similar than that of GM. The effect of particle shape as assessed by the Shape Factor proved to be insignificant for PFA-pastes, however it is believed to be partly responsible for the higher water demand of blended and cement pastes as apposed to that of PFA pastes due to the irregular shape of cement particles.

The effect of grading slope of the PFA proved to be significant and it was found that PFA-types with the largest range in particle-size distribution ("most continuous") produced cement/PFA-pastes with the lowest water demands.

Performance tests to assess the quality of PFA described by ASTM as well as B.S.-specifications is performed by replacing part of cement in a standard reference mix by PFA and adjusting the water content as to achieve the same workability as the reference mix. The compressive strength is then measured after a standard period of time subjected to standard curing conditions. An activity index is then calculated as the strength ratio of the PFA-containing mortar to that of the control containing no PFA. The activity index thus depends partially on the ability of a PFA-type to reduce the water content of a mixture to which it is incorporated into. It also depends on the true pozzolanic activity of the PFA, which is a chemical reaction and can thus be influenced by reaction conditions and reactant particle size.

It was found that subjected to curing conditions used for this study, the strength obtained for mortars was a function only of the water content in terms of water/binder ratio. Thus for these conditions it can be concluded that for the PFA-types used only their ability to reduce water demand determine their relative strength activity. This may not hold true for different curing conditions as the chemical (pozzolanic) activity of PFA that also contributes to its activity index may be more pronounced for finer PFA-types especially when curing temperatures are raised.

Scope for further research include the assessment of different cement types and curing conditions in combination with the five PFA-types used. By using different cement types that differ in terms of particle size it will be possible to manipulate the overall particle size distribution of the binary cement/PFA system. This may prove to be very significant with regards to size specifications for PFA where the R_{45}-value is currently being employed. This specification was developed with regards to the replacement of ordinary Portland cement with PFA, which is coarser than some other cements like the SABS I 42.5R used for this dissertation.

More scope for further research includes the assessment of curing conditions applied for PFA activity tests. Conditions used for this study was limited to curing cubes wrapped in plastic at room temperature. The pozzolanic reaction is a chemical reaction and most chemical reactions are accelerated by a rise in temperature as well as a decrease in particle size of the reactants (PFA).

Lastly it was shown in this study that the J-tube could be used as a two-point workability test apparatus that can measure relatively small changes in workability of cementitious pastes. Further development of the apparatus can make it feasible as an on-site quality control tool. Possible uses include the development and testing of road-repair grouts where PFA is incorporated to maximize workability and minimize segregation.

REFFERENCES

Abrahams, D.A. 1918. *Design of concrete mixtures, Bulletin no 1.* Structural Materials Research Laboratory, Chicago, pp. 1-20.

Anderson, P. 1990. *Control and monitoring of concrete production.* PhD thesis. Technical University of Denmark.

ASTM C109-80: *Standard Test Methods for Compressive Strength of Hydraulic Cement.* ASTM Annual Book, Vol 04.02. 1993.

ASTM C618: *Standard Specification for Coal Fly Ash and Raw Calcined Natural Pozzolans for use as a Mineral Admixture in Concrete.* ASTM Annual Book, Vol 04.02. 1993.

ASTM C939: *Standard Test Methods for Flow of Grout for Preplaced-Aggregate Concrete (Flow Cone Method).* ASTM Annual Book, Vol 04.02. 1998.

ASTM C311-77: Part 29-32. *Standard Methods of Sampling and Testing Fly Ash and Natural Pozzolans for Use as a Mineral Admixture in Portland-Cement Concretes.* ASTM Annual Book, Vol 04.02.

ASTM C311-98a. *Standard Methods of Sampling and Testing Fly Ash and Natural Pozzolans for Use as a Mineral Admixture in Portland Cement-Concretes.* ASTM Annual Book, Vol 04.02. 1998.

Bai, J. Wild, S. Sabir, S. and Kinuthia, J.M. 1999. Workability of concrete incorporating pulverized fuel ash and metakaolin. *Magazine of Concrete Research*, Vol 51, No 3, June, pp 207-216.

Banfill, P.G.F. 1990. Use of the Viscocoder to study the rheology of fresh mortar. *Magazine of Concrete Research*, Vol 42, No 153, December, pp 213-221.

Banfill, P.G.F. 1994. Rheological methods for assessing the flow properties of mortar and related materials. *Construction and Building Materials*, Vol 8, No 1, pp. 43-51.

Beaupre, D. Mindess, S. and Pigeon, M. 1994. Rheology of fresh shotcrete. *Special Concretes: Workability and Mixing.* Ed Peter J.M. Bartos. E&F.N. Spon, London.

Boch, G.L. and Willis, J.P. 1990. *The chemical and mineral compositions and particle size distribution of fly ash from three South African power stations*. South African Coal Ash Association. First national symposium. CSIR, May.

Brown, J.H. 1980. *The effects of two different pulverized fuel ashes upon the workability and strength of concrete.* Cement and Concrete Association. Technical Report 42.563. Wexham Springs.

B.S. 1881: Part 102. 1983. *Method for Determination of Slump.* London: British Standards Institution.

B.S. 1881: Part 103. 1993. *Method for Determination of Compacting Factor.* London: British Standards Institution.

B.S. 1881: Part 104. 1983. *Method for Determination Vebe-time.* London: British Standards Institution.

B.S. 1881: Part 105. 1985. *Method for Determination of Flow of Fresh Concrete.* London: British Standards Institution.

B.S. 3892: Part 1. 1997. *Specification for Pulverized Fuel Ash for Use with Portland Cement.* London: British Standards Institution.

B.S. 3892: Part 3. 1997. *Specification for Pulverized Fuel Ash for Use with Portland Cement.* London: British Standards Institution.

Cornelissen, H.A.W. and van den Berg, J.W. 1998. Fly ash customization for defined performance concretes. *Fly Ash, Silica Fume, Slag and Natural Pozzolans in Concrete: Proceedings of the Sixth CANMET/ACI/JCI International Conference.* Bangkok.

Cornelissen, H.A.W. and Gast, C.H. 1993. Upgrading of fly ash for utilization in concrete. *Fly Ash, Silica Fume, Slag and Natural Pozzolans in Concrete. Proceedings of the International Conference.* Istanbul. ACI SP 132, Vol. 1, pp 457-470.

Costa, U. and Masazza, F. 1986. *Il Cemento,* Vol 41, p 397.

Cusens, A.R. 1956. The measurement of the workability of dry concrete mixtures. *Magazine of Concrete Research,* Vol 8, No 22, pp 23-30.

De Larrard, F. Sedran, T. Hu, C. Szitkar, J.C. Joly, M. and Derkx, F. 1996. Evolution of the Workability of Superplastisized Concrete: Assessment with BTRHEOM. *Proceedings of the International RILEM Conference on Production Materials and Workability of Concrete.* Eds Paisly, P.J.M. Bartos, D.C. Marrs and D.J. Cleland. June, pp377-388.

De Larrard, F. Sedran, T. Hu, C. Szitkar, J.C. Joly, M. and Derkx, F. 1997. A new Rheometer for soft-to-fluid fresh concrete. *ACI Materials Journal,* Vol 94, No 3, May-June, pp 234-243.

Dewar, J.D. 1999. *Computer Modeling of Concrete Mixtures.* E&F.N. Spon, London.

Diamond, C.R. and Bloomer, S.J. 1977. A consideration of the DIN flow table. *Concrete,* Vol 11, No 1, pp 29-30.

Ferraris, C.F. and de Larrard, F.1998. Modified slump test to measure the Rheological parameters of fresh concrete. *Cement, Concrete and Aggregates, CCAGDP, Vol 20, No 2, December, pp 241-243.*

Glanville, W.H. 1947. *The grading of aggregates and the workability of concrete, 2nd edition.* Road Research Technical Paper No. 5. London, HMSO.

Govier, G.W.1972. *The flow of complex mixtures in pipes*. Robert E. Kriegler Publishing Company, Florida, p 58.

Grzezezryk, S. and Lupowski, G. 1997. Effect of content and perticle size distribution of high calcium fly ash on the Rheological properties of cement paste. *Cement and Concrete Research,* Vol 27, No 6, pp 907-916.

Grieve, G.R.H. 1991. *The influence of two South African fly ashes on the properties of concrete.* PhD thesis. University of Witwatersrand.

Hobbs, D.W. 1980. The effect of pulverized fuel ash upon the workability of cement paste and concrete. *Magazine of Concrete Research,* Vol 32, No 113, December, pp 219-226.

Hobbs, D.W. Workability and water demand. *Special Concretes: Workability and Mixing. Rilem Workshop,* March, 1993.

Hobkins, C. J.1984. *The Properties of Pulverized Fuel Ash and their Influence on the Behaviour of Cement Pastes. And Concrete.* PhD thesis. University of Leeds.

Hopkins, C.J. and Cabrera, J.G. 1994. The Shape Factor: A parameter to assess the effect of PFA on the flow properties of cement pastes and concrete. *International Symposium on Cement and Concrete Science.* Beijing, Peoples Republic of China.

Homma, A. Yamamoto, Y. and Kitzukata, Y. 1998. Testing method of Rheological chatarisitcs of high fluid concrete. *Concrete Under Severe Conditions 2: Enviroment and Loading. Proceedings of the second International Conference on Concrete Under Severe Conditions.* Tramso, Norway, pp 1864+.

Hu, C. de Larrard, F. and Gjorf, O.E. 1995. Rheological testing and modeling of fresh high performance concrete. *Materials and Structures,* Vol 28, pp 1-7.

Hughes, B.P. and Al-Ani, M.N.A. 1989. PFA fineness and its use in concrete. *Magazine of Concrete Research,* Vol 41, No 147, June, pp 99-105.

Iyer, R.S. and Stanmore, B.R.1995. Surface area of fly ashes. *Cement and Concrete Research,* Vol 25, No 7, pp 1403-1405.

Jiang, W. and Roy, D.M. Rheology in hydration and setting. *Hydration and Setting of Cements.* Ed A. Norrat, J.C. Mutin. C&F.N. Spon, London.

Johansen, V. and Anderson, P. 1993. Particle Packing and Concrete Properties. *Material Science of Concrete II,* pp 111-147.

Kruger, J.E. 1999. *Origen, History and Properties of South African Fly Ash and Portland Fly Ash Cements, Guide 2.* South African Coal Ash Association, March.

Lee, S. Sakai, E. Daimon, M. and Bang, W.K. 1999. Characterization of fly ash directly collected from electrostatic precipitator. *Cement and Concrete Research,* Vol 29, pp 1791-1797.

Mooney, M. (1931). *Journal of Rheology,* Vol. 2, P. 210

Morat, E. Paya, J. and Manzo, J. 1993. Influence of different size fractions of fly ash on the workability of mortars. *Cement and Concrete Research*, Vol 23, No 4, July, pp 863-874.

Neville , A.M. and Brooks, J.J. 1998. *Concrete Technology.* Updated. Longman Group, U.K.

Okamura, H. and Ozawa, K. 1994. State of the art self-compacting concrete. *Journal of Japanese Society of Civil Engineers,* Vol 24, No 496, pp 1-8.

Olorunsogo, F.T. 1990. *Effect of Particle Size Distribution of Ground Granulated Blast Furnace Slag on Some Properties of Slag Cement Mortar.* PhD thesis. University of Leeds.

Popovics, S. 1994. Effect of the fineness of fly ash on the flow and compressive strength of portland cement mortars. *New Concrete Technology: Robert E. Philleo Symposium.*

Rabinowitsch, B. Z. (1929). *physic. Chem., Ser. A.,* 145, 1

Rendchen, K. 1985. Einflu der Granulometrie von Zement auf die Eigenschaften des Frishbetons und das Festigkeits- und Verformensverhalten des Festbetons. VDZ, Dusseldorf, Schriftenreihe fur den Zementindustrie, Heft 45, p. 189.

SABS method 862-1, *Concrete tests – Consistence of freshly mixed concrete – Slump test*, Pretoria: South African Bureau of Standards, 1994.

SABS 1491: Part 2. *Standard Specifications for the use of fly ash as a replacement for Portland cement*, Pretoria: South African Bureau of Standards, 1994.

Sakai, E. Hashino, S. Otlba, Y. and Daimon, M. 1997. The fluidity of cement pastes with various types of inorganic powders. *Proceedings of the 10th International Congress on the Chemistry of Cement,* Gottenburg, Sweden, June, Vol 2.

Sumner, M.S., Hepner, M.N. and Moir, G.K. 1989. The influence of a narrow cement particle size distribution on cement paste and concrete water demand. *Ciments, Betons, Platres, Chaux,* No. 778, March, pp. 164-168.

Tattersall, G.H. and Banfill, P.G.F. 1983. *The rheology of fresh concrete*. Pitman. London.

Tattersall, G.H. 1991. Workability and Quality Control of Concrete. E&FN Spon, London.

Visvanathan, K. 1993. *Indian Chemical Engineer, pp117-121.*

Vom Berg, W. 1979. Influence of specific surface of solids upon the flow behaviour of cement pastes. *Magazine of Concrete Research,* Vol 31, No 109, December, pp 211-216.

Wimpenny, D.E. and Ellis, C. 1987. Oil pressure measurement in the two-point workability apparatus. *Magazine of Concrete Research,* Vol 39, No 140, pp 169-173.

APPENDIX A: FLOW DATA FOR PRELIMANARY J-TUBE TESTS

1. Flow Curves

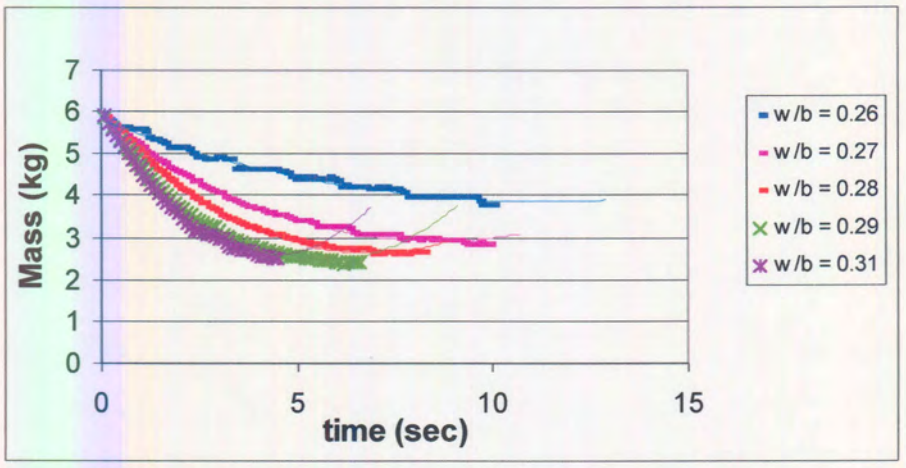

Figure A1: Flow curves for preliminary J-tube tests.

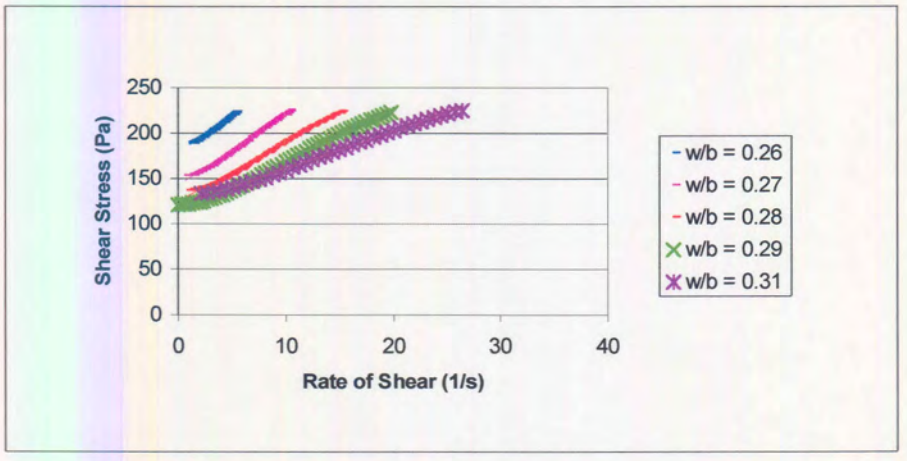

Figure A2: Bingham curves for preliminary J-tube tests.

2. Bingham Equations

Table A1: Bingham equations for preliminary flow curves.

W/b ratio	Bingham equation
0.26	$Y = 8.5x + 177$
0.27	$Y = 8.0x + 141$
0.28	$Y = 6.7x + 124$
0.29	$Y = 5.7x + 112$
0.31	$Y = 4.1x + 120$

APPENDIX B: FLOW DATA FOR J-TUBE TESTS

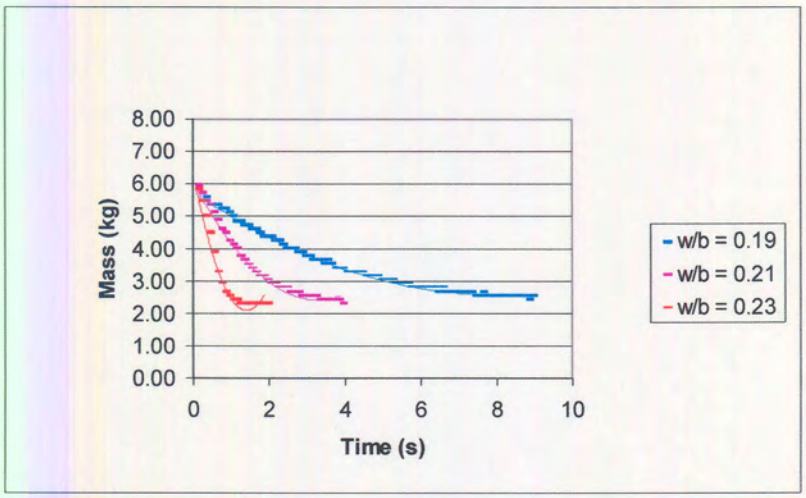

Figure B1: Flow curve of PFA-A.

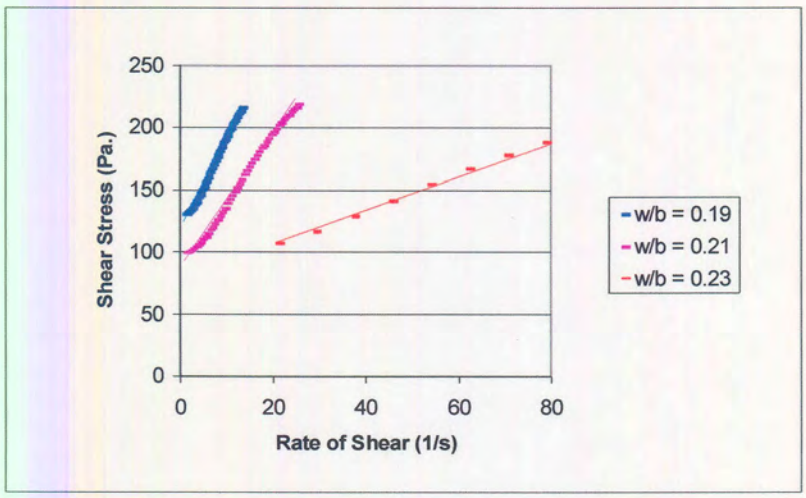

Figure B2: Bingham curve of PFA-A.

Table B1: Bingham equations for PFA-A.

W/b ratio	Bingham equation
0.19	$Y = 7.6x + 119$
0.21	$Y = 5.4x + 87.5$
0.23	$Y = 1.3x + 81.0$

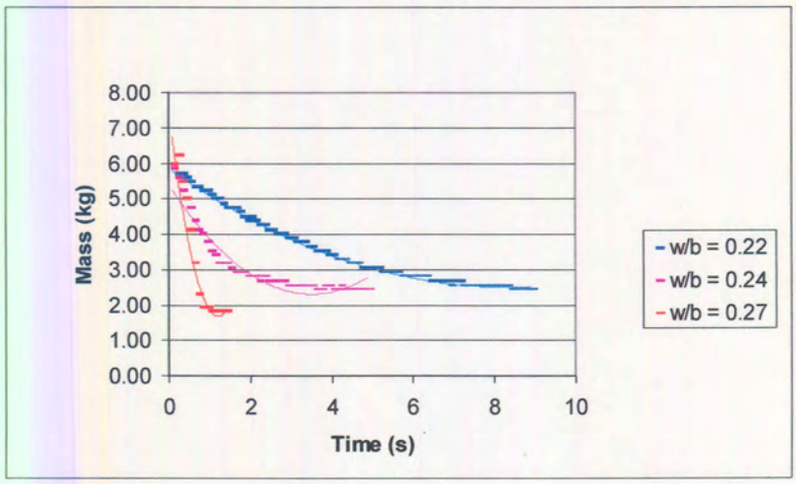

Figure B3: Flow curve of PFA-B.

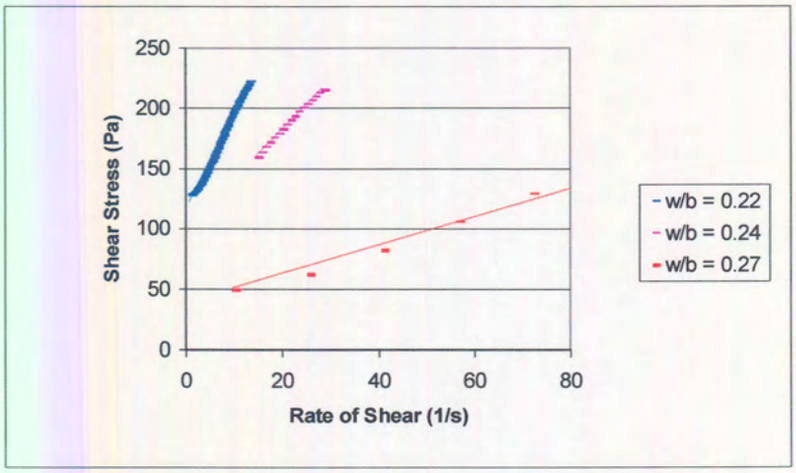

Figure B4: Bingham curve of PFA-B.

Table B2: Bingham equations for PFA-B.

W/b ratio	Bingham equation
0.22	$Y = 8.3x + 116$
0.24	$Y = 4.1x + 102$
0.27	$Y = 1.2x + 39.6$

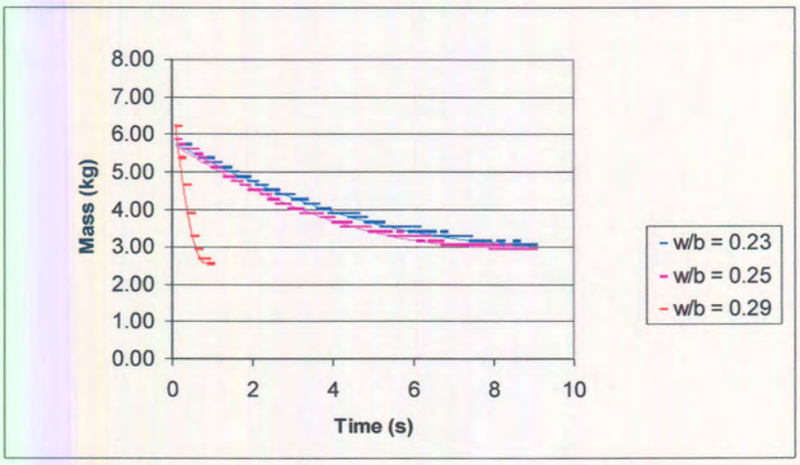

Figure B5: Flow curve of PFA-C.

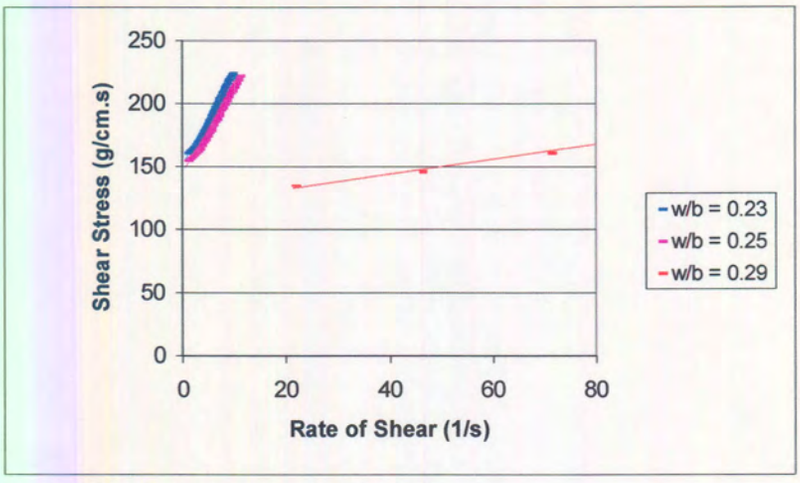

Figure B6: Bingham curve of PFA-C.

Table B3: Bingham equations for PFA-C.

W/b ratio	Bingham equation
0.23	$Y = 7.9x + 150$
0.25	$Y = 7.1x + 144$
0.29	$Y = 0.6x + 120$

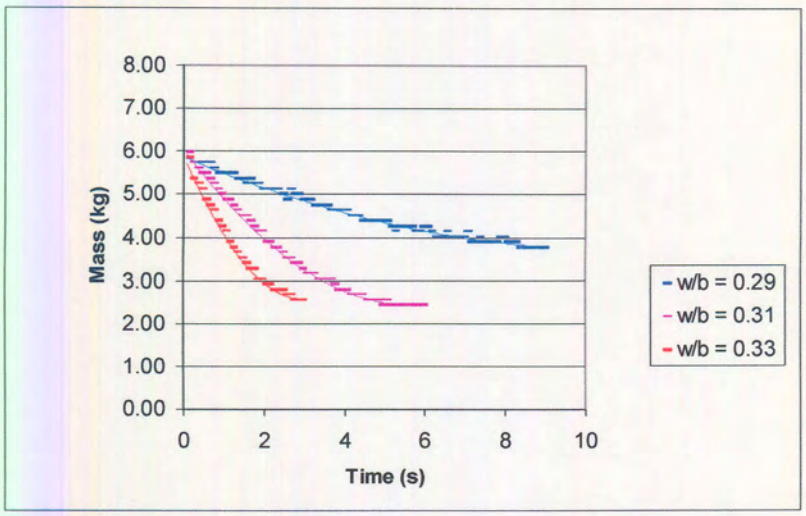

Figure B7: Flow curve of PFA-D.

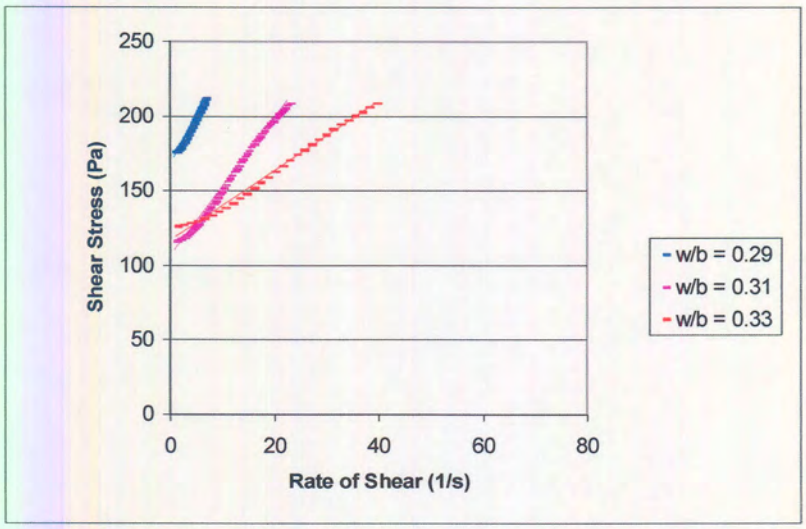

Figure B8: Bingham curve of PFA-D.

Table B4: Bingham equations for PFA-D.

W/b ratio	Bingham equation
0.29	$Y = 6.5x + 167$
0.31	$Y = 4.6x + 106$
0.33	$Y = 2.3x + 117$

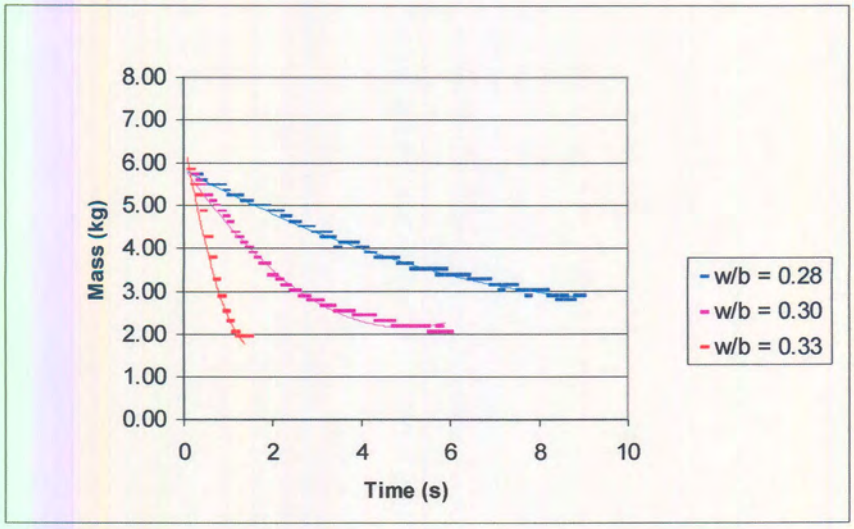

Figure B9: Flow curve of PFA-E.

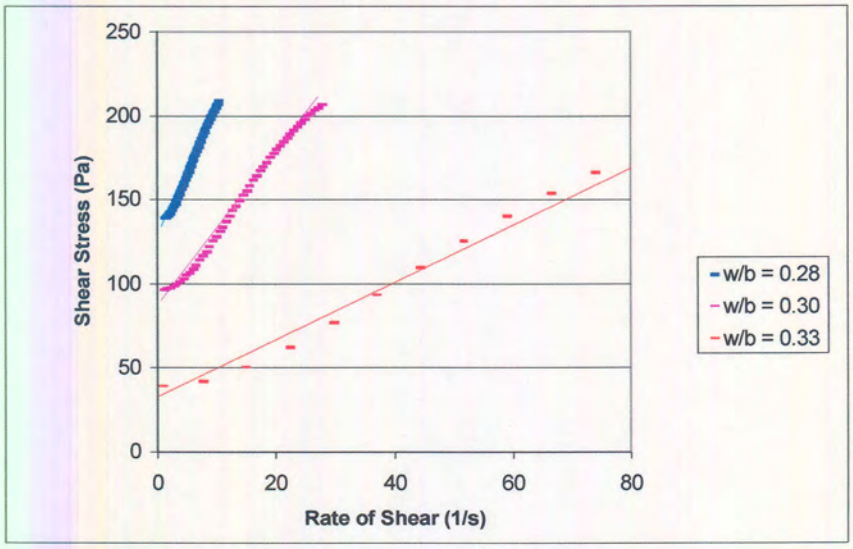

Figure B10: Bingham curve of PFA-E.

Table B5: Bingham equations for PFA-E.

W/b ratio	Bingham equation
0.28	$Y = 8.2x + 128$
0.30	$Y = 4.6x + 89.0$
0.33	$Y = 1.7x + 32.8$

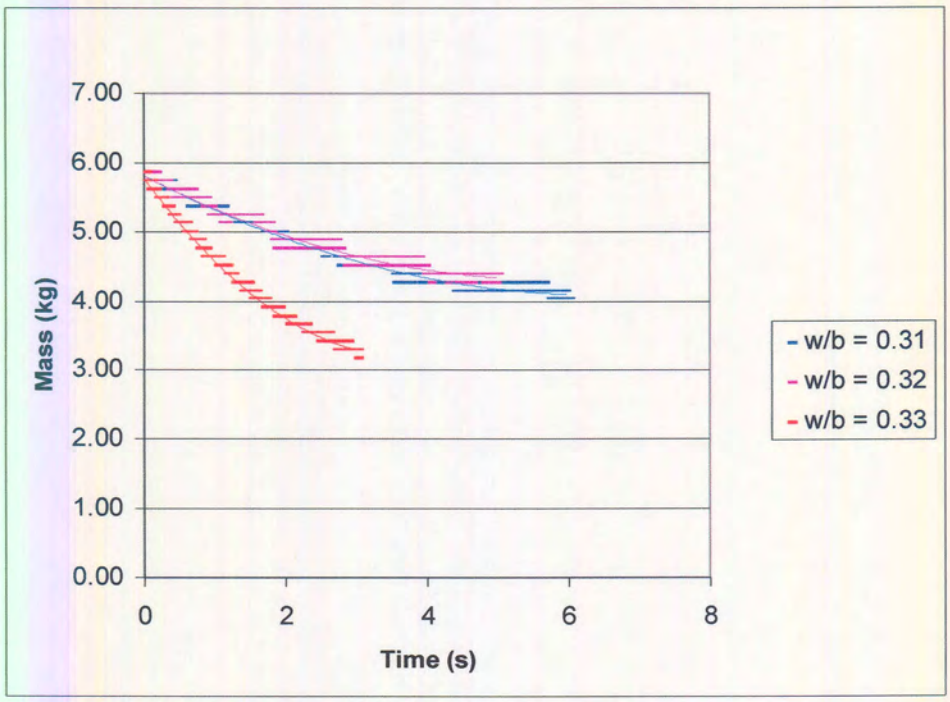

Figure B11: Flow curve for CEM I 42.5R.

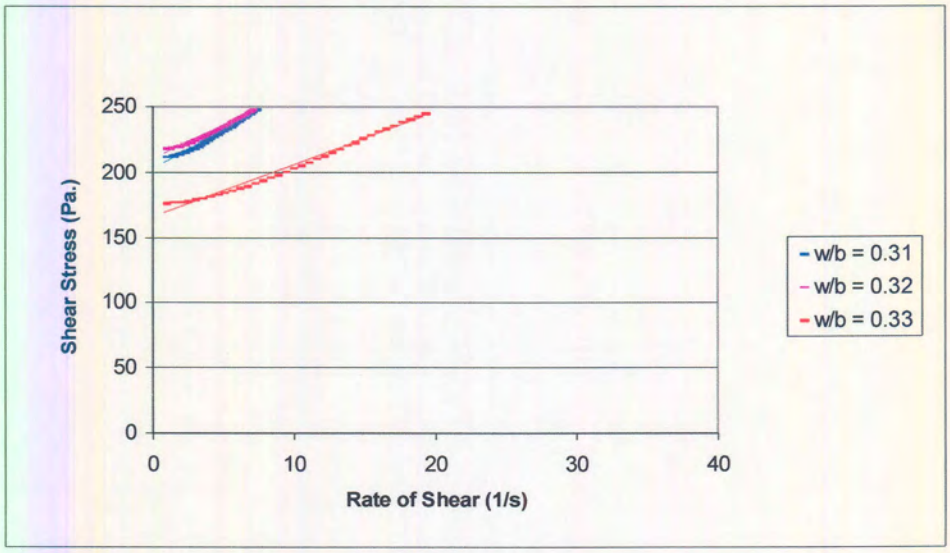

Figure B12: Bingham curve for CEM I 42.5R.

Table B6: Bingham equations for CEM I 42.5R.

W/b ratio	Bingham equation
0.31	$Y = 5.9x + 203$
0.32	$Y = 4.9x + 201$
0.34	$Y = 4.0x + 166$

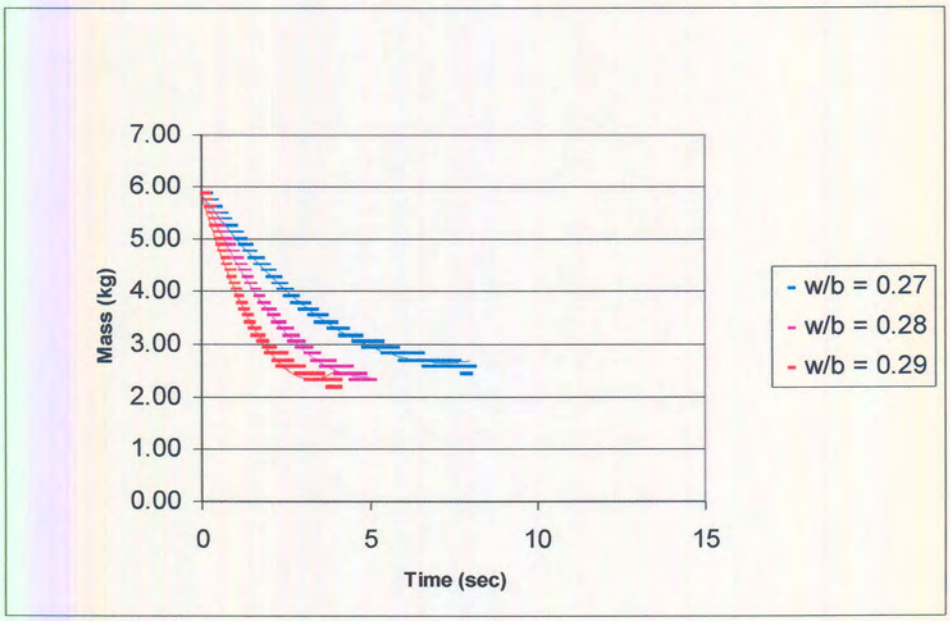

Figure B13: Flow curve for Blend-A.

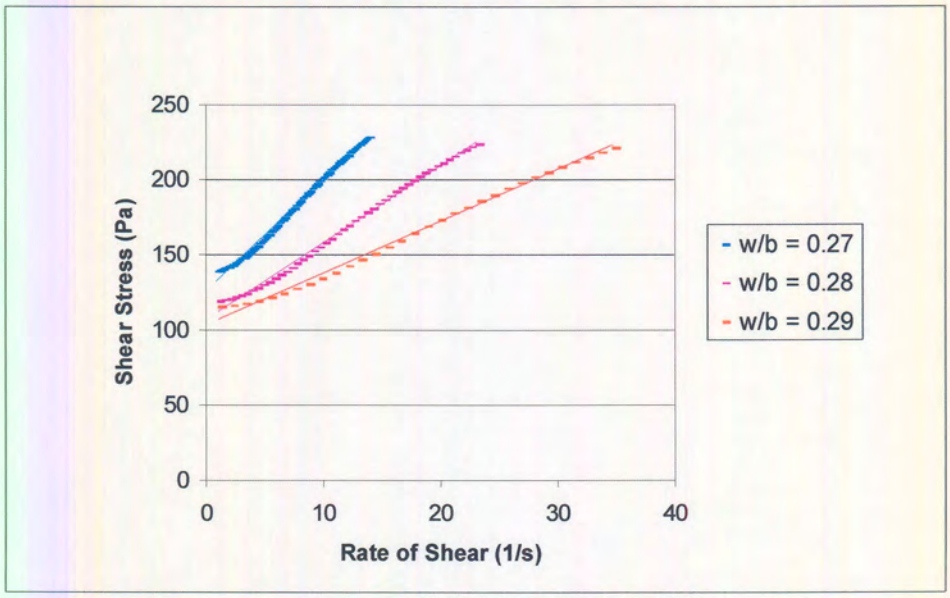

Figure B14: Bingham curve for Blend-A.

Table B7: Bingham equations for Blend-A.

W/b ratio	Bingham equation
0.27	$Y = 7.8x + 126$
0.28	$Y = 5.4x + 107$
0.29	$Y = 3.6x + 104$

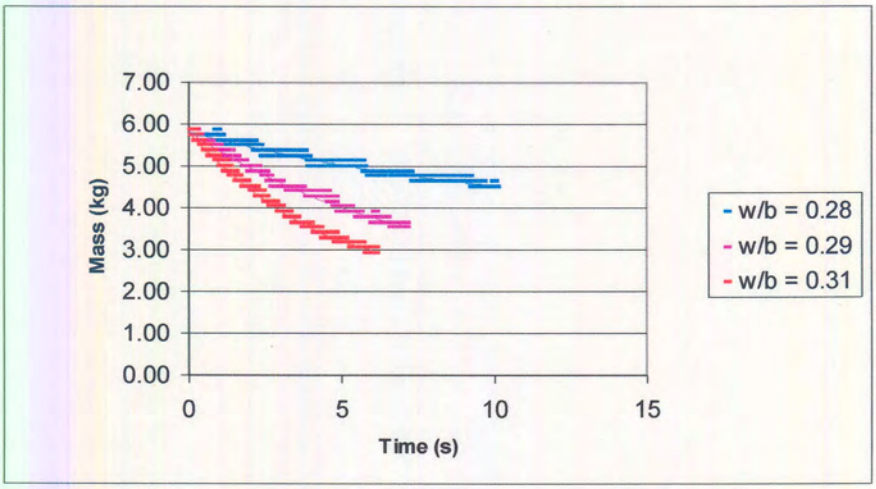

Figure B15: Flow curve for Blend-B.

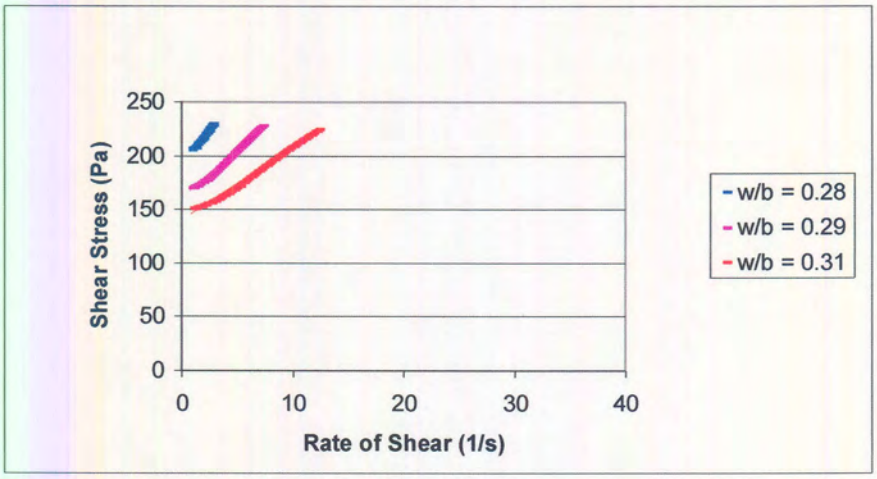

Figure B16: Bingham curve for Blend-B.

Table B8: Bingham equations for Blend-B.

W/b ratio	Bingham equation
0.28	$Y = 13x + 195$
0.29	$Y = 9.7x + 1591$
0.31	$Y = 6.9x + 140$

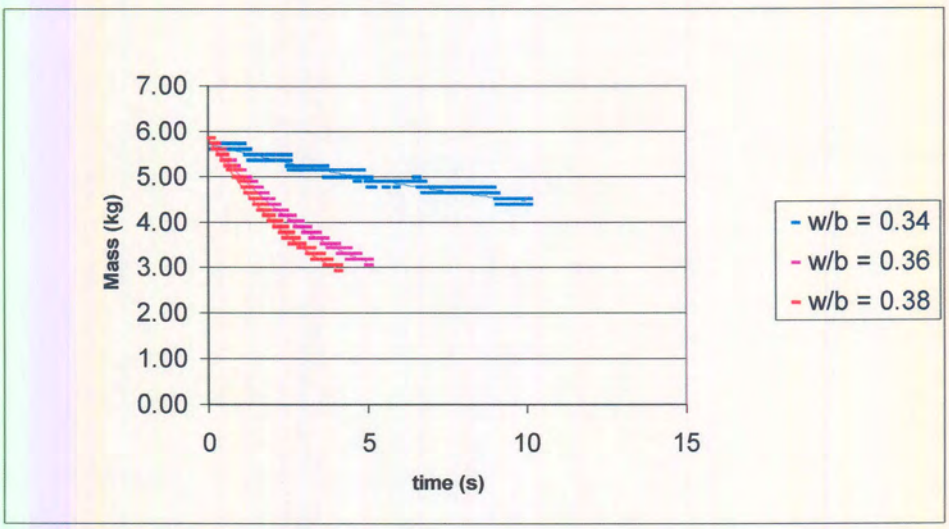

Figure B17: Flow curve for Blend-C.

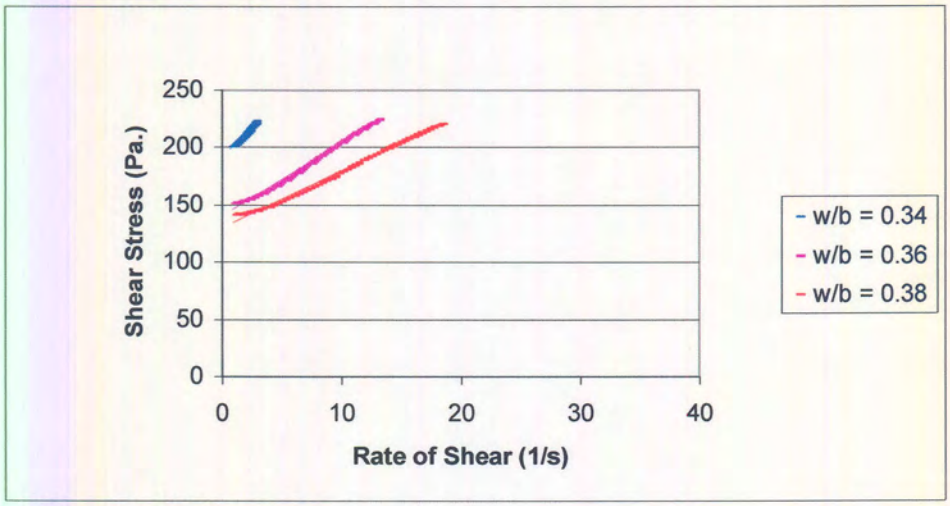

Figure B18: Bingham curve for Blend-C.

Table B9: Bingham equations for Blend-C.

W/b ratio	Bingham equation
0.34	$Y = 11.6x + 190$
0.36	$Y = 6.5x + 140$
0.38	$Y = 4.9x + 131$

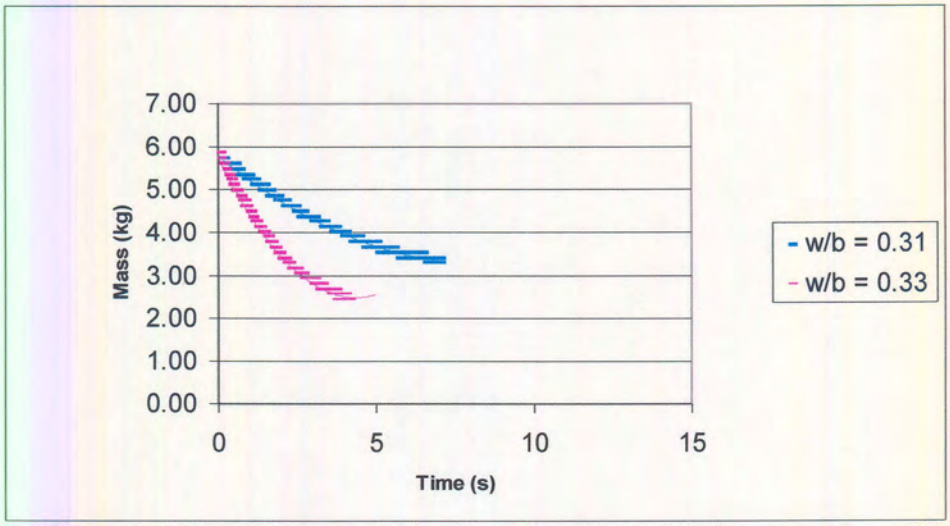

Figure B19: Flow curve for Blend-D.

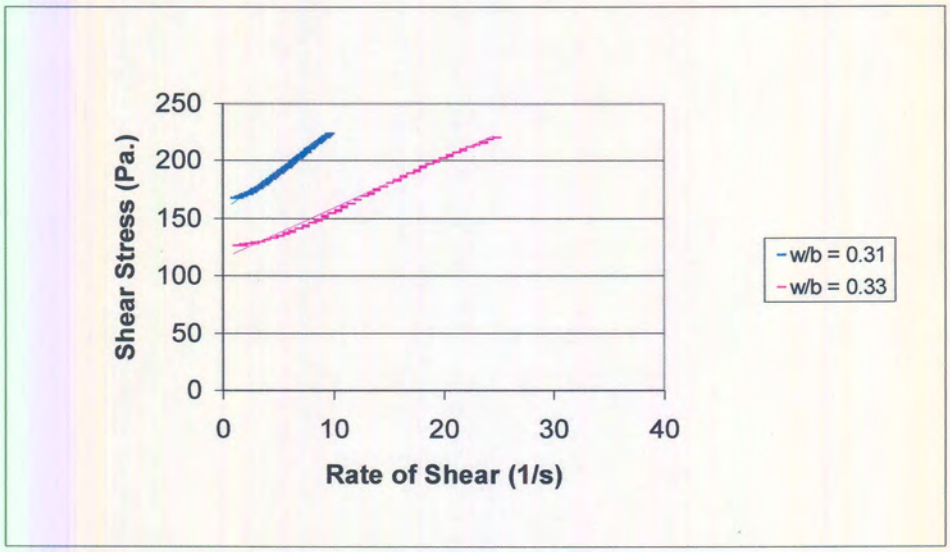

*Figure B20: Bingham curve for Blend-D.**

* The mixture made with a w/s ratio of 0.30 had insufficient workability and could therefore not be measured in the J-tube.

Table B10: Bingham equations for Blend-D.

W/b ratio	Bingham equation
0.31	Not measurable
0.31	$Y = 6.9x + 157$
0.33	$Y = 4.4x + 115$

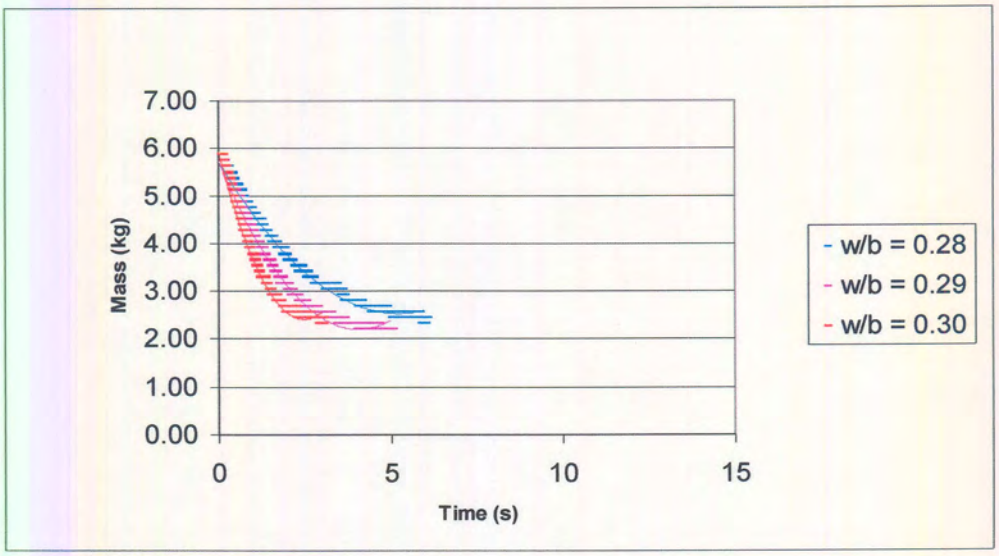

Figure B21: Flow curve for Blend-E.

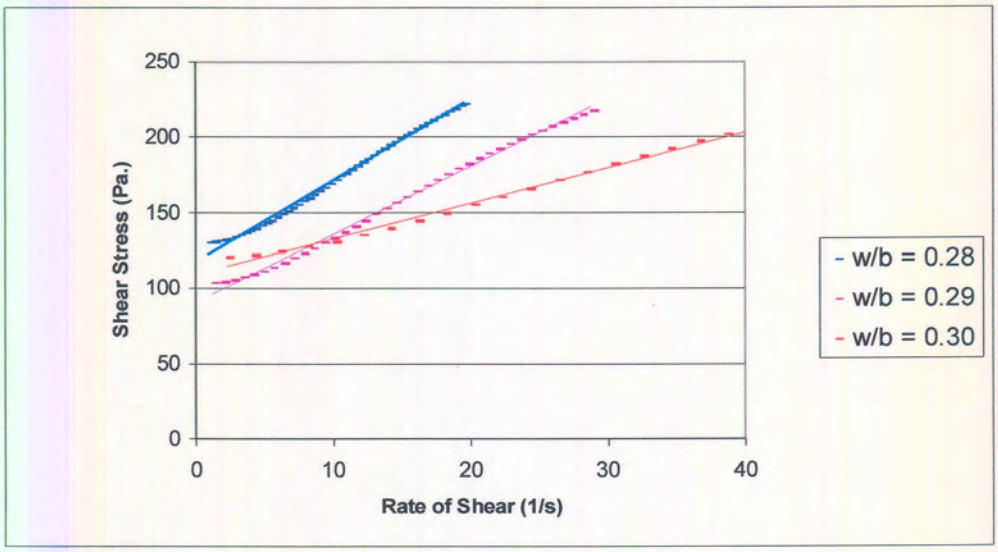

Figure B22: Bingham curve for Blend-E.

Table B11: Bingham equations for Blend-E.

W/b ratio	Bingham equation
0.28	$Y = 5.4x + 118$
0.29	$Y = 4.5x + 91$
0.30	$Y = 2.4x + 108$